



**Cinvestav**

CENTER FOR RESEARCH AND ADVANCED  
STUDIES (CINVESTAV-IPN)

ZACATENCO UNIT

DEPARTAMENT OF MOLECULAR BIOMEDICINE

MOLECULAR AND FUNCTIONAL  
CHARACTERIZATION OF HYDROPHOBIC  
NONSTRUCTURAL PROTEIN OF DENGUE VIRUS  
SEROTYPE 2

THESIS

PRESENTED BY

GAURAV SHRIVASTAVA

TO OBTAIN THE DEGREE OF

DOCTOR IN SCIENCE

IN THE SPECIALIZATION OF  
MOLECULAR BIOMEDICINE

THESIS SUPERVISOR  
DRA. LETICIA CEDILLO BARRÓN

Mexico City, Federal District.

August, 2017

DIRECTOR

**Dr. Leticia Cedillo Barrón**

Principal Investigator, Department of Molecular Biomedicine  
CINVESTAV-IPN, MEXICO CITY, MEXICO

ASSESSORS

**Dr. Rosaura Hernández Rivas**

Principal Investigator, Department of Molecular Biomedicine  
CINVESTAV-IPN, Mexico City

**Dr. Nicolás Villegas Sepúlveda**

Principal Investigator, Department of Molecular Biomedicine  
CINVESTAV-IPN, Mexico City

**Dr. Miguel Ángel Vargas Mejía**

Principal Investigator, Department of Molecular Biomedicine  
CINVESTAV-IPN, Mexico City

**Dr. Porfirio Nava**

Principal Investigator, Department of Physiology Biophysics y  
Neuroscience  
CINVESTAV-IPN, Mexico City

**Dr. Tomás David López Díaz**

Principal Investigator, Institute of biotechnology  
UNAM, Mexico

This thesis was carried out in the Department of Molecular Biomedicine of the Center for Research and Advanced Studies of the National Polytechnic Institute (CINVESTAV-IPN), under the supervision of **Dr. Leticia Cedillo Barrón.**

For the accomplishment of the doctorate degree, the National Council of Science and Technology (CONACYT), an institution to which I thank for the economic support provided during the development of this work, granted the scholarship with scholarship number (372598).

## ACKNOWLEDGEMENT

With the grace of almighty and blessings of my elders the research enthusiasm inside was fostered at this one of the greatest research facilities of Mexico “Center for Research and Advanced Studies of the National Polytechnic Institute (CINVESTAV-IPN), Mexico City”. I would like to start by thanking CINVESTAV-IPN for giving me an opportunity to pursue my doctorate at this excellent institution.

I consider myself extremely fortunate to be mentored by **Dr. Leticia Cedillo Barrón**. I will forever be grateful for her exceptional guidance during the course of my doctorate research and also for my future career plans. She is not only a brilliant scientist but also a friend, philosopher and guide to me, she played an important role as my supervisor and encouraged and challenged me throughout my doctorate project-training program. She has been very kind and patient with me when I took the time to learn and make mistakes during the initial stages of research. Dr. Leticia Cedillo Barrón provided me with complete freedom, resources and collaborations to experiment and explore in my projects and has always made herself available for questions and insightful discussions. Over the years, she has helped me better my writing and presentation skills and mould myself into a better scientist.

I would also like to convey my sincere gratitude to my thesis research advisory committee- Dr. Nicolás Villegas Sepúlveda, Dr. Tomás David López Díaz, Dr. Rosaura Hernández Rivas, Dr. Miguel Ángel Vargas Mejía, Dr. Porfirio Nava for providing invaluable guidance through my all projects. Their suggestions and comments have tremendously helped me in steering my projects in the right direction. I thank all the professors of the department, that without their advice and ideas this project would not be the same. I would like to thanks Ma. de Jesus Maqueda Villegas for her administrative help and support.

My special thanks to Dr. Julio García Cordero to who I look up to as great scientist, he has not only patiently helped me in various aspects of my research project, but also have grown to be my life-long friend. Thanks for your patience and above all for your friendship.

With deep sense of veneration and obligation from the core of my heart, I avail this opportunity to express my thanks to my labmates: Moises Leon, Sofia, Paola, Alfredo, Joseline, Moises Gomez, Giovanni and Mayra for their indispensable and able guidance inspirational ideas and support. I would like to thank the lab technician Froylán Ramírez Gómez, for his help and his dedication to maintain the lab material and facilities of this laboratory in good conditions. I would like to thank members of other labs (Samantha, Diana, Bere, Carolina, Karla, Mercedes, Ali, Abraham, Macario, Raul, Pili) in the department who I had the opportunity of working and becoming good friends with.

Life in CINVESTAV-IPN was more enjoyable and joyous because of a wonderful set of friends outside of my lab. I would like to thank Shiv, Neeshu, Joice, Satyam, Khemlal, Digpal, Goldi, John, Rajesh, Saira, Rigel, Alvaro, Francisca, Paco etc. who have stood by me through the hard times and continue to be great friends even after having left CINVESTAV-IPN.

My thesis is dedicated to my mother (Lt. Sarita Shrivastava) for nursing me with affection and love and for her encouragement and prays for my successful life. My head and heart bow down before my beloved Father Mr. Yogendra Shrivastava and my beloved family members Prashant, Shalu, Abhinav, Namrata, whose blessing and exhilaration have always animated me to rise against problems and face them smilingly. They kept me enthusiastic throughout my educational career, which enabled me to acquire the present gratification.

Finally, I give thanks to God, who makes all things possible.

Date: 31<sup>st</sup> August, 2017

Place: Mexico City

**(Gaurav Shrivastava)**

## INDEX

❖ INDEX OF FIGURES	V
❖ INDEX OF TABLES	VI
❖ ABBREVIATIONS	1
❖ ABSTRACT	4
❖ RESUMEN	6
❖ INTRODUCTION	8
1. EPIDEMIOLOGY	8
2. DENGUE INFECTION AND PATHOGENESIS	9
3. CHARACTERISTICS OF VIRUS	10
4. REPLICATION CYCLE	12
5. STRUCTURAL PROTEINS	14
6. NON-STRUCTURAL PROTEINS	14
7. HYDROPHOBIC PROTEINS OF DENGUE VIRUS	15
8. PERMEABILATION OF MEMBRANES	18
9. VIROPORINS	19
9.1. Structural characteristics and classification of viroporins	20
9.2 Functions of viroporins	21
9.2.1 Membrane Permeability	21
9.2.2 Effect of calcium homeostatis on viral infections	22
9.2.3 Reorganization of membrane & vesicular traffic	23
9.2.4 Induction of apoptosis by viroporins	24
9.2.5 Viroporins and the viral life cycle	25
10. ACTIVATION OF INFLAMMASOME	28
10.1 Inflammasome	28
10.1.1 NLR Family	31
10.1.2 Inflammasome activation during viral infection	33

10.1.2.1 NLRP3 Inflammasome	33
10.1.2.1.1 RNA virus	36
10.2 Activation of Inflammasome by viroporins	39
10.3. Activation of Inflammasome by dengue virus	42
❖ BACKGROUND WORK	43
❖ JUSTIFICATION	45
❖ HYPOTHESIS	46
❖ OBJECTIVES	46
❖ PARTICULAR OBJECTIVES	46
❖ MATERIAL AND METHODS	47
1. Propagation and purification of Dengue Virus Serotype 2	47
2. Virus Titration	47
3. <i>In silico</i> analysis of the NS2A protein	47
4. Amplification of the NS2A sequences	48
5. Cloning of NS2A in prokaryotes	49
6. Cloning of NS2A in eukaryotic vector	51
7. Analysis of recombinant clone	52
7.1 Extraction of plasmid DNA	52
7.2 Confirmation of NS2A DNA construct	52
8. Bulk preparation of NS2A plasmid by Maxiprep	52
9. Analysis of the recombinant proteins expression	53
9.1. Induction of NS2A recombinant protein	53
9.2. Induction of NS2A-GFP protein expression in HMEC-1 cells	54
10. Permeability assays using <i>E. coli</i> pLysS bacteria	55
11. Purification of the NS2A protein by preparative gels	55
12. Generation of anti-NS2A polyclonal antibody	56
13. Cellular localization of NS2A protein	56
14. Cross-linking test with Glutaraldehyde	56
15. Purification of the membrane	57

16. Preparation of liposomes and encapsulation of FITC	57
17. SDS-PAGE and Immunoblotting	58
18. Mitochondrial Membrane Potential Assay	58
19. Knockout of Inflammasome gene by CRISPR-CAS9 Technology	59
19.1 CRISPR	60
19.2 lentiCRISPRv2 (one vector system)	60
19.3 Designing of Guide RNA targeting NLRP3, CASPASE-1, ASC	61
19.4 Cloning of guide RNA in lentiCRISPRv2 plasmid	64
19.5 Transformation	64
19.6 Confirmation of the clones by colony PCR	64
19.7 Transfection, Transduction & Selection	65
❖ RESULTS	67
1. <i>In silico</i> analysis of NS2A sequence of DENV-2 and JEV	67
2. Cloning of NS2A protein in prokaryotic and eukaryotic system	69
3. Bacterial expression and purification of the DENV NS2A protein	70
4. Production of polyclonal antibody against NS2A protein	72
5. Evaluation of lytic activity of NS2A in <i>E.coli</i>	73
6. Oligomerization of NS2A Protein	74
7. Evaluation of lytic activity of NS2A in eukaryotic membrane	75
8. Expression and localization of NS2A-GFP in HMEC-1 cells	77
9. Dengue activates the NLRP3 inflammasome	79
10. NS2A and NS2B proteins activate NLRP3 inflammasome	82
11. Confirmation of viroporin effect in inflammasome by CRISPR-CAS9	86
12. Viroporin mediated inflammasome is dependent of NLRP3 and Caspase-1	88
13. Regulation of Ca <sup>++</sup> in Inflammasome activation	90
14. Viroporins activate NLRP3 inflammasome through mitochondrial ROS	91
❖ DISCUSSION	94
❖ CONCLUSION	103
❖ PERSPECTIVE	103



❖ LIST OF PUBLICATIONS	104
❖ REFERENCES	105

## INDEX OF FIGURES

Figure 1.	Geographical distribution of DENV infection in 2016	9
Figure 2.	Structural changes during the maturation of Dengue virus	11
Figure 3.	Genome of Dengue virus	11
Figure 4.	Replication cycle	13
Figure 5.	Membrane topology of DENV NS2A	17
Figure 6.	Viroporins functions during the viral life cycle	27
Figure 7.	Molecular sensors associated with the antiviral innate immune response	30
Figure 8.	Domain organization and cellular localization of pattern recognition receptors	32
Figure 9.	Mechanisms of virus mediated NLRP3 activation	35
Figure 10.	Cloning of NS2A protein in prokaryote	50
Figure 11.	Cloning of NS2A protein in eukaryote	51
Figure 12.	Schematic of the RNA-guided Cas9 nuclease	60
Figure 13.	Cloning of sgRNA of NLRP3, ASC and Caspase 1	61
Figure 14.	CRISPR: Target selection and reagent preparation	62
Figure 15.	<i>In silico</i> analysis of the amino acid sequence of NS2A	68
Figure 16.	Cloning of NS2A protein	69
Figure 17.	Expression and purification of NS2A protein from bacteria and confirmation of NS2A association with bacterial membranes	71
Figure 18.	Production of a polyclonal antibody against the NS2A protein	73
Figure 19.	NS2A protein expression arrests the growth of E. coli and affects the permeability of bacterial membranes.	74
Figure 20.	Oligomerization of NS2A protein	75
Figure 21.	NS2A lytic effect on Liposome	76
Figure 22.	Expression and localization of NS2A protein in HMEC-1 cells.	78
Figure 23.	NLRP3 inflammasome activation by DENV-2	81
Figure 24.	NLRP3 inflammasome activation by DENV viroporin NS2A and NS2B	85
Figure 26.	Confirmation of inflammasome activation by viroporin by CRISPR-CAS 9.	87
Figure 27.	NLRP3 and caspase-1 specific activation of inflammasome by NS2A & NS2B	88

Figure 28.	Requirement of increased intracellular Ca <sup>++</sup> concentration for NLRP3 inflammasome activation by NS2A and NS2B	91
Figure 29.	DENV viroporins induce the NLRP3 inflammasome through mitochondria	92

## INDEX OF TABLE

Table 1.	Characterized viroporins in different viruses	19
Table 2.	Inflammasomes activated by viroporins	41
Table 3.	NS2A oligonucleotide for PCR amplification	49
Table 4.	NS2A oligonucleotide for cloning in pEGFPN1 vector	51
Table 5.	Guide RNA specific to NLRP3, Caspase-1, ASC	63
Table 6.	Reagent cocktail for colony PCR	65
Table 7.	Transfection reaction cocktail	66
Table 8.	Percent similarity and identity between JEV and DENV NS2A	68

## ABBREVIATIONS

2-ME	2-mercaptoethanol
Aim-2	Absent in melanoma 2
ASC	Apoptosis-associated speck-like protein containing a CARD
ATP	Adenosine triphosphate
BSA	Bovine serum albumin
CARD	Caspase recruitment domain
C-terminal	Carboxy terminal
DENV-2	Dengue Virus serotipo 2
DF	Dengue Fever
DHF	Dengue Hemorrhagic Fever
dsRNA	Double stranded RNA
DSS	Dengue shock syndrome
DAMP	Danger associated molecular pattern
DAPI	4',6-diamidin-2-phenylindole
DNA	Deoxyribonucleic acid
dsDNA	Double strand Deoxyribonucleic acid
<i>E.coli</i>	<i>Escherichia coli</i>
E	Envelop Protein
EDTA	Ethylene-diaminetetraacidic acid
ELISA	Enzyme linked immunosorbent assay
ER	Endoplasmic reticulum
FACS	Fluorescence activated cell sorting
FITC	Fluorescein isothiocyanate
GFP	Green fluorescent protein
HRP	Horseradish peroxidase
Hpi	Hours post infection
IPTG	Isopropyl $\beta$ -D-1-thiogalactopyranoside
IF	Immunofluorescence
IFN	Interferon

IL	Interleukin
IRF	Type I IFN regulatory transcription factor
JEV	Japanese encephalitis Virus
kDa	Kilodaltons
M	Membrane protein
MEM	Minimum essential medium
MOI	Multiplicity of infección
mRNA	RNA messenger
N-terminal	Amino terminal
NS1	Non structural Protein 1
NS2A	Non structural Protein 2A
NS2B	Non structural Protein 2B
NS3	Non structural Protein 3
NS4A	Non structural Protein 4A
NS4B	Non structural Protein 4B
NS5	Non structural Protein 5
NTP	Nucleotide triphosphate
NF-κB	Nuclear factor-κB
NLRs	NOD-like receptors
NLRP3	NACHT,LRR,PYD domains containing protein 3
NLRC4	NLR family CARD domain containing protein 4
NOD	Nucleotide-binding oligomerization domain
O.D	Optical Density
ORF	Open reading frame
prM	Pre-membrane protein
PAGE	Polyacrylamide gel electrophoresis
PEG	Poly ethylene glycol
RdRP	RNA dependent RNA polymerase
RPM	Revolutions per minute
ROS	Reactive oxygeb species
PAMP	Pathogen associated molecular pattern

PBS	Phosphate buffered solution
PCR	Polymerase chain reaction
PE	Phosphatidyl-ethanolamine
PFA	Paraformaldehyde
RLRs	RIG like receptors
PRRs	Pattern recognition receptors
PFU	Plaque Forming Unit
UTR	Untranslated region
SDS	Sodium dodecyl sulphate
FBS	Fetal Bovine serum
ssRNA	Single stranded RNA
TGN	Trans-golgi network
TNF	Tumoral necrosis factor
TBE	Tris - base EDTA
TE	Tris-EDTA buffer
UV	Ultra violet
WB	Western blot
WT	Wild type

## ABSTRACT

During viral infections, virus hijacks the host cell machinery, specially virus generates new structures or compartments from the host cellular membranes and used for different stages of its infection cycle. Additionally, it has been reported that the permeability of the membrane is modified during viral infection, in this respect; we have identified the presence of specific viral protein called viroporin. Viroporins are viral genome-encoded low-molecular weight ion channel proteins. Viroporins are highly hydrophobic, contain transmembrane regions that allow them to be associated with membranes, and the ability to oligomerize and thereby form channels or pores in the membrane where they attach, compromising membrane permeability. In the flaviviridae family, a number of viroporins are described in Japanese encephalitis virus (JEV); however, although Dengue virus (DENV) encodes a small and highly hydrophobic protein, NS2A, the viroporin activity of this molecule needs complete evaluation. Our study showed for the first time, Dengue virus NS2A proteins behaves as a viroporin. In this report, we have performed *in silico* analysis, which has identified six putative membrane-interacting motifs in the DENV NS2A protein and sequence similarities with the NS2A protein from JEV, which possesses the membrane-destabilizing ability. We found that recombinant DENV NS2A localizes to both endoplasmic reticulum and mitochondrial membranes in cultured cells. Additionally, expression of DENV NS2A protein in an *E. coli* pLysS strain led to permeabilization of bacterial membranes. Moreover, the protein forms homo-oligomers and are responsible to permeabilize the eukaryotic membrane model (liposomes). In addition, Several RNA virus viroporins have demonstrated to play a crucial role in innate immune response by inducing the NLRP3 inflammasome. Dengue stimulates the Nod-like receptor NLRP3 specific inflammasome. However, the viral factor by which dengue virus activates the NLRP3 inflammasome is unknown. In this study, we investigated the activation of NLRP3 inflammasome in endothelial cells following DENV infection. Our results showed that DENV infection triggers the NLRP3 expression, ASC oligomerization, caspase-1 activation and subsequently secretion of IL-1 $\beta$ . Further, dengue viral protein was analyzed to investigate the role in the activation of inflammasome. We have demonstrated that proposed viroporins of dengue virus i.e NS2A and NS2B stimulates the NLRP3 inflammasome pathway. Viroporin activity of NS2A and NS2B was required for the activation of inflammasome complex by dengue virus and was sufficient to activate inflammasome complex in LPS primed endothelial

cells. NS2A and NS2B have shown to elevate the expression of NLRP3, oligomerization of ASC, activation of caspase-1 followed by secretion of IL-1 $\beta$  in cell supernatant. NS2A was found to redistribute the NLRP3 from cytoplasm to perinuclear space and colocalize with NLRP3. In addition, NS2A and NS2B activation of inflammasome was found to be NLRP3 and caspase-1 dependent. Elevation of the cytoplasmic Ca<sup>++</sup> level was important in viroporins-induced NLRP3 inflammasome activation as chelation of Ca<sup>++</sup> did not induce viroporins-induced IL-1 $\beta$  secretion. In addition, NS2A was found to modify mitochondria membrane morphology and NS2A and NS2B viroporins were showed to decrease mitochondria membrane potential. In continuation, generation of ROS was important in viroporins-induced NLRP3 inflammasome activation, as chelation of ROS did not induce viroporins-induced IL-1 $\beta$  secretion. These results indicate that DENV activates the NLRP3 inflammasome by stimulating Ca<sup>++</sup> flux from intracellular storages to the cytosol or by inducing ROS from mitochondria and highlight the importance of viroporins, transmembrane pore-forming viral proteins, in virus-induced NLRP3 inflammasome activation.



## RESUMEN

Durante las infecciones virales, el virus secuestra la maquinaria de la célula hospedera, induciendo la formación de nuevas estructuras o compartimentos de las membranas de las células del huésped y la utiliza para diferentes etapas de su ciclo de infección. Además, se sabe que la permeabilidad de la membrana se modifica durante la infección con diferentes virus y varias proteínas, son responsables de este fenómeno, tales como las vioporinas. Las vioporinas son proteínas de bajo peso molecular codificadas en genoma viral. Las vioporinas son altamente hidrófobas, contienen regiones transmembranales que les permiten asociarse con las membranas y tienen la capacidad de formar oligómeros y por lo tanto formar canales o poros en la membrana donde se unen, comprometiendo la permeabilidad de la membrana. En la familia Flaviviridae, se han descrito varias vioporinas presentes en el virus de la encefalitis japonesa (JEV); Sin embargo, aunque el virus del Dengue (DENV) codifica una proteína pequeña y altamente hidrófoba, NS2A, la actividad como vioporina nunca se había evaluado. En este trabajo nosotros mostramos, por primera vez, que la proteína del virus del Dengue NS2A se comporta como una vioporina. En este trabajo, hemos realizado análisis *in silico*, que ha identificado seis motivos putativos de interacción de la proteína NS2A de DENV y similitudes con la secuencia de la proteína de JEV, la cual posee la capacidad de desestabilización de la membrana. Se encontró que la recombinante DENV NS2A se localiza tanto en el retículo endoplásmico como en las membranas mitocondriales en cultivos celulares. Además, la expresión de la proteína NS2A en una cepa pLysS de *E. coli* condujo a la permeabilización de las membranas bacterianas. La proteína forma homo-oligómeros y son responsables de permeabilizar un modelo de membrana eucariótica (liposomas). Además, varias vioporinas de virus de RNA han demostrado desempeñar un papel crucial en la respuesta inmune innata al inducir el inflamasoma NLRP3. Una de las reacciones fundamentales de la respuesta inmune innata a la infección vírica incluye el procesamiento y liberación de citoquinas pro-inflamatorias, incluyendo IL-1 $\beta$  e IL-18. El dengue estimula el receptor tipo Nod específico, NLRP3, el cual es parte de la vía de activación del inflamasoma. Sin embargo, se desconoce el factor viral por el cual el virus del dengue activa el inflamasoma NLRP3. En este estudio, se investigó la activación de

este inflammasoma en las células endoteliales después de la infección por Dengue. Nuestros resultados mostraron que la infección del dengue desencadena la expresión de NLRP3, la oligomerización de ASC, la activación de caspasa-1 y por último la secreción de IL-1  $\beta$ . Posteriormente, la proteína viral del dengue se analizó para investigar el papel en la activación del inflammasoma. Hemos demostrado que las proteínas propuestas como vioporinas del virus del dengue, es decir, NS2A y NS2B, estimulan la vía del inflammasoma NLRP3. La actividad como vioporinas de NS2A y NS2B fue requerida para la activación del complejo de inflammasoma por el virus del dengue y fue suficiente para activar el complejo del inflammasoma en células endoteliales cebadas con LPS. NS2A y NS2B han demostrado elevar la expresión de NLRP3, la oligomerización de ASC, la activación de la caspasa-1 seguido por la secreción de IL-1 $\beta$  en el sobrenadante celular. Se encontró que NS2A redistribuye la proteína NLRP3 desde el citoplasma al espacio perinuclear y colocaliza con NLRP3. La expresión de ambas vioporinas desencadena la estructura puntiforme de ASC que corresponde a la activación del complejo del inflammasoma. También, se encontró que la activación del inflammasoma debida a NS2A y NS2B es dependiente de NLRP3 y caspasa-1. La elevación de las concentraciones citoplasmicas de Ca<sup>++</sup>, fue importante en la activación del inflammasoma NLRP3 inducida por vioporinas, ya que la quelación de Ca<sup>++</sup> no indujo la secreción de IL-1 $\beta$ . Además, se observó que NS2A modifica la morfología de la membrana mitocondrial y que las vioporinas NS2A y NS2B disminuyen el potencial de la misma. Por otra parte, la generación de ROS fue importante en la activación del inflammasoma inducida por las vioporinas, ya que la quelación de ROS no indujo la secreción de IL-1 $\beta$ . Estos resultados indican que el DENV activa el inflammasoma NLRP3 estimulando el flujo de Ca<sup>++</sup> de los depósitos intracelulares al citosol o induciendo ROS de las mitocondrias, resaltando la importancia de las vioporinas, proteínas transmembranas formadoras de poro, en la activación del inflammasoma NLRP3 inducida por el virus.

## **INTRODUCTION**

### **1. EPIDEMIOLOGY**

#### **DENGUE VIRUS**

Dengue is an acute febrile disease caused by the mosquito borne dengue viruses (DENVs).

The causal agent of this infection is the dengue virus (DENV) from which 4 serotypes (DENV-1 to DENV-4) have been described, *Aedes aegypti* being the main vector transmitting the infection. They are the members of the flaviviridae family, genus flavivirus (1). The virus is distributed in tropical and subtropical areas including urban and suburban America, Southeast Asia, Eastern Mediterranean, and Western Pacific and in rural areas of Africa (Fig 1). Several factors have contributed to spread of the disease, such as rapid population growth, migration of population from rural to urban areas, lack of potable water, improper disposal of organic waste and the redistributing of vector (2). To date, the WHO estimates 390 million dengue infections per year (95% credible interval 284–528 million), of which 96 million (67–136 million) manifest clinically including the severe cases. Another study regarding the prevalence of dengue estimates that 3.9 billion people in 128 countries are at risk of infection with dengue viruses (2). In most cases, the disease is self-limiting with either mild flu-like symptoms or acute febrile illness called dengue fever (DF). Among 2-5% of patients may develop more lethal form of the disease called dengue hemorrhagic fever and dengue shock syndrome (DHF/DSS) characterized by hemorrhagic manifestations i.e capillary leakage, thrombocytopenia and hypovolemic shock (3). Nowadays, the major public health concern and one of the most frequent diseases caused by arbovirus worldwide resulted from DENV. The abundant alteration for the dynamics of transmission and global epidemiology was demonstrated by DENV (3). The factors that define the severe forms of the disease are multiple, from the coincidence of a secondary infection with a heterologous serotype, to factors that depend on the mosquito, the isolate and the serotype, among others.

Distribution of dengue, worldwide, 2016

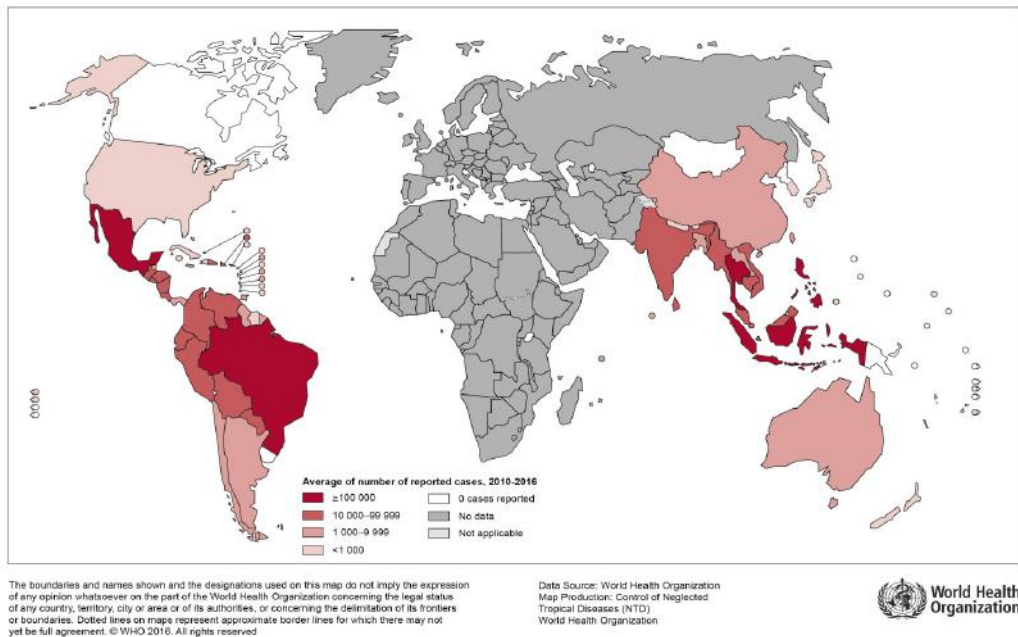


**Fig 1. Geographical distribution of DENV infection in 2016.** Outline red countries are areas where the disease has been reported. (WHO 2016)

## 2. DENGUE INFECTION AND PATHOGENESIS

Dengue virus infection begins with the bite of a virus-carrying mosquito to the humans. After a incubation period of 4 to 7 days, the infected individual may experience acute fever accompanied by non-specific signs and symptoms such as: frontal headache, retro orbital pain, fever, arthralgia, myalgia; these symptoms are associated with classical dengue fever, which is common in adults and rarely fatal (4). In contrast, DHF and DSS, affect mainly children aged 1-15 years. Severe forms are characterized by circulatory problems and hemorrhagic manifestations that include vascular changes, thrombocytopenia and clotting disorders, which mainly cause vascular damage and loss of fluid in patients. Patients with DSS show micro hemorrhages, which decrease the blood pressure and subsequently deteriorates the condition of patient. Shock duration is very short; patients may die within range from 8 to 24 hours (4). Until now, the pathogenic mechanisms of severe forms of the disease are not fully understood, in part due to the absence of an animal model that reproduce the signs and symptoms of the

disease. Therefore, the severe form of dengue is multifactorial; since it depends on viral factors and host factors, play a crucial role in the pathogenesis of disease. Some studies have suggested that certain viral genotypes are associated with the incidence of severe forms of disease. In this respect, the virus serotype 2 of asiatic origin are responsible for severe forms of primary infections in central American countries, whose nucleotide sequences of E, prM, NS4B, and NS5; were different from the strains more prevalent in America (5). Additionally, other studies have reported the changes in the 5' and 3' untranslated regions of viral RNA, that affect directly in the viral replication rate, which can influence the virulence of virus (6).

### **3. CHARACTERISTICS OF VIRUS**

Structurally, Dengue virus consists of 3 proteins: C (Capsid), M (membrane) and E (envelope). The capsid protein is associated with viral genome (RNA) and the M and E proteins are immersed in the membrane covering the nucleocapsid particle. The virus has an icosahedral morphology of approximately 50 nanometers. Cryoelectronic microscopy studies revealed 2 architectures of the viral particle: one immature form, which is composed of 60 asymmetric trimers constituted by the prM-E heterotrimer, which is inserted into the surface of the viral particle simulating the spike forms. This architecture prevents premature fusion of the E protein during virus maturation events (7). In contrast, the mature virus has a relatively smooth surface formed by 30 rafts; each of these structures contain 3 antiparallel homodimers of the protein E, which are organized into an icosahedral structure (Fig. 2), (8).

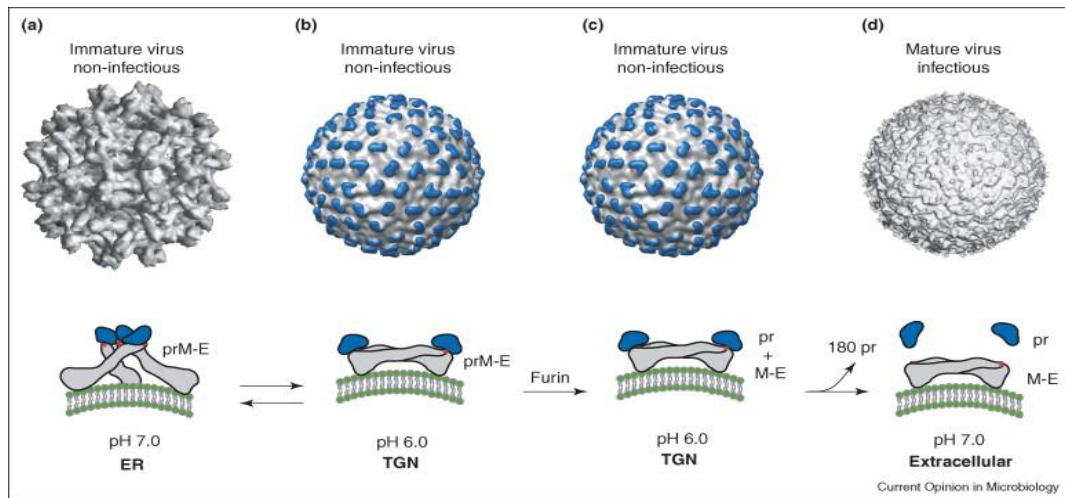


**Fig 2. Structural changes during the maturation of Dengue virus:** A) Organization of heterotrimer constituted by the E-prM proteins in the endoplasmic reticulum, spiral appearance of the viral particle. B) and C) show the changes that occur on the heterotrimer to form a heterodimer of the E-prM proteins in the trans-golgi network. (D) Release of the Pr portion of the M protein by the action of the protease furine, Smooth appearance of the viral particle (8).

The viral genome consists of a positive sense, single stranded RNA with an approximate length of 10.7 kb. This string contains a 5' untranslated region (UTR) of about 100 nucleotides and a 3' end UTR that consist of about 400 nucleotides. Both regions i.e 3' end and 5' end are highly structured and are required for successful replication of DENV (8). The genome contains one single open reading frame (ORF) that encodes for a polyprotein that is processed by viral and host protease to form 3 structural and 7 non structural proteins. (3)

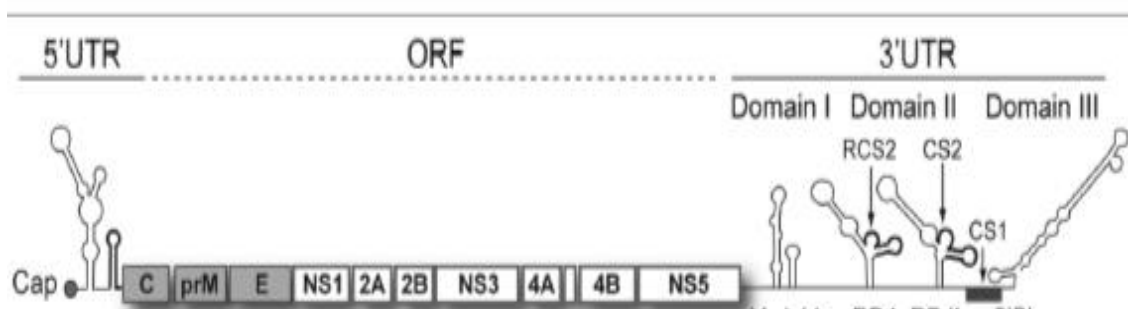


**Fig 3. Genome of Dengue virus.** The different elements that constitute the genome of the virus: 5' UTR region, sequence that encodes the 7 methyl guanosine (CAP); followed by the framework of open reading (ORF), with structural proteins are in gray colour and non-structural proteins are in white colour. Finally the 3'UTR region is located, with the 3 domains which are mentioned in the text (8)

#### 4. REPLICATIVE CYCLE

DENV enters through the skin of the host during the bite of the female mosquito *Aedes aegypti* at the level of epidermis and dermis where, virus potentially infects resident cells expressing the viral receptor (s). In this precise moment the local innate immune response starts, which could be crucial for the evolution of the infection. (9) (10). It is proposed that the virus enters to the target cell by two mechanisms. A) Receptor mediated endocytosis and B) antibody mediated facilitation. Once the virus is in an endosome / lysosomal vesicle, the acidic pH of the compartment induces the conformational changes in the E protein, exposing the fusogenic loop peptide, and allowing the release of the nucleocapsid to the cytoplasm. Once the nucleocapsid is released in the cytoplasm, the genetic material of the virus is exposed to the translation machinery in the endoplasmic reticulum of the cell. Viral RNA is immediately read as a messenger and translated into a polyprotein. Simultaneously the negative sense replicative intermediate is produced which serves as a template to form the viral genome. Further, the newly synthesized genome is translated, replicated to form a new intermediary or assembled with the nucleocapsid to form a new virion. The virion assembly begins in the ER lumen, when positive sense genomic RNA is associated with C protein to form the nucleocapsid and acquire the endoplasmic reticulum envelope from the host. The assembly continues in the intracellular vesicles, where reorganization of membranous structures is observed accompanied by a rapid maturation of the virion (11). A hallmark of dengue infection is the redistribution and reorganization of cellular membranes. The nonstructural proteins perform these changes. In the vesicles, the immature particle contains the prM protein that is non-covalent associated to the E protein in a heterodimeric complex, prevents the premature exposure of the fusogenic peptide of E protein (18). The membrane vesicles transport the virions through the exocytic pathway of the trans-golgi network. During this process, the maturation of the virion is characterized by the proteolytic processing of the prM protein to induce the association of mature M protein with E protein. Finally the cytoplasmic transporter vesicles are fused with plasma membrane of the cell, allowing the mature virions to be released to the extracellular space by secretory exocytosis (Fig. 4) (12)(13)(14).

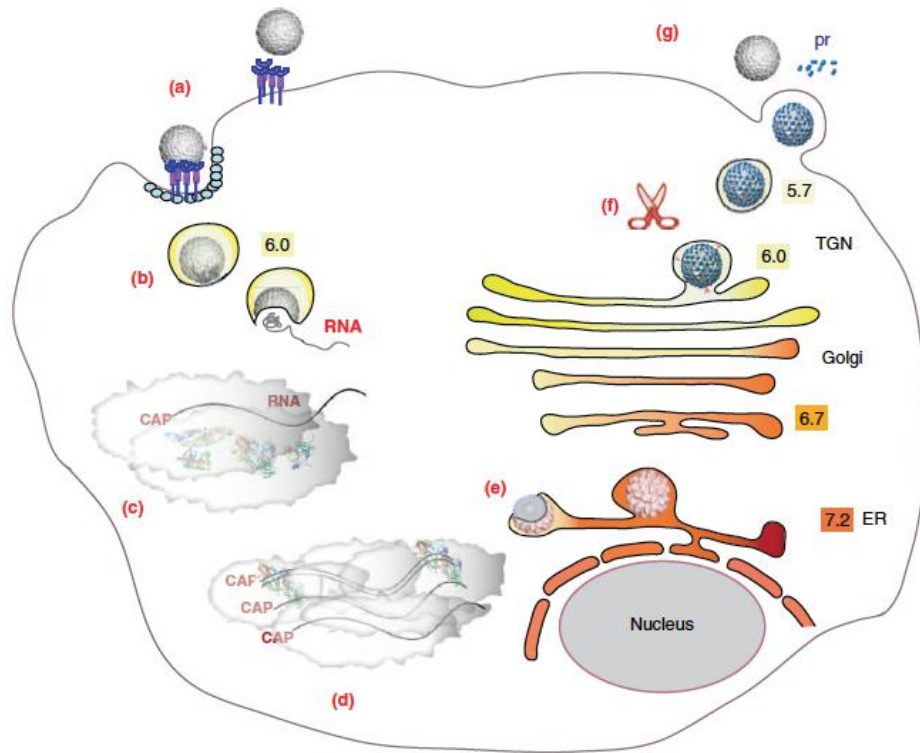


**Fig 4: DENV replication cycle.** The various steps in the flavivirus life cycle : A) virions binding to cell surface attachment molecules and receptors, and are internalized through endocytosis. B) Due to the low pH of the endosome, viral glycoproteins mediate fusion of viral and cellular membranes, allowing disassembly of the virion and release of vRNA into the cytoplasm. C) vRNA is translated into a polyprotein that is processed by viral and cellular proteases. D) Viral NS proteins replicate the RNA genome. E) Virus assembly occurs at the endoplasmic reticulum (ER) membrane, where C protein and vRNA are enveloped by the ER membrane and glycoproteins to form immature virus particles. F) Immature virus particles are transported through the secretory pathway, and in the acidic environment of the trans-Golgi network (TGN), furin mediated cleavage of prM drives maturation of the virus. F) Mature virus is released from the cell. (15)



## 5. STRUCTURAL PROTEINS

The capsid protein (**C**) is a structural component of the nucleocapsid with molecular weight of 12 to 14 kDa and carries positive charge. The sequence homology between the members of the flaviviridae family is very low, however some hydrophobic and hydrophilic residues are maintained. The **prM** protein is a glycoprotein precursor of the matrix protein M with a molecular weight between 18.1 and 19 kDa. This precursor cleaves to give rise to the M protein and the terminal amino fragment pr whose function is unknown and the processing is associated with maturation or release of the virion (16). The envelope protein (**E**) is the major structural component of all flaviviruses with molecular weight of 53 to 54 kDa. It is known that this protein participates in several biological events such as receptor binding and membrane fusion. Protein E presents three structural and functional domains. The central domain I is involved in the conformational change. Domain II, participates in the fusion of viral and endosomal membranes for virus stripping towards the cytoplasm. Finally domain III contains the highest number of neutralizing antibody-inducing epitopes. Experimental evidences suggest that domain III have the cell receptor-binding site (17)(16)(18)(19).

## 6. NON-STRUCTURAL PROTEINS

Flavivirus **NS1** is a multifunctional 48-kDa glycoprotein and is an essential component of the viral replicase (20) (17)(21). In addition, NS1 are highly immunogenic and contribute to the pathogenesis of flavivirus infection in a host. NS1 has been suggested to facilitate immune complex formation, elicit autoantibodies that react with platelet and extracellular matrix proteins, damage endothelial cells via Ab-dependent complement-mediated endocytosis, and directly enhance infection (22)(23)(24)(25)(26)(16). Flavivirus NS1 also exhibits immune-evasion via binding to complement proteins and modifying or antagonizing their functions (27)(28)(29)(30). The **NS3** protein is highly conserved among different members of the flaviviridae family, has molecular weight of 68 to 70 kDa. This protein has been attributed four different activities; protease, nucleoside triphosphatase (NTPase), helicase as well as RNA triphosphatase (31)(32)(33) (34)(27)(28)(29). This protein participates in the proteolytic hydrolysis activity of the viral polyprotein between NS2A and protein C proteins as well as between the NS2A / NS2B, NS2B / NS3, NS3 / NS4A, NS4A / NS4B and NS4B / NS5 proteins. NS3 proteolytic activity is associated with the formation of a complex (NS3-NS2B)

with the viral protein NS2B (31)(33)(30). The **NS5** protein is the largest protein among the non-structural protein with molecular weight of 105 kDa. NS5 amino terminal contains a methyl transferase domain which is responsible for the methylation of the Guanine cap N-7 and ribose 2'-O. NS5 protein also has RNA-dependent RNA polymerase domain (RdRp) at its carboxyl end terminus and is precisely responsible for the replication of the viral genome. In addition, NS5 also contain a GDD domain, which is present most of the proteins with RNA-dependent RNA polymerases activity. NS5 play a very important function during dengue viral pathogenesis by participating in the synthesis of the viral replication intermediates (16).

## **7. HYDROPHOBIC PROTEINS OF DENGUE VIRUS**

The viral genome encodes 4 non-structural hydrophobic proteins, however very little is known about their functions and properties. These proteins are NS2A, NS2B, NS4A and NS4B. Although, the amino acid sequence of these proteins show a low identity among the different members of the genus of the flavivirus, however, they share similar physicochemical and structural characteristics such as size, hydrophobicity and potential hydrophobic transmembrane regions (35).

Flavivirus **NS2A** is a 22-25 kDa hydrophobic trans-membrane protein that plays a critical role in virus life cycle (36)(37)(38)(39)(40). NS2A N-terminus is processed in the endoplasmic reticulum (ER) lumen by a membrane bound host protease and C terminus is processed in cytoplasm by NS2B/NS3 viral protease (32)(41). Recent topological study of DENV NS2A has demonstrated eight predicted transmembrane segments (pTMSs; pTMS1 to pTMS8) and five integral transmembrane segments (pTMS3, pTMS4, pTMS6 to pTMS8) that span the lipid bilayer of the endoplasmic reticulum (ER) membrane (Fig 5). DENV-2 NS2A protein has been found to be involved in DENV RNA synthesis and virion assembly/maturation. A mutagenesis study within the first integral transmembrane segment revealed that the R84A mutation did not affect viral RNA synthesis but blocked the intracellular formation of infectious virions (37). Another mutagenesis study revealed that several NS2A mutations, G11A, E20A, E100A, Q187A, and K188A, impaired virion assembly without specifically affecting viral RNA synthesis (42). Kunjin virus (KUNV) NS2A has shown to interact with the 3'UTR of viral RNA and other components (NS4A) of the replication complex, stating the involvement of NS2A in viral RNA replication (38). Several studies have demonstrated that

flavivirus NS2A contributes in the assembly and secretion of the virion (39)(40) (42)(43). It has shown that KUNV NS2A was located in vesicle packet and bound strongly with UTR of kunjin RNA and with replicase component (NS3 and NS5) (38). A model was proposed in which NS2A is directly involve in transporting RNA from sites of RNA replication across virus-induced membranes to adjacent sites of virus assembly, with NS2A acting as a viroporin (43)(40). In addition flavivirus NS2A as a viroporin was further hypothesized in a study where JEV NS2A protein has shown to cause membrane permeability (35).

The viral NS2A protein has also shown to be involved in the inhibition of IFN pathways and its effector responses. In this aspect, studies in kunjin (KUNV) virus have identified the NS2A protein as an inhibitor of IFN- $\beta$  gene transcription (44)(45). NS2A flaviviruses target the JAK-STAT signaling pathway to prevent the induction of antiviral ISG with possible antiviral activity as NS2A has shown to enhance replication of IFN-sensitive virus by blocking nuclear localization of STAT1 (46)(47). Further it was found that a single amino acid substitution in NS2A (Ala30 to Pro [A30P]) dramatically reduced its inhibitory effect of IFN- $\beta$  promoter driven transcription (44). A single NS2A mutation (A30P) in the WNVKUN genome elicits more rapid induction and higher levels of synthesis of IFN- $\alpha/\beta$  indicates the importance of single amino acid in NS2A in interferon induction (44). Flavivirus NS2A also exerts apoptotic role. In the regards, a mutation in westnile NS2A protein (A30P) reduced viral cytopathicity in cells and virulence in mice (44). Further a study has demonstrated the role of westnile virus NS2A protein in virus induced cell death independently of IFN $\alpha/\beta$  response by showing the effect of different amino acid substitutions at position 30 (48). Recently, hydrophobic regions of NS2A is investigated and observed a specific NS2A peptide “dens25” has strong interaction with membranes and due to its membrane modulating capabilities this region might be involved in membrane rearrangements and thus be important for the viral cycle (49).

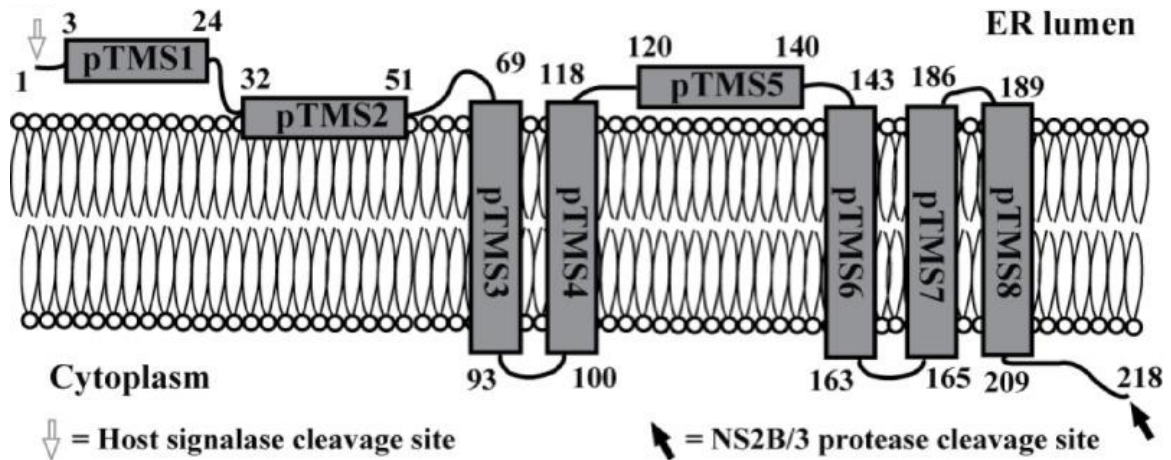


**Fig 5. Membrane topology of DENV NS2A.** A Membrane topology model of DENV-2 NS2A on the ER membrane. The N-terminal 68 residues are located in the ER lumen; pTMS1 does not associate with the membrane, whereas pTMS2 is likely to peripherally associate with ER membrane. pTMS3, pTMS6, and pTMS8 span the membrane from lumen to cytosol, whereas pTMS4 and pTMS7 span the membrane from cytosol to lumen. The C-terminal 9 residues are located in cytosol (37).

The **NS2B** protein is the smallest among the 4 hydrophobic proteins encoded by the genome of the DENV. The molecular weight of NS2B protein is about 15 to 17 kDa that consists of 131 amino acids. In contrast to the other hydrophobic proteins, very little is known about function of NS2B. It has been shown that NS2B amino acid residues position from 67 to 80 directly interact with the NS3 protein and serve as a critical role as a cofactor for NS3 protease activity. In addition, NS2B has shown to interact with the membrane of the endoplasmic reticulum (27). Recently we have demonstrated that NS2B hydrophobic domain has membrane active regions that can modulate the permeability of prokaryotic and eukaryotic membrane. In addition, we have demonstrated that NS2B protein can form self oligomers and form pore like structures in erythrocytes membranes suggesting that NS2B play a role as a viroporin in dengue virus genome (50). In addition, DENV NS2B targets the DNA sensor cyclic GMP-AMP synthase (cGAS) for lysosomal degradation to avoid the detection of mitochondrial DNA during infection and subsequently inhibits type I interferon production in the infected cell (51).

Flavivirus **NS4A** is a small multifunctional hydrophobic protein with a molecular weight of 16 kDa. (38). NS4A colocalizes with double-stranded RNA and promotes membrane rearrangements that harbor viral replication complexes (52). NS4A has identified as a sole mediator to protect cell from cell death during dengue virus infection via activating the PI3K-

dependent autophagy, suggesting a critical determinant of flavivirus replication (53). NS4A is reported to antagonize the host antiviral response defence by recruiting and interacting with eukaryotic initiation factor eIF4AI and escaping the translation inhibition mediated by PKR (54). NS4A has shown to associate with MAVS and prevents the binding of MAVS to RIG-I, resulting in the repression of RIG-I-induced IRF3 activation and, consequently, the abrogation of IFN production (55).

Flavivirus **NS4B** is a hydrophobic protein with molecular weight of 27 kDa that consists of 255 amino acids (56). Recent studies have shown that DENV NS4B protein participates in inhibiting the interferon response, since it block kinases involved in the phosphorylation of STAT-1 and thereby inhibits the signaling cascade (47). NS4B colocalizes with in the replication intermediates and interacts with the NS3 protein, suggesting the involvement of NS4B in viral replication events (57).

## **8. PERMEABILIZATION OF MEMBRANE**

Various evidences have demonstrated the ability of viruses to permeabilize different membranous systems during infection, which further triggers the different mechanisms to allow replication or the propagation of new viral progeny (58)(59)(60)(61). Animal viruses induce changes in the permeability of membranes in 2 well defined moments: 1) During entry of viral particle to the cytoplasm, a number of molecules of different size are capable of entering in the cytoplasm simultaneously with the viral particle, this process is called early permeabilization; 2) Late permeabilization occurs when there is an active translation of viral messenger RNA, whose products are associated with different membranous cell systems and are responsible for modifying the permeability of membranes (62). Molecular events through which viruses modify the permeability of the membranes in late stages of the infection could play an important role in cytopathic and cytolytic mechanisms such as collapse of ionic gradient and apoptosis. One of the main characteristics of late stage permeability is the expression of viral genes. Many of the viral proteins have the ability to associate with the cell membrane systems, those are: 1) glycoproteins which are involved in the mechanisms of entry and stripping; 2) scaffold proteins, which participate in the formation of specialized structures where replication and viral assembly processes occurs 3) viroporins, that are associated with different membranes and participates in modifying the permeability of membranes (62).

## 9. VIROPORINS

The viral proteins that can induce the increase in host cell membrane permeability are classified as viroporins. Viroporins are an emerging class of virally encoded membrane proteins that promote viral entry, penetration, replication and release (62). These proteins modify the integrity of host membranes thereby stimulating the progression of viral infection and are often critical for virus production. Viroporins increase the host cell membrane permeability and balance the disturbance among the corresponding intracellular ions (e.g., Na<sup>+</sup>, K<sup>+</sup>, Ca<sup>2+</sup>, Cl<sup>-</sup>, H<sup>+</sup>) (63)(64)(65)(66). Viroporins also frequently contain basic and aromatic amino acids residues adjacent to the transmembrane domain(s) that help in membrane binding and are sometimes required for ion conductance. In some cases, a single viroporin has been critical for more than one step, demonstrating that these proteins serve multifaceted and versatile functions (67). Several viroporins are described in both enveloped and non-enveloped viruses (Table 1).

**Table 1:** Characterized viroporins in different viruses

FAMILY	VIRUS	VIROPORIN	REFERENCE
PICORNAVIRUS	POLIO VIRUS	2B, VP4, 2BC, 3A	Lama, 1992, Danthi 2003
	COXSACKIE VIRUS	2B	Van Kuppeveld,1997
TOGAVIRIDAE	SINDBIS VIRUS	6K	Sanz M, 2003
RETROVIRUS	HIV-1	VPU, VPR	Gonzalez, 1998
PARAMYXOVIDAE	RESPIRATORY SINTICIAL VIRUS	SH	Perez, 1995
REOVIRIDAE	BLUETONGUE	NS3	Han, 2004
	ARV	P10	Boledon, 2002
FLAVIVIRADAE	HCV	P7, NS4A	Madan, 2008, Carrere-Kremer et al., 2002
	JEV	NS2B, NS2A	Chang, 1999
RHABDOVIRIDAE	BEFV	10P	Mc Milliam, 1997
CORONAVIRIDAE	SAS-CoV	E, 3A	Liao 2006
PAPILLOMAVIRIDAE	VPH	E5	Wetherill 2012
POLYOMAVIRIDAE	JC POLYOMAVIRUS	AGNOPROTEIN, VP4	Suzuki et.al 2010
	SIMIAN VIRUS	VP1,VP2,VP3,VP4	Kristina M et.al, 2008
ORTHOMYXOVIDAE	INFLUENZA VIRUS	M2	Lamb 1985, Pinto 1992

## **9.1 STRUCTURAL CHARACTERISTICS AND CLASSIFICATION OF VIROPORINS**

Viroporins are small proteins with a sequence of about 50 to 140 amino acids. However, some evidences have suggested that viroporin are ever greater in size (68)(69). Viroporins are small, hydrophobic proteins that are able to oligomerize and form channels in membranes to modulate membrane permeability towards small ions and molecules. The insertion of viroporins within membranes, followed by their oligomerisation creates a typical hydrophilic and aqueous channel, with hydrophobic amino acid residues facing the phospholipid bilayer and hydrophilic residues forming part of the aqueous channel pore. Additionally, basic amino acid residues and domains rich in aromatic amino acids disturb the organisation of the lipid bilayer, thus contributing to membrane destabilization (70). Viroporins share some common structural characteristics and signature motifs that are the basis for their identification. (62). Viroporins have the property of being associated with the membranes of the different organelles and further induces the change of membrane permeability once inserted in them (43). Viroporins are virulence factors encoded by diverse families of RNA and DNA viruses of clinical interest that include hepatitis C virus (HCV), human immunodeficiency virus (HIV-1), JC polyomavirus, human papilloma virus (HPV), influenza A virus (IAV), coronaviruses, picornaviruses (polioviruses), and togaviruses (71).

## 9.2 FUNCTIONS OF THE VIROPORINS

Viroporins are multifaceted proteins that exert pleiotropic effects on several viral and cellular processes. The activity of viroporins is not only due to the formation of transmembrane pores as oligomers, but also to their capacity to interact with other viral and cellular proteins. The principal activity of viroporins is to promote virus assembly and egress from infected cells. In general, viruses lacking the viroporin gene are very much weakened and the production of progeny viruses is very low. Viroporins also play an important role in the regulation of antiviral innate immune responses, especially in inflammasome activation, to ensure the completion of the viral life cycle.

### 9.2.1 Membrane permeability

The change in membrane permeability is a common phenomenon observed during the infection of different animal viruses (58)(62). Notably, transgenic expression of the individual viroporin of animal viruses in host cells mimics the membrane permeability phenomenon (62)(58). Their transgenic expression in bacterial, yeast and mammalian cells have helped in analyzing their mode of action, as their expression increases the membrane permeability in different cell types (62)(72)(73). This phenomenon has been evaluated in different cellular or artificial systems. A lot of tests are available to analyze the changes in membrane permeability by analyzing the entrance of ions or small molecules within the cell, or the release of small molecules into the culture medium during the expression of the gene encoding viroporin. One of these tests called "Patch Clamping", which consists of microinjecting viroporin messenger RNA to *xenopus* oocytes and measure the transport of ions with a potential ability of a protein to form pores or channels, as shown for viroporin activity of M2 influenza virus (74). Additionally, the change of permeability in bacterial systems has been evaluated during the expression of viroporin. This protocol involve the use of protein synthesis inhibitor (Hygromycin B), the inhibitory effect of the proteins synthesis occurs only in those bacteria transformed with the plasmid encoding viroporin that form the pore and allows the hygromycin to enter inside the cell and subsequently arrest the protein synthesis (75)(69)(76). The phenomenon of change in membrane permeability due to viroporins was also observed in the liposome and erythrocytes. Finally, results obtained from these tests suggest that the size of the molecules that are transported by the viroporins are about 800 to 1000 Da. In addition, it



is suggested that the ion transport is in favor of a concentration gradient leading to depolarization of the membrane as a result of a change in membrane potential (62)(77)(78).

### **9.2.2 Effects of calcium homeostasis on viral infections**

Calcium is one of the molecules that participate in the signals translation as a second messenger within the cells and regulates diverse cellular processes such as: the activation of receptors, ion channels, enzymes and transcriptional factors. During the virus infection cycle, changes in calcium homeostasis is observed where viral proteins can act as follows: 1) modifying the permeability of the membranes organelles that serve as storage of calcium; 2) viral proteins with calcium binding motifs, which culminates in the activation of these proteins, or the assembly or disassembly of the viral particle; 3) viral proteins interact with cellular factors that are involved in the regulation of cellular calcium, or the signaling pathways that are activated by calcium ion (79). The endoplasmic reticulum is one of the cellular organelles involved in the calcium homeostasis and considered as a main store of calcium. Recent evidence has shown that the flow of ion between the endoplasmic reticulum and mitochondria plays an important role in the activation of cellular mechanisms such as apoptosis, autophagy and the innate immune response. During the virus infections such as enterovirus, poliovirus, coksakivirus, the increased levels of intracellular calcium were found. This phenomenon was observed between 2-4 hours post-infection, which coincides with the *de novo* synthesis of viral proteins. Further experiment shown that transgenic expression of 2B protein of enterovirus have shown to localize in endoplasmic reticulum, mitochondria, Golgi apparatus and the plasma membrane, which are organelles that are involved in calcium homeostasis. Additionally, it was demonstrated that the 2B protein forms homo-multimers that are assembled into the membranes of the endoplasmic reticulum, Golgi apparatus and plasma membrane and forms pores that subsequently alter calcium levels in the cells. Finally, it has been proposed that changes in the calcium homeostasis plays 3 important roles during the infection cycle of the enterovirus: 1) Inhibit the trafficking of intracellular proteins and improve the viral replication, as well as inhibiting the host the antiviral response; 2) Induce an anti-apoptotic activity in the infected cell thereby allowing the assembly of the viral particle; and (3) the alteration of the plasma membrane potential, which would allow the lysis of the cell and subsequent release of the viral particles (79)(80). Additionally, during the first stages

of rotavirus infection, it was observed that NSP4 glycoprotein is widely distributed in the endoplasmic reticulum. Further, Exogenous expression of NSP4 in insect and mammalian cell has demonstrated that NSP4 alters the permeability of endoplasmic reticulum causing an increase in the concentration of cytosolic calcium. (81).

On the other hand, hepatitis C p7 viroporin is a highly hydrophobic protein. Studies have shown that p7 is mainly located in different regions of the endoplasmic reticulum and associated with mitochondria. Various studies using purified protein have demonstrated that p7 are assembled in hexamers on artificial membranes or liposomes. Additionally, it was evaluated whether p7 possesses activity as an ion channel, for the flow of potassium, sodium and calcium, being more selective for calcium ion (82).

### **9.2.3 Reorganization of membranes and vesicular traffic**

To promote replication, many viruses induce a profound reorganization of the intracellular membranes. The participation of the vesicular traffic as well as the different components of lipid metabolism are involved in the reorganization of cell membrane (83). These phenomena have also been reported in cells expressing viroporins such as 2B non-structural protein of picornavirus that carries out the reorganization of membranes when it was expressed exogenously in different cells. Finally, the origin of these new membrane structures is found to generate from the endoplasmic reticulum. In addition, these phenomena have also been reported in other viroporins such as NSP4 from rotavirus, and E protein from coronavirus (67)(73). The process of assembly of the viral particle, occurs mainly in the cytoplasm of the cell where various cellular factors are utilized for this process. Viruses as mentioned above, can modify the morphology of the cellular membranes, as well as its permeability and these phenomenons participate importantly in vesicular traffic during infection. It has been reported that the trafficking of viral and cellular glycoproteins proteins can be delayed by the activity of viroporin such as M2 protein of Influenza virus and p7 protein through a monensin-like “ionophore” activity that promotes proton redistribution in a manner that prevents acidification of intracellular compartments. This loss of acidification can prevent structural modifications or rearrangements of viral glycoproteins. Thus, in some instances viroporin-mediated inhibition of intracellular-vesicle acidification may be important for the production of infectious viral particles(67) .

#### **9.2.4 Induction of apoptosis by viroporins**

Programmed cell death (apoptosis) represents one of the mechanisms for the maintenance, dissemination and eradication of pathogens in infected cells. In this process morphological and biochemical changes occur including reduction in cell volume, chromatin condensation and nuclear fragmentation. Consequently cells eventually become small and generate discrete bodies known as apoptotic bodies. On the other side biochemical changes include loss of structural integrity and bioenergetic of the mitochondrial, activation of catabolic enzymes (proteases of the caspase family, nucleases), exposure of phosphatidylserine on the outer face of the plasma membrane and loss of integrity of the plasma membrane (84). In recent years, a large number of viral proteins have been reported that regulate in a positive or negative manner the apoptotic response during infection. In this regard, viral factors may be classified in one of the following subgroups: 1) pro-apoptotic proteins that are inserted into the mitochondrial membrane, promote mitochondrial membrane permeabilization through amphipathic  $\alpha$ -helices domain; they belong to viroporins 2) pro-apoptotic proteins that indirectly promote the permeability of the mitochondrial membrane by the activation of factors encoded by the host; 3) anti-apoptotic modulators which have sequences BH 1-4 multidomain (also called as Bcl2-viral proteins) 4) anti-apoptotic modulators which inhibit apoptosis by other mechanisms (84).

The mechanism by which viroporins exert apoptotic effect on the infected cell is not fully understood. A study showed that 7 viroporins encoded by different viruses expressed in mammalian cells (SV 6K, MHVA59 E, IAV M2, PV 2B, 3A, HCV p7, NS4A) induced an apoptotic response (85). In that experiment BHK cells were transduced with a set of replicons, which encode different proteins and morphological changes pertaining to apoptosis were observed using TUNEL staining such as DNA fragmentation and presence of apoptotic bodies. Additionally, the processing of eIF4GI and PARP were also observed. Localization of viroporins on mitochondria was determined by immunofluorescence assays, identified the expression of these proteins induces abnormal perinuclear distribution in contrast to control cells. Thus it suggests a package alteration in mitochondrial morphology during the early stages of apoptosis, similar to what observed with the effect of other viral proteins that have viroporin activity (HBx of HBV and E1E4 of HPV). Finally in this study it was shown that the

NS4A, 2B viroporins induce the release of cytochrome C with 50% and 60%, of cells expressing these proteins. Thus this study suggests that the expression of viroporins induce apoptosis by intrinsic pathway (85). Additionally, 2 viroporins (NSP4-Rotavirus and p13-HTVL1) have demonstrated to activate the apoptotic response, and was localized in mitochondria. Additionally, study shown the presence of NSP4 and P13 in the inner mitochondrial membrane. Additionally, it was established that the expression of these proteins causes morphological changes of the mitochondria as well as dissipation of the mitochondrial membrane potential, culminating in the activation of apoptosis (86)(87). The NSP4 protein induces the apoptosis by interacting with proteins such as ATN or VDAC, which are involved in controlling the transition pore of mitochondrial permeability. Although the viroporin activity is not compromised by this interaction, viroporin need the property of insertion to the membranes to fulfill this effect (87). On the other hand, the p13 protein has been shown to have a direct effect on mitochondria extracted from rat hepatocytes. p13 protein has demonstrated to mobilizes potassium ion that controls the potential of the inner mitochondrial membrane. The increased potassium in the mitochondrial matrix, leads to the loss of membrane potential, which culminates in the release of apoptotic factors. Additionally, it was demonstrated that this loss of potential associated with increase of  $K^+$ , and is involved in changes in calcium homeostasis, by mobilizing calcium ion from the endoplasmic reticulum to the mitochondria (88).

### **9.2.5 Viroporins and the viral life cycle**

Viroporins play role from entry to egress of viral particle. IAV M2 viroporin is linked to viral entry (74)(89). During entry, membrane pores are usually formed by viral glycoproteins or capsids, depending on whether the virions are enveloped or not. The formation of pores in endosomes dissipates the proton gradient and propels viral capsids into the cytosol, and it is suggest that it is unlikely that the majority of known viroporins participate in this process (90). In support of this, studies have shown that the entry and infectivity of IAV and HCV are not hindered by the presence of a defective M2 viroporin or in the absence of p7 viroporin, respectively (91)(65)(92). Conversely, a study that examined p7 inhibitor compounds demonstrated that HCV entry is partially impeded in the presence of some of these compounds, suggesting that HCV requires p7 for entry into the cell (93). Although the data are

conflicting, it is proposed that viroporin-mediated permeabilization is generally not required for viral entry, as this is induced by virus particles. Thus, the cell permeabilization that is induced by virus particles appears to have a different function to the permeabilization functions of viroporins (90)(94). Although viroporins participate in different steps of the viral life cycle, such as cell entry and genome replication, the main activity of viroporins is their involvement in virion assembly and the release from infected cells. Viruses, defective in viroporins are unable to accomplish proper assembly and release from cells (67). During the maturation of both enveloped and non-enveloped viruses, the insertion of viroporins in the membrane leads to the dissipation of membrane potential. It is proposed that viroporin insertion breaks the chemoelectrical barrier by conducting ions across membranes, thus dissipating the membrane potential of the plasma membrane or of internal vesicles and thereby stimulating budding (95). Therefore, in enveloped viruses, the dissipation of membrane potential can be coupled to viral release. In the process of budding, membrane fission begins with the formation of a membrane neck, which is followed by self-merging of the inner monolayer of the neck. Subsequent self-merging of the outer monolayer of the neck results in the virus particle pinching off from the plasma or vesicle membrane. Membrane depolarization is accompanied by a reduction in the surface charge density of the membrane, and it has been argued that this reduces the repulsion between contacting monolayers and therefore enhances the contacts that are required for fission (96). In this manner, the production of viruses and vesicles, even those of non-viral origin, is promoted (96)(97). IAV M2 increases proton conductance across the membrane and may act as a Na<sup>+</sup> antiporter; however, there is no pH gradient at the plasma membrane, which is the site of IAV budding (98)(97)(99). M2 localizes at the neck of budding virions and is necessary for this process (100). The role of viroporins are summarized in the Fig. 6 (67).

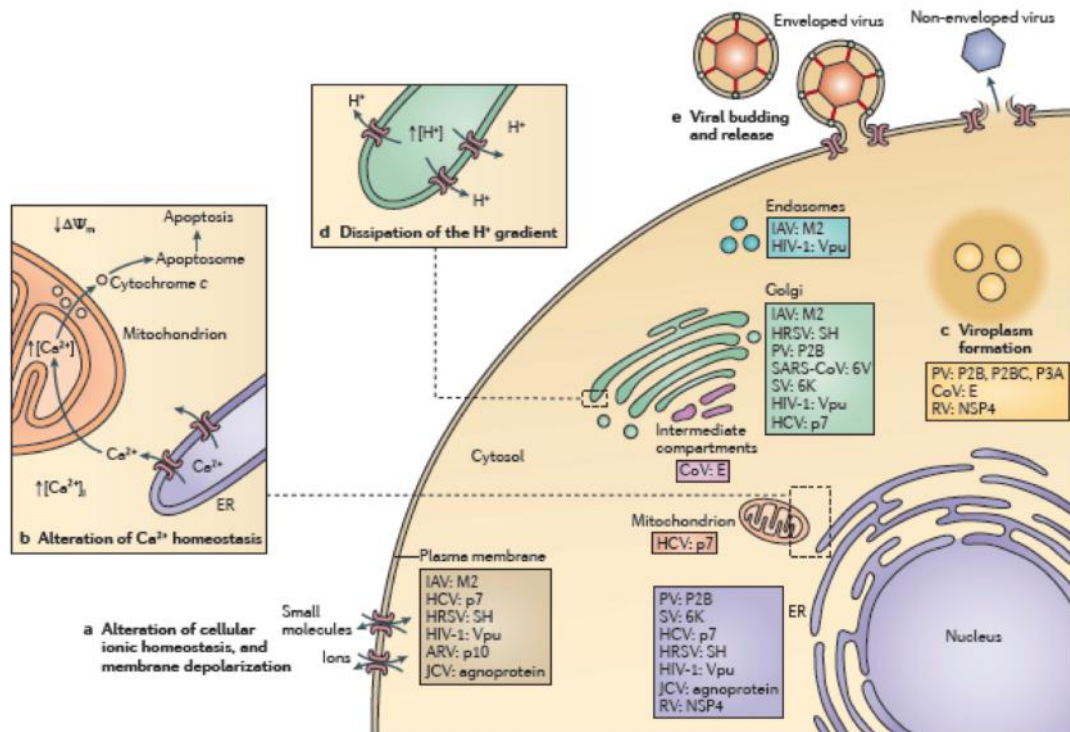


**Fig 6. Viroporins functions during the viral life cycle.** **a** | Alteration of plasma membrane potential. Viroporins that are located at the plasma membrane can dissipate the ionic gradient across the membrane, leading to depolarization. **b** | Alteration of cellular Ca<sup>++</sup> homeostasis. The poliovirus (PV) viroporin protein 2B (P2B) assembles pores in the ER membrane and induces the release of Ca<sup>++</sup> from the ER lumen into the cytosol. Uptake of Ca<sup>++</sup> by the mitochondria can lead to dissipation of the inner-mitochondrial-membrane potential ( $\Delta\Psi_m$ ), permeabilization of the outer mitochondrial membrane and, finally, the release of cytochrome *c*. In the cytosol, cytochrome *c* promotes the formation of the so-called apoptosome, a molecular platform that is involved in apoptosis. **c** | Certain viroporins, such as P2B, polyprotein P2BC and P3A from PV or envelope small membrane protein (E) from coronavirus (CoV), induce intracellular membrane remodelling to generate new membrane vesicles (called the viroplasm) that serve as viral replication sites. **d** | Dissipation of the proton gradient in the Golgi and the *trans*-Golgi network. The viroporins influenza A virus (IAV) matrix protein 2 (M2) and hepatitis C virus (HCV) p7 reduce the acidification of vesicular acidic compartments by equilibrating the proton concentration with the cytosol. Alteration of the intracellular ionic gradient in the vesicular system impairs glycoprotein trafficking. **e** | During the viral replication cycle, viroporins play an essential part in assembly, budding and release of the viral progeny (101).

## **10. ACTIVATION OF INFLAMMASOME**

### **10.1 INFLAMMASOME**

The innate immune system is the first line of defence differentiating ‘self’ from ‘non-self’. To detect and promptly respond to diverse groups of micro-organisms, the innate immune system appoints a range of germline-encoded pattern recognition receptors (PRRs) to detect pathogen-associated molecular patterns (PAMPs), which are conserved microbial components (102)(103). PRRs are expressed by cells of the innate immune system such as macrophages, monocytes, dendritic cells, and neutrophils, as well as epithelial cells and cells of the adaptive immune system. A wide range of PRRs have been characterised, such as retinoic acid-inducible gene (RIG)-I-like receptors (RLRs), Toll-like receptors (TLRs), nucleotide-binding oligomerisation domain (NOD)-like receptors (NLRs), and the absent in melanoma 2-like receptors (ALRs). Among these PRRs, TLRs detect PAMPs in the endosome and extracellular space, whereas NLRs, RLRs, and ALRs play a crucial role in sensing pathogens in the intracellular compartment (Fig. 7) The activation of PRRs results in the initiation of an innate immune response involving a cascade of signalling events that contribute to the differentiation and maturation of immune cells and the secretion of cytokines and chemokines, which also builds a base for the adaptive immune response (104). Cytosolic surveillance is performed by intracellular nucleic acid-sensing PRRs, including RNA-sensing RIG-like helicases (RIG-I and MDA5) and DNA-sensing PRRs (DAI and AIM2). The outcome of PAMP detection by PRRs is determined by the complex interplay between the invading microbe and responding cell. When the helicase domain of either RIG or MDA5 detects viral RNA in the cytoplasm, the caspase recruitment domain (CARD) is exposed to interact with the N-terminal of mitochondrial adaptor protein (MAVS) via its own CARD domain. This CARD–CARD interaction results in the dimerisation of MAVS in the mitochondria to form a protein complex called the MAVS signalosome, which enables the activation of NF- $\kappa$ B and the production of type I interferon (IFN). Once the innate immune system has been activated, it elicits the secretion of cytokines and chemokines, which subsequently induce the expression of adhesion molecules and costimulatory molecules to further activate the adaptive immune

response (105)(106)(107)(108)(109)(110)(111)(112). Among the proinflammatory cytokines, IL-1 $\beta$  is involved in a range of biological processes such as apoptosis, pyroptosis, cell differentiation, proliferation, and regulation of the inflammatory immune response (113). While the production of many proinflammatory cytokines are principally regulated at the transcriptional level, IL-1 $\beta$  and IL-18 require an additional proteolytic event that is regulated in two steps. The first regulatory step is stimulation via TLRs or RLRs, which induces the synthesis of IL-1 $\beta$  and IL-18 as inactive precursors. The second regulatory step involves posttranslational processing; this is required for the secretion and bioactivity of these cytokines and is catalysed by inflammasome activation (Fig. 7) (114)(115)(116). The inflammasome is a multiprotein complex that regulates the autocleavage process, which in turn activates caspase-1 and generates the p10/p20 tetramer. This further converts inactive IL-1 $\beta$  and IL-18 into their active forms (117). The inflammasome plays an important role in the innate immune pathway and regulates at least two protective responses of the host: the secretion of proinflammatory cytokines (IL-1 $\beta$  and IL-18) and the induction of pyroptosis, which is a form of cell death (118)(119)(103). Although several studies have identified diverse inflammasomes with activities against a broad range of pathogens, certain inflammasomes, such as the NLRP3, AIM2, and RIG-I inflammasomes, have been found to be highly specific and important in mediating the host response to viral infection (112,120).



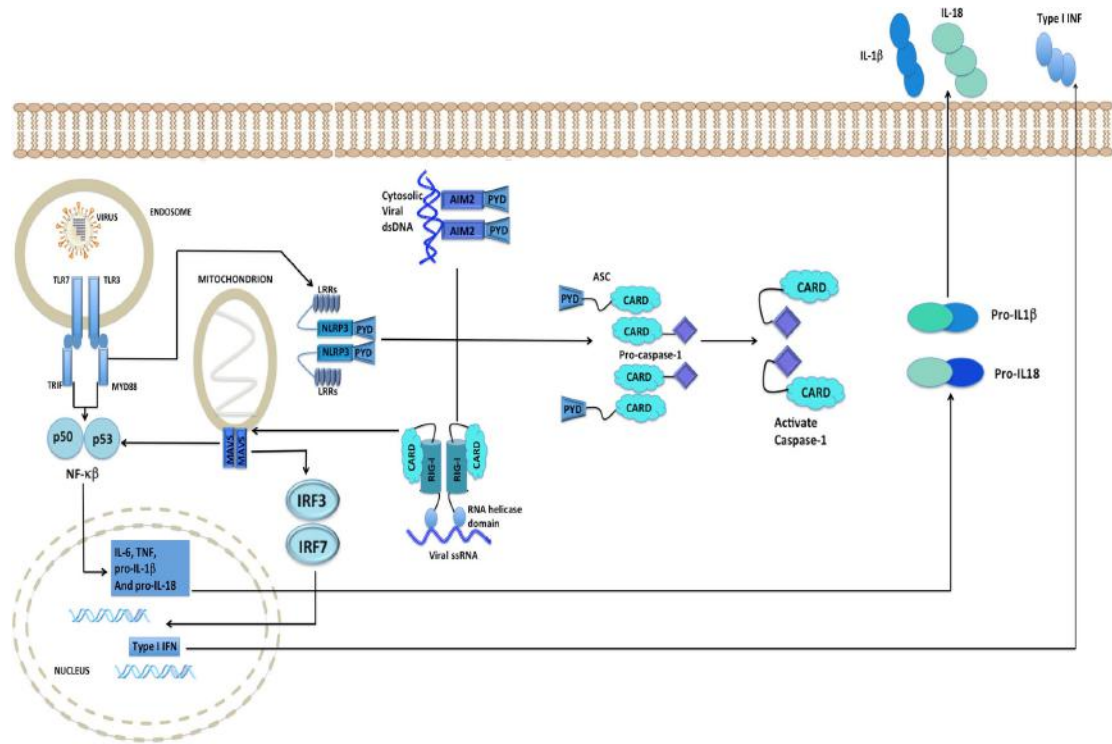


**Fig 7. Molecular sensors associated with the antiviral innate immune response.** Cells susceptible to viral infection have evolved a defence mechanism based on the recognition of pathogen-associated/danger associated molecular patterns (PAMPs/DAMPs) of viral origin, including viral RNA and DNA. The recognition process is mediated by molecules distributed in several cellular compartments and culminates in the activation of NLR proteins and the inflammasome to initiate signalling and the production of proinflammatory cytokines, which leads to the amplification of the antiviral immune response. In the endosome, viral PAMPs are sensed by TLR-7 and TLR-3, and trigger a signal that activates the transcription factor NF- $\kappa$ B to promote the gene expression of cytokines including pro-IL-1 $\beta$  and pro-IL-18. In addition, RIG-1 recognises viral PAMPs via its helicase domain and further interacts with adapter proteins localised in mitochondria such as virus-induced signalling adapter, which contains CARD domains. This signalling culminates in the phosphorylation and activation of transcription factors such as IRF3 and IRF7, which in turn induce the transcription of type I IFN and the production of IL-1 $\beta$ . Finally, after recognizing viral PAMPs and DAMPs, NLRs (NLRP3) and AIM2 self-oligomerise and, via their PYD domains, recruit adapter molecules such as ASC that contain caspase recruitment domains. This mechanism triggers the activation of caspase-1, which processes pro-IL-1 $\beta$  and pro-IL-18 into their active forms (121).

### 10.1.1 NLR family

The innate immune system is able to respond promptly against invading pathogens as a first line of defence. Sensing of microbial pathogens by the innate immune system relies on the specific host-receptor detection of their molecular signatures, which comprise PAMPs and danger-associated molecular patterns (DAMPs). Host PRRs are germline-encoded and include a number of families of leucine-rich repeat (LRR)-bearing proteins in plants and animals. Recent studies have identified 2 protein families, the RIG-like helicases (RLHs) and the NLRs, that perform intracellular scrutiny for PAMPs and DAMPs, while the Toll-like receptors (TLRs) comprise key sensors for extracellular microbe detection (122)(123)(124). Furthermore, numerous NLR family proteins stimulate innate and adaptive immune responses (125). NLRs initiate host defence after recognising microbial products or intracellular danger signals, through the activation of the NF- $\kappa$ B response and inflammatory caspases (126). NLRs are characterised as central molecular platforms that establish signalling complexes such as inflammasomes and NOD signalosomes. Structurally, the members of the NLR family are multi-domain proteins composed of a common central NOD domain, C-terminal LRRs, and N-terminal caspase recruitment (CARD) or pyrin (PYD) domains. LRRs play crucial role in the processes of ligand sensing and autoregulation that initiate NLR signalling, whereas the CARD and PYD domains mediate homotypic protein-protein interactions for downstream signalling (127)(128). Thus, the active multiprotein signalling platform (e.g. the inflammasome or nodosome) is formed by oligomerisation of the NACHT domains (which is present in all NLR family members) in an ATP-dependent manner, which further allows the attachment of adaptor molecules and effector proteins, eventually leading to an inflammatory response (128)(129). Members of the NLR family have been further classified into 3 subfamilies based on the sequences of their NACHT domains: NODs (NOD1–2, NOD3/NLRC3, NOD4/NLRC5, NOD5/NLRX1, CIITA), NLRPs (NLRP1–14, also called NALPs), and IPAF (NLRC4 and NAIP) (Fig 8).

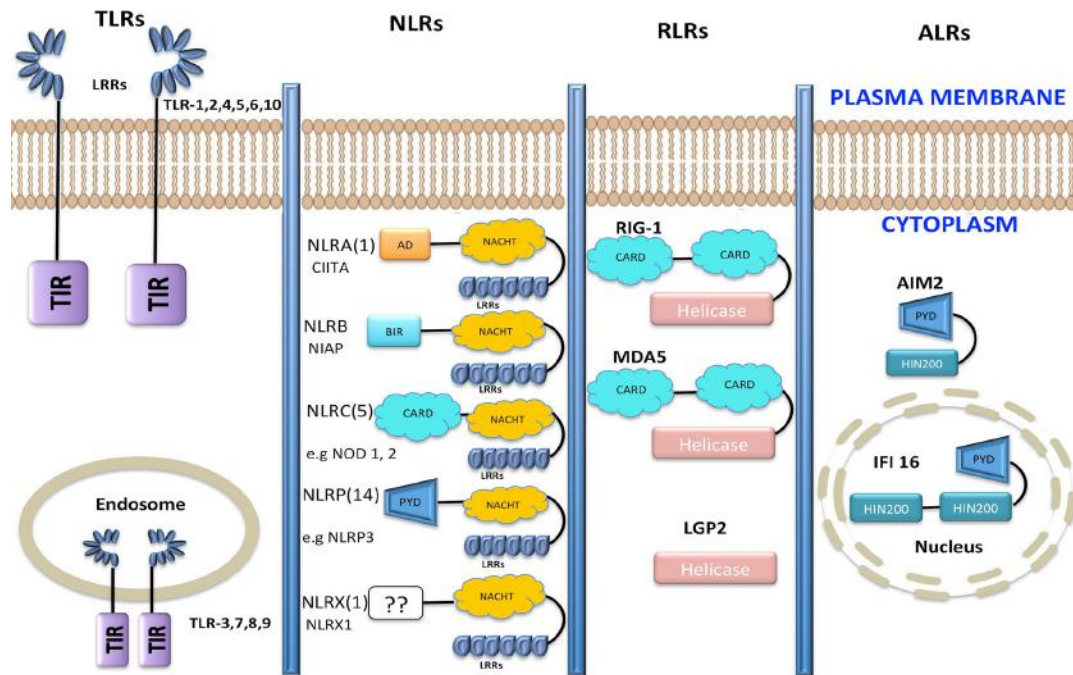


**Fig. 8 Domain organisation and cellular localization of pattern recognition receptors.** Toll-like receptors (TLRs), NOD-like receptors (NLRs), RIG-I-like receptors (RLRs), and AIM2-like receptors (ALRs) are displayed with their cellular localisation. TLRs are confined to the plasma membrane and endosomes. TLRs comprise leucine-rich repeat (LRR) domains and a Toll/interleukin-1 receptor (TIR) domain that facilitates downstream signalling. NLRs are present in the cytosol and are classified into five subfamilies based on their effector domain. Structurally, NLRs contain an N-terminal effector domain, a NACHT domain, and LRR domains. The effector domain can be an acidic activation domain (AD), baculovirus IAP repeat (BIR) domain, caspase recruitment domain (CARD), pyrin domain (PYD), or a domain without homology to other NLR subfamily members. RLRs are expressed in the cytoplasm and consist of CARD domains and an RNA helicase domain, except for LGP2, which lacks CARD domains. ALRs are localised in the cytoplasm and nucleus; they consist of a PYD domain and a certain number of HIN200 domains, which bind dsDNA (121).

## **10.1.2 Inflammasome activation during viral infection**

### **10.1.2.1 NLRP3 inflammasome**

The NLRP3 inflammasome is the best studied inflammasome and seems to be activated by many families of viruses, suggesting a common pathway for viral detection and response by the host cell (130). The structural arrangement of NLRP3 (the order of its domains from *N*-terminus to *C*-terminus) is PYD–NOD–LRRs. Structurally; the NLRP3 inflammasome comprises the adaptor protein apoptosis-associated speck-like protein containing CARD (ASC) and procaspase-1. NLRP3 forms a homo-oligomer during activation via its NOD domain and further interacts with ASC through its PYD domain. ASC, in turn, interacts with procaspase-1 through its CARD domain, forming the complete NLRP3 inflammasome complex (131). The activation of NLRP3 inflammasome leads to the activation of caspase-1 and the production of mature IL-1 $\beta$  and IL-18 (132). For its full activation, the NLRP3 inflammasome requires 2 signals. The first signal (priming signal) can be produced by receptors of the TLR, NLR, or RIG-I-like receptor (RLR, or by a cytokine receptor; this first signal leads to transcriptional activation of the genes encoding pro-IL-1 $\beta$  and pro-IL-18 (133). The second signal arises from the different stress signals associated with host cell/tissue damage [(134)]. Three key mechanisms are associated with NLRP3 inflammasome activation (Figure 10). Firstly, NLRP3 activators such as alum, silica, nigericin, and asbestos stimulate the production of reactive oxygen species (ROS) by nicotinamide adenine dinucleotide phosphate (NADPH) oxidase, which stimulates an efflux of potassium ions (K<sup>+</sup>) leading to the activation of NLRP3 inflammasome (135)(136). The second mechanism is the “lysosomal rupture model” in which NLRP3 activators (silica, asbestos, etc.) primarily form aggregates, which are phagocytosed and induce the release of cathepsin B by lysosome rupture. Released cathepsin B further activates NLRP3 (135). Lastly, the “ion channel model” posits that a high concentration of extracellular ATP can induce the formation of cell membrane pannexin-1 pores and K<sup>+</sup> efflux through the P2X7 ATP-gated ion channel, assisting the influx of PAMPs and DAMPs, which play a crucial role in NLRP3 activation (137). However, intracellular ion fluxes have been found to be the most crucial danger signal and amplify inflammasome recruitment. Several studies have demonstrated that in response to a broad range of stimuli, including ultraviolet light irradiation, membrane

attack complex (MAC) formation generates pores that allow the influx of calcium ions ( $\text{Ca}^{2+}$ ), which increases the cytosolic  $\text{Ca}^{2+}$  concentration (138)(139)(140). Further  $\text{Ca}^{2+}$  accumulation in the mitochondrial matrix leads to the loss of mitochondrial membrane potential, triggering NLRP3 activation and secretion (141). In addition,  $\text{K}^+$  efflux has also been shown to trigger inflammasome activation in response to several stimuli including mitochondrial and lysosomal damage, ROS, and extracellular  $\text{Ca}^{2+}$ . These findings indicate that inflammasomes are stringently regulated by intracellular ion concentrations and ion imbalances serve as the central trigger for their activation (142). A growing body of evidence regarding the mechanisms of inflammasome activation suggests that in several viral infections, viral products such as viroporins may alter cell membrane permeability and change the ionic milieu of cell membranes. Such changes in the properties of the cell membrane can play a significant role in NLRP3 inflammasome activation (Figure 9) (143)(144).

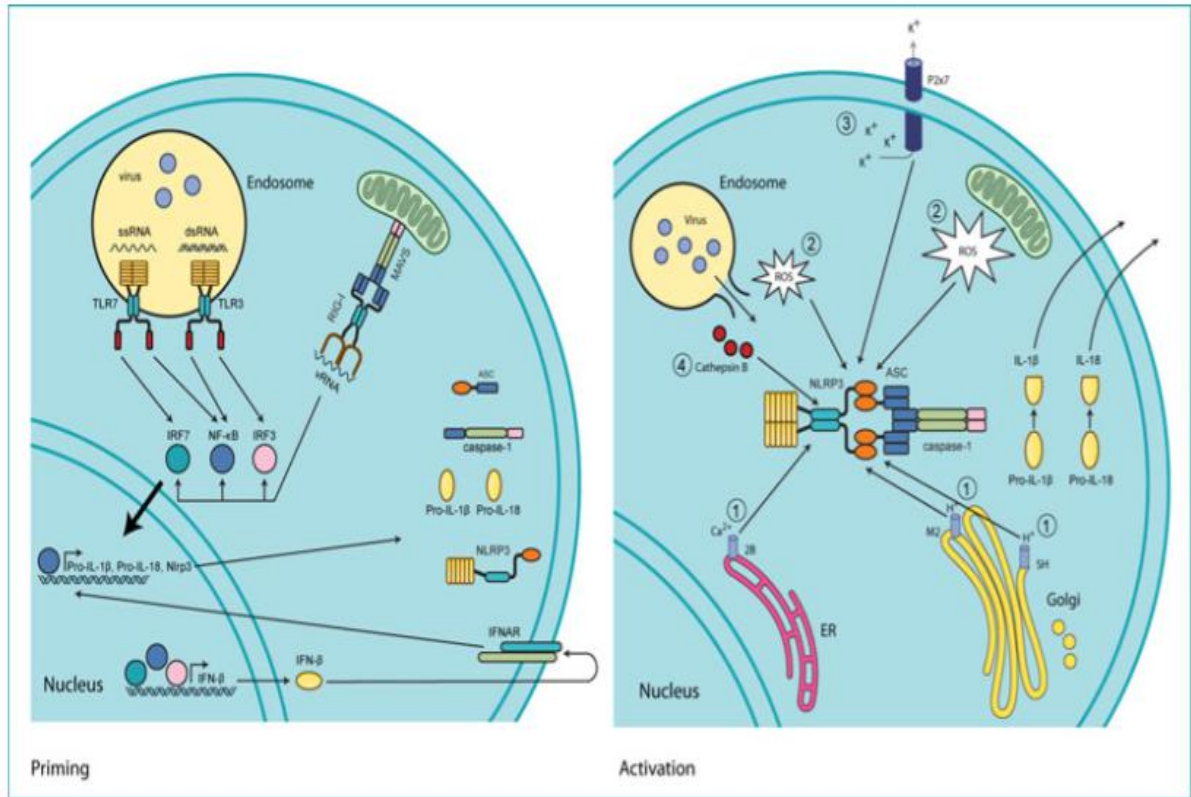


**Fig. 9 Mechanisms of virus mediated NLRP3 activation.** (Priming) During virus infection, viral genomic RNA (vRNA) consisting of either single-stranded RNA (ssRNA) or double-stranded RNA (dsRNA) is recognized by endosomal (TLR3 or TLR7) or cytoplasmic (RIG-I) pattern recognition receptors. This activates the transcription factor NF-κB and induces the production of inflammasome components and substrates like NLRP3, pro-IL-1β, and pro-IL-18, thus ‘priming’ the inflammasome for activation. Similarly, transcription factors IRF3 and IRF7 induce the expression or type I interferons, like IFN-α and IFN-β, which then feedback through the type I IFN receptor (IFNAR) to induce production of the same components and substrates NLRP3, pro-IL-1β and pro-IL-18. (Activation) Following priming, the NLRP3 inflammasome is assembled and activated in response to virus-induced damage-associated molecular patterns (DAMPs). Four main sources of DAMPs exist. (i) Virus-encoded viroporins like M2, SH, and 2B allow for ion leakage from intracellular organelles into the cytosol; (ii) The generation of reactive oxygen species resulting from PRR signaling, ER, and mitochondrial stress, or virus-induced damage to endosomes; (iii) The P2x7 ion channel is opened in response to extracellular ATP from damaged or necrotic cells allowing for potassium efflux; and (iv) During entry, virus infection damages endosomes and releases proteases such as cathepsin B into the cytosol (145).

#### 10.1.2.1.1 RNA viruses

Cumulative work has demonstrated that many RNA viruses are able to activate “the NLRP3 inflammasome”. The first evidence came from an *in vitro* study on flock house virus, rotavirus, Sendai virus, and influenza A virus, which demonstrated that viral dsRNA activates caspase-1 in murine macrophages (146). Later, other RNA viruses, such as encephalomyocarditis virus (EMCV) and vesicular stomatitis virus (VSV), were studied in murine dendritic cells (DCs) and macrophages, and the results indicated that IL-1 $\beta$  secretion was NLRP3-dependent (147). Further, no production of IL-1 $\beta$  was observed when the cells were incubated with ultraviolet light-treated (i.e., inactivated) virions, suggesting that inflammation activation requires viral replication. Moreover, the survival rates of caspase-1-deficient and wild-type mice did not differ upon infection with EMCV and VSV, indicating the minor role of IL-1 $\beta$  in the host defence against these viruses (147). Recently, it was shown that EMCV viroporin 2B, but not viral RNA, can activate the NLRP3 inflammasome (148). Upon the expression of EMCV viroporin 2B, NLRP3 was redistributed to the perinuclear space, where it colocalize with viroporin 2B. In addition, viroporin 2B increases the Ca<sup>2+</sup> concentration in the cytoplasm, promoting IL-1 $\beta$  secretion (148). Measles virus infection was found to activate the NLRP3 inflammasome in THP-1 cells, resulting in the secretion of IL-1 $\beta$  (149). Human rhinovirus (HRV) and its viroporin 2B protein activate the NLRP3 and NLR family CARD-containing 5 (NLRC5) inflammasome [(150)]. When bronchial cells were infected or transfected with HRV and its viroporin 2B protein, respectively, NLRP3 was found to interact with NLRC5 and ASC and colocalised with viroporin 2B and NLRC5 in the Golgi apparatus. Viroporin 2B of HRV leads to the activation of NLRP3 inflammasome by increasing the cytosolic Ca<sup>2+</sup> concentration as treatment with BAPTA-AM (a Ca<sup>2+</sup> chelator) and verapamil (a Ca<sup>2+</sup> channel inhibitor) blocks HRV-induced IL-1 $\beta$  release and caspase-1 activation [(150)]. Previous studies in Huh7.5 hepatoma cells or THP-1 macrophages demonstrated that hepatitis C virus (HCV) induces IL-1 $\beta$  production and NLRP3 inflammasome activation in a ROS and K<sup>+</sup> channel-dependent manner (151)(152). More specifically, it has been shown that HCV genomic RNA and viroporin P7 protein activate inflammasome activation, and its activation was found to be ASC- and NLRP3-dependent (153). Among all RNA viruses, influenza virus is the best studied in

regards to its capabilities to interact with and activate the NLRP3 inflammasome (154)(155). Studies investigating the role of the NLRP3 inflammasome in the development of the adaptive immune response have yielded controversial results; the development of adaptive immunity was found to be mainly dependent on inflammasome activation, but was NLRP3-independent (156) (157). Recently, studies on the mechanism underlying NLRP3 activation during influenza virus infection have suggested that the priming signal for activation of the NLRP3 inflammasome is provided following the recognition of viral RNA by TLR7, with subsequent IL-1 $\beta$  production (158). Influenza virus provides the second signal for NLRP3 inflammasome activation by inserting its ion channel protein M2 into the trans-Golgi network. This disturbs the ionic milieu, leading to K<sup>+</sup> efflux and ROS production, and ultimately resulting in the activation of the NLRP3 inflammasome (158). In addition, secretion of IL-1 $\beta$  and IL-18 by blood bone marrow-derived macrophages (BMMs) was observed when the cells were infected with wild-type influenza virus, but not when they were infected with a mutated influenza virus expressing non-functional M2 protein. Furthermore, lipopolysaccharides-primed BMMs and blood bone marrow derived DCs were found to activate the NLRP3 inflammasome when they were transduced with a recombinant lentivirus expressing the M2 protein. Therefore, it has been suggested that the ion channel activity of M2 protein plays a crucial role in the activation of the NLRP3 inflammasome [(158)]. Other RNA viruses, such as respiratory syncytial virus (RSV), have been found to activate the NLRP3 inflammasome, resulting in the activation of caspase-1 and release of IL-1 $\beta$ . In this case, NLRP3 inflammasome activation was ROS and K<sup>+</sup> efflux-dependent [(159)]. Additionally, one study demonstrated that viroporin SH from RSV provides the second signal for activation of the NLRP3 inflammasome; a mutant RSV lacking the viroporin SH gene was unable to induce caspase-1 maturation and IL-1 $\beta$  release, in contrast with the wild-type RSV. Further, treatment with 5-(*N,N*-hexamethylene)amiloride, which is an inhibitor of the HCV p7 channel, together with a Na<sup>+</sup>/H<sup>+</sup> ion channel inhibitor was shown to inhibit the secretion of IL-1 $\beta$  (160). These findings suggest that NLRP3 can be activated by virus-encoded viroporins due to their ability to disrupt the cellular ion balance. In the context of human immunodeficiency virus (HIV) infection, NLRP3 inflammasome activation was observed during the early onset of the HIV disease and HIV infection has been shown to



activate the NLRP3 inflammasome and IL-1 $\beta$  secretion in DCs from healthy individuals, but not in those from HIV-positive individuals (161). In addition to the aforementioned viruses, several other RNA viruses have been reported to activate the NLRP3 inflammasome.

A recent study on mice infected with West Nile virus (WNV) demonstrated that the infection is able to induce IL-1 $\beta$  secretion, caspase-1 maturation, and ASC expression. (162)(163). Additionally, mice infected with other members of the Flavivirus family, such as Japanese encephalitis virus, show IL-1 $\beta$  and IL-18 secretion and caspase-1 maturation in an NLRP3-dependent, K<sup>+</sup> and ROS-mediated manner. Furthermore, NLRP3 depletion results in reductions of caspase-1 activity and of IL-1 $\beta$  and IL-18 secretion (164). Dengue virus (DENV) also induces the NLRP3 inflammasome in infected platelets *in vitro* and in those obtained from DENV-infected patients. This activation was found to be ROS and K<sup>+</sup> channel-mediated. IL-1 $\beta$  secretion from platelets plays a crucial role in increased human microvascular endothelial cell permeability *in vitro* and also vascular permeability in clinical cases (165). Further investigation regarding the mechanism of inflammasome activation by DV demonstrated that C-type lectin domain family 5 member A (CLEC5A) interacts directly with DENV, triggering NLRP3 inflammasome activation (166). In addition, Rift Valley fever virus (RVFV) also induces the formation of an inflammasome complex containing NLRP3 and MAVS-dependent inflammasome in which MAVS localizes with NLRP3 during the RVFV infection and, and knockout mice showed a reduced production of IL-1 $\beta$  in bone marrow-derived DCs infected with RVFV (167). Recently, a study on human chikungunya virus (CHIKV) infection showed a high expression of NLRP3 and caspase-1 activation that led to the secretion of IL-1 $\beta$  (168).

## 10.2 Viroporins in inflammasome

Although multiple virus-encoded proteins exhibit viroporin properties, the involvement of these viroporins in the activation of the NLRP3 inflammasome is rarely reported. These proteins mainly include Respiratory syncytial virus (RSV) small hydrophobic (SH) protein, Influenza virus M2 protein, Rhinovirus 2B protein, Encephalomyocarditis virus (EMCV) 2B protein and Hepatitis C virus (HCV) p7 protein (169). Multiple lines of evidence suggest that changes in cytoplasmic ions result in NLRP3 activation by viruses. During influenza virus infection, genomic RNA stimulate TLR7 signaling and pro-IL-1 $\beta$  transcription, M2 protein of the influenza virus was necessary as a second signal to stimulate the activation of the NLRP3 inflammasome (170). Furthermore, the M2 protein help in IAV uncoating in endosome by allowing the entry of protons into virions. The M2 protein not only exhibits viroporin properties but also regulates the pH balance between the lumen of the trans-Golgi complex and the cytosol; as a result, the acidity of intracellular vesicles and the acidity inside the organelles are reduced. Wild-type influenza virus was shown to activate inflammasome and secretes IL-1 $\beta$  and IL-18 in infected host cells, and a recombinant retrovirus expressing the M2 protein was demonstrated to activate the NLRP3 inflammasome in LPS-stimulated cells. The histidine 37 residue in the transmembrane domain of the M2 protein was found critical for the proton selectivity of the M2 protein. Retrovirus harboring a mutation at histidine 37 residue position shows that the levels of IL-1 $\beta$  induced by this mutant recombinant virus were higher than those of the wild-type M2 recombinant retrovirus. Moreover, the secretion of IL-1 $\beta$  and the accumulation of the M2 protein in the golgi apparatus were significantly enhanced in the cells infected by the wild-type influenza strain in the presence of monensin (a Na<sup>+</sup>-H<sup>+</sup> anti porter in the trans-Golgi network). In addition golgi apparatus-disrupting drug brefeldin A blocked the secretion of IL-1 $\beta$  and induce the M2 protein to localize in the endoplasmic reticulum. Therefore, the cellular localization and the biological activity of the M2 viroporin were involved in NLRP3 inflammasome activation (170). Study demonstrated a role of RSV in activating inflammasome and producing IL-1 $\beta$ . In vitro, RSV was demonstrated to trigger the activation of the NLRP3/ASC inflammasome via the following mechanisms: after host cells were infected, TLR2/myeloid differentiation primary response 88 (MyD88)/nuclear factor  $\kappa$ B (NF- $\kappa$ B), which was the first signal, was activated; afterward, the NLRP3/ASC

inflammasome, together with the second signal from ROS and a potassium current, was activated. Both signals induce caspase-1 activation and subsequent IL-1 $\beta$  secretion (171). The RSV SH protein is a viroporin that can enhance membrane permeability and promote the entry of ions and small molecules into host cells through the membrane pores formed by its oligomers. An SH-deficient RSV mutant could not induce the activation of the NLRP3/ASC inflammasome and the subsequent secretion of IL-1 $\beta$ ; as such, the RSV SH was necessary to activate the NLRP3 inflammasome. RSV-infected cells can be treated with drugs that inhibit viroporin activity; the treatment also suppressed inflammasome activation. This result suggests that SH viroporin or lipid rafts are involved in inflammasome activation. After RSV infects host cells, the RSV SH protein accumulates in the lipid rafts of the Golgi apparatus, thereby forming a positive ion-permeable specific pore. These positive ion fluxes induce the transport of NLRP3 from the cytosol to the Golgi apparatus and promote the NLRP3 activation. However, these studies have confirmed the involvement of SH viroporin in inflammasome activation on the basis of this phenomenon (172). EMCV viroporin 2B also plays an important role in NLRP3 inflammasome activation. EMCV viroporin 2B has shown to induce IL-1 $\beta$  release and distribute the localization of NLRP3 and co-localize with NLRP3 in the perinuclear space. The calcium ion channel activity of the 2B protein in the endoplasmic reticulum and the Golgi apparatus was necessary for IL-1 $\beta$  secretion. In addition, thapsigargin and the Ca<sup>++</sup> ionophore ionomycin significantly increased the calcium concentration in the cytosol and further induced IL-1 $\beta$  release into EMCV-infected cells. By contrast, the calcium chelator BAPTA-AM inhibited IL-1 $\beta$  release induced by EMCV infection or 2B protein expression(173). Human rhinovirus (HRV) infection or 2B protein expression has shown to induce NLRP3-dependent caspase-1 cleavage and IL-1 $\beta$  production. In respiratory tract cells, which are either infected by HRV or transfected with the 2B protein alone, NLRP3 binds to NLRC5 and ASC, which is co-localized with NLRC5 and the 2B protein in the Golgi apparatus (174). 2B mediated secretion of IL-1 $\beta$  were inhibited in the presence of Brefeldin A. In addition, cells infected with HRV in the presence of BAPTA-AM or verapamil significantly inhibited the IL-1 $\beta$  release and caspase-1 activation(174). Hepatitis C virus (HCV) has shown to activate NLRP3 inflammasome and induces IL-1 $\beta$  production in hepatoma Huh7.5 cells or THP-1 macrophages cells (175)(176). The ROS inhibitor

diphenyliodonium and the potassium channel inhibitor glibenclamide blocked HCV-induced IL-1 $\beta$  production. The genomic RNA of HCV and p7 viroporin also triggers NLRP3 inflammasome activation; this genomic RNA also induces the oligomerization of ASC and the maturation of caspase-1 in THP-1 cells via NLRP3 (175). In continuation, production of IL-1 $\beta$  was blocked in the presence of the ROS inhibitor in a dose-dependent manner. Therefore, HCV induces NLRP3 inflammasome activation via the genomic RNA of HCV and the ROS model (177). More recently, the pore-forming protein from other viruses has been shown to regulate NLRP3 inflammasome activation. The 2B protein from several picornaviruses, including poliovirus and enterovirus 71 were shown to induce NLRP3 cytoplasmic relocation and inflammasome activation in an intracellular Ca<sup>++</sup>-mediated manner (169). The fact that viroporin proteins from five different viruses are capable of NLRP3 activation strongly indicates that this is a common mechanism of virus sensing by the NLRP3 inflammasome. There is a list of viruses reported to activate NLRP3 through viroporin or unknown factor depending manner (Table 2) (178). In summary, the viroporin activity of viruses can disrupt the balance of intracellular ion concentration. Responses to this imbalance activate the NLRP3 inflammasome. However, ion channel protein blockers affect this activation process. Hence, viroporins can represent a novel group of molecules that activate the NLRP3 inflammasome. Specific viroporin blockers or ion chelators can be used as effective antiviral drugs.

**Table 2:** Inflammasomes activated by viroporins

PRR	Virus	Activator	Possible mechanisms involved in activation
NLRP3	Influenza virus	M2 viroporin, PB1-F2, and vRNA <sup>a</sup>	Mitochondrial biological function [ $\Delta\Psi(m)$ ] and Mfn2, H <sup>+</sup> , cathepsin B, and ROS
	EMCV	2B viroporin	Mitochondrial biological function [ $\Delta\Psi(m)$ ] and Mfn2, Ca <sup>2+</sup> flux
	HRV	2B viroporin	NLR5 and Ca <sup>2+</sup> flux
	RSV	SH viroporin	Monovalent cation
	HCV	vRNA	ROS and K <sup>+</sup> efflux
	JEV		ROS and K <sup>+</sup> efflux
	Sendai virus		MAVS
	RVEV		MAVS
	Dengue virus	?????	CLECSA
	HSV-1, VSV, WNV, rabies virus, and VACV Ankara	??	
NLRP1	LCMV		
AIM2	VACV and mCMV	dsDNA	
RIG-I	Influenza virus	dsRNA replication intermediates	MAVS, type I IFN, and IFNAR1
	VSV	dsRNA replication intermediates	K <sup>+</sup> efflux

## **11. Activation of inflammasome by DENV**

Endogenous pyrogens (ex. IL-1 $\beta$ ) that are induced during dengue virus infection cause the fever, the primary symptom during the infection (179). IL-1 $\beta$  has been shown to be regulated by caspase-1 through the activation of inflammasome complex ((180)). Among EPs, IL-1 $\beta$  and TNF- $\alpha$  play a vital role in inducing fever in host (181)(182). Proinflammatory cytokine IL-1 $\beta$  has shown to play a crucial role during DENV infection as IL-1 $\beta$  has demonstrated to increase the endothelial permeability, dysregulated hemostasis and thrombosis (181)(182)(183)(184)(185)(186). Although dengue virus pathogenesis is not fully exposed, recent evidence supports a central role for proinflammatory cytokines in endothelial activation and plasma leakage during DV infection (179)(187)(188). As thrombocytopenia is detected in mild and severe forms of DENV infection, the role of platelet activation in dengue pathogenesis has demonstrated by increasing the expression of IL-1 $\beta$  in platelets and platelet-derived microparticles from patients with dengue or after platelet exposure to dengue virus in vitro. Further, microparticle released through the activation of NLRP3 inflammasome and caspase-1-dependent IL-1 $\beta$  secretion by platelets during DENV infection. Inflammasome activation and platelet shedding of IL-1 $\beta$ -rich microparticles correlated with signs of increased vascular permeability. Moreover, microparticles from DENV-stimulated platelets induced enhanced permeability in vitro in an IL-1 $\beta$  dependent manner (M.-F. Wu, 2013)(Hottz et al. 2013). In addition, study reported the increased caspase-1 gene expression in DV-infected cultured cells (189). In addition, DENV has shown to induce high levels of IL-1 $\beta$  and IL-18 from GM-M $\Phi$  (inflammatory macrophage) and cause cell death (pyroptosis). Moreover, up-regulation of proIL-1 $\beta$ , pro-IL-18, and NLRP3 associated with caspase-1 activation was observed in DENV-infected GM-M $\Phi$  whereas blockade of CLEC5A/MDL-1, a C-type lectin critical for dengue hemorrhagic fever and Japanese encephalitis virus infection, inhibits NLRP3 inflammasome activation and pyroptosis in GM-M $\Phi$ (190). Altogether, these observations indicated that inflammasome activation may play critical roles in the pathogenesis of DENV infection. However, the molecular mechanism through which DV activates inflammasome is still elusive till date.

## **BACKGROUND WORK**

Dengue virus infects host cells and causes cytopathic effect. During infection, DENV induces host cell membrane rearrangement, reorganization as well as changes in the membranes permeabilization that strongly involved in the replication and processing of the viral polyprotein. However, it's unknown whether any of dengue virus proteins involved in membrane permeabilization for such an effect (191). Furthermore apoptosis has been implicated as a cytopathology mechanism in response to infection with DENV. Several studies have identified viral proteins responsible for activating apoptosis during infection. M protein of DENV-4 and other members of the flavivirus, has identified in a study that M protein ectodomain (amino acids 1-40) activates apoptotic mechanisms in mouse neuroblastoma cells and human hepatoma cells. Our group have demonstrated the activation of apoptosis by demonstrating the activation of caspase 3 and proteolytic cleavage of PARP-1 due to NS2B-NS3 (192). Thereby, it is suggested that during infection these proteins could activate apoptotic pathways in order to alter vascular permeability and thus produce manifestation associated with pathogenesis of the disease. Regarding to other pathologic effects caused by viral proteins, the viroporins have been demonstrated to play several important role during different steps in virus life cycle including virus entry, replication, egress, as well as in causing apoptosis and inducing innate immune response by causing the permeability of the host membranes and changing the ionic milieu of the host cell (67). Different flaviviral proteins have been characterized as viroporins as example hepatitis C (p7, NS4A) and japanese encephalitis virus (NS2A, NS2B, NS4A, NS4B) (85)(35). The latter belongs to the DENV family for which any of the proteins identified in the Japanese encephalitis virus could behave similar in DENV. Although, studies regarding the functions of hydrophobic proteins from DENV and JEV are not sufficient, however their proteins share similar physicochemical properties, suggests a common function. Our group has showed that NS2B protein of DENV-2 behaves as a viroporin. NS2B protein of DENV was characterized and demonstrated that NS2B protein allows Hygromycin B (cell membrane impermeable, protein translator inhibitor) by forming the pores to cell, which inhibited both, cellular and viral protein synthesis in infected cells. Additionally, over expression of the DENV NS2B protein induced permeability changes in an inducible *E.coli* system. In continuation, it was

illustrated that purified NS2B protein was able to modify the permeability of erythrocyte membranes resulted in the assembly of oligomeric structures, which resembles as pore (50). Finally apoptosis activity of NS2B was observed and demonstrated that NS2B partially localized with the mitochondria and activated caspase 9, caspase 3, and PARP. Therefore these results demonstrated that DENV-2 NS2B protein behaves as a viroporin and causes apoptosis in intrinsic mediated pathway.

Multiple lines of evidence suggest that viroporins activates NLRP3 Inflammasome by changing cytoplasmic ion concentration. Specifically, it has shown that viroporin were enough to activate inflammosome and it was necessary for virus to induce inflammasome (178). Additionally, it have been shown that viroporin interacts with mitochondria and induce the disruption of mitochondrial membrane potential (85). Disruption in mitochondria induces ROS that further triggers NLRP3 activation (193). In dengue virus infection, it has reported that DENV infection leads to assembly of NLRP3 inflammasomes, activation of caspase-1, and IL-1 $\beta$  secretion (194). As mentioned above JEV NS2A that shares structural and functional activity with DENV NS2A has also demonstrated to behave as a viroporin with membrane permeability capacity. Therefore it will be relevant to evaluate the role of DENV NS2A, which could behaves as viroporin and could be responsible for activation the inflammasome in DENV infection and impart a significant role in dengue virus pathogenesis.

## **JUSTIFICATION**

Cumulative studies or evidences have provided the information regarding to the structure, life cycle and pathogenesis of disease caused by the dengue virus. One of the most prominent features of flavivirus infection is a dramatic proliferation of intracellular membranous structures, including rough endoplasmic reticulum (RER) and golgi complex, within which virus particles accumulate. DENV is known to hijack the host cellular machinery by increasing plasma membrane permeability, remodelling of host cell membrane, causing a loss of cellular ion gradients and leakage of essential compounds from the cell, which leads to apoptosis. Growing body of evidences indicate that the expression of one single gene from certain animal viruses is sufficient to modify membrane permeability. These viral proteins are called viroporins. Reported viroporins have shown specific characteristics such as small hydrophobic protein, potential membrane-spanning hydrophobic domains as well as stretch of basic and aromatic amino acids. During DENV infection, DENV induces several cyto-pathological events such as apoptosis by viral protease (NS2B-NS3) and M protein. These proteins triggers apoptotic response either by disturbing mitochondrial membrane potential or by activation of caspase-9, however there is no evidence to illustrate any of these proteins have the properties and characteristics like a viroporin. Flavivirus (JEV) hydrophobic nonstructural proteins NS2A, NS2B have been shown to behave viroporin like activity that alter the permeability of the membranes, and sometimes associated with apoptotic phenomena, and promotes viral pathogenesis. Little is known about the functions of the DENV hydrophobic proteins (NS2A, NS2B, NS4A, NS4B). However, our group has reported recently that DENV-2 NS2B behaves as a viroporin since it can alter the permeability of cellular membranes. The results suggested that NS2B is able to modulate membrane permeability to facilitate critical steps in viral replication cycles. In addition NS2B has been found partially distributed to the inner mitochondrial membrane and further NS2B triggers caspase 3, caspase 9, and PARP activation. Further characterization of other hydrophobic proteins of DENV-2 is important; specially NS2A, which structural properties suggest NS2A as a viroporin. In addition, studies in flaviviruses such as kunjun virus, Japanese encephalitis virus also supports this hypothesis about the role of NS2A as a viroporin. Therefore it will be very relevant to evaluate and characterize the role of



NS2A and to analyze whether NS2A functions in DENV-2 genome as a viroporin apart from its role in synthesis, replication and assemble of DENV-2. It is relevant to address the role of NS2A as viroporin and associated functions as membrane permeability, osmotic imbalance of calcium, induction of apoptosis, localization and function on cell organelle. Further analyzing the role of proposed NS2A viroporin in inducing NLRP3 inflammasome in dengue virus infection would be very important to unravel the molecular mechanism of inflammasome in DENV pathogenesis. Better definition of the functional aspects of viroporins will certainly draw greater enthusiasm for developing therapeutics that target the interesting family of membrane channels.

### **HYPOTHESIS**

The nonstructural protein NS2A has viroporin activity and both NS2A and NS2B activate NLRP3 inflammasome.

### **OBJECTIVE**

1. Evaluate the role of viroporin activity of nonstructural NS2A protein of DENV-2
2. Characterize the role of NS2A and NS2B proteins in inflammasome activation

### **PARTICULAR OBJECTIVE**

1. Cloning, expression and purification of NS2A protein in eukaryotic and prokaryotic system.
2. Evaluate the viroporin activity of NS2A in prokaryotic and eukaryotic system.
3. To assess the capability of NS2B and NS2A protein of DENV-2 in the activation of NLRP3 inflammasome.
4. To characterize the mechanism of NS2A and NS2B to mediated NLRP3 inflammasome activation

## **MATERIALS AND METHODS**

### **1. Propagation and purification of DENV Serotype 2**

Dengue virus used in this work was isolated from a classic Dengue-2, with a large homology to New Guinea serotype 2. Mosquito C6/36 cells derived from *Aedes albopictus* were grown in MEM supplemented with 10% fetal bovine Serum (FBS) (Gibco Carlsbad, CA) at 34°C. Baby hamster kidney (BHK- 21) cells were cultured at 37°C in the presence of 5% CO<sub>2</sub> in MEM supplemented with 10% FBS, 1 IU penicillin/mL, 1 mg/mL streptomycin and 2.4 ng/mL of amphotericin B at final pH 8. The virus stock was prepared by infecting a C6/36 cell monolayer in 75 cm<sup>2</sup> tissue culture flasks at 75% – 85% confluence. When the infected monolayer showed cytopathic effects, the cells and supernatant were homogenized and diluted in a 40% polyethylene glycol solution in 2M NaCl (Sigma-Aldrich St. Louis, MO) and incubated at 4°C overnight. The suspension was centrifuged at 6000 rpm for 1 hour. The virus was resuspended in 1/15 of the total volume with a glycine buffer (Tris 50 mM, Glycine 200 mM, NaCl 100 mM and EDTA 1 mM) and 1/30 of the total volume of FBS. The virus was homogenized, aliquoted and frozen at -70°C until use.

### **2. Virus Titration**

The virus was titrated by the standard plaque-forming assay technique using BHK-21 cells. Briefly, tenfold serial dilutions of virus stock in Hank's salt solution (Gibco Carlsbad, CA) were used to infect monolayers of BHK-21 cells in 24-well plates. After incubation at 37°C for 1 hour, the infected cells were overlaid with MEM Eagle modified medium (Gibco Carlsbad, CA) with 3% carboxymethyl cellulose (Sigma-Aldrich St. Louis, MO). After 5 days, the resulting plaques were stained with naphthol blue-black solution to quantify the plaque forming units (PFUs).

### **3. *In silico* analysis of the NS2A protein**

To identify the degree of homology of the NS2A protein of the Dengue virus, with NS2A protein of Japanese encephalitis, we used the clustal W2 program, which is a tool that performs a phylogenetic analysis, based on comparing the alignments of multiple sequences of the proteins of interest. The sequences were obtained from the NCBI database. For the Dengue

virus, NS2A sequence was retrieved from accession number (AF038403) and for Japanese encephalitis the NS2A sequence was retrieved from accession number (AAF34187); the sequences were aligned and percent homology was calculated. In addition, a kyte-doolittle analysis was done, which defines the values relative hydrophobicity of amino acids, according to the degree of interaction of polar solvents with amino acids. The more positive values are more hydrophobic and these are related to transmembrane regions within the protein. Therefore, it helped us to identify the profile of hydrophobicity, as well as prediction of possible transmembrane regions, for this DAS Trans-membrane prediction was used. Next, topological representations of the DENV NS2A protein were generated using the Socs MEMSAT program.

#### **4. Amplification of the NS2A sequence**

The sequence encoding for NS2A protein was obtained by RT-PCR. Briefly C6/36 cells were infected with Dengue-2 virus at 5 MOIS. When the cells formed syncytial structure, the supernatant was removed and the cells were treated with 1mL of Trizol (Invitrogen), mixed and incubated 5 minutes at room temperature. Further 200  $\mu$ l of chloroform (sigma) was added, the mixture was homogenized vigorously and incubated for 3 minutes and centrifuged at 12000 rpm for 5 minutes at 4°C. The aqueous phase was recovered (where the RNA is found) and 500  $\mu$ l of isopropanol (sigma) was added and incubated for 10 minutes at room temperature and further, centrifuged at 12,000 rpm for 10 minutes at 4°C. The supernatant was removed and the precipitate was washed with 1 mL of 75% ethanol and centrifuged at 7500 rpm for 5 minutes at 4°C. The pellet was allowed to dry at room temperature and finally resuspended in 15  $\mu$ l in DEPC (Invitrogen) water. Subsequently the sample was treated with 0.75  $\mu$ l DNase I 1u/ $\mu$ l, 2.5 u/ $\mu$ l of 10X Buffer (Invitrogen) and 6.75  $\mu$ l of DEPC water, the mixture was incubated for 15 minutes at 37°C, and further incubation at 65°C for 15 minutes and finally RNA was maintained at 4°C. With RNA sample, a reverse transcription reaction was performed and the cDNA was obtained. To do this, 3  $\mu$ g of RNA was mixed in a reaction tube with 1.5  $\mu$ l of 1.25 mM hexamers, 6  $\mu$ l 5X first strand buffer, 1.2  $\mu$ l 10 mM dNTPs, 3  $\mu$ l DTT 0.1M, 1  $\mu$ l super script 200 u/ $\mu$ l (Invitrogen), the mixture was made up to 30  $\mu$ l with injectable water. The reaction mixture were subjected to following reaction conditions in the thermal cycler (applied Biosystems): 50 minutes at 42°C, 15 minutes at 70°C, 15 minutes at 4°C (in

this cycle RNase H was added, Invitrogen), 20 minutes at 37°C and 4°C. Finally the NS2A sequence was amplified from the synthesized cDNA. Oligonucleotides were designed to amplify the NS2A sequence (Table 3). The PCR reaction was carried out and amplified product was resolved on a 1% agarose gel and identified the band corresponding to the calculated size. Further the PCR product is purified, run in 1% agarose gel and the band of interest was purified with the QIAQuick Gel extraction kit (QIAGEN). The final volume (20 µl) was stored at 20°C for its future application.

**Table 3:** NS2A oligonucleotide for PCR amplification

OLIGONUCLEOTIDE	SEQUENCE	TM
NS2AF	CACCATGGGACATGGGCAGATT	52
NS2AR	CCTTTTCTTGTTGGTTCTTGAA	52

### 5. Cloning of NS2A in prokaryotic vector

To express the NS2A protein, PET151 / D-TOPO (Invitrogen) vector was used which consists of the following elements: bacteriophage T7 promoter sequence, which allows high levels of expression of the protein of interest in an IPTG-inducible manner; the lac operon sequence; A ribosome binding site, a sequence that encodes 6 histidine, Sequence of the V5 epitope, cloning site TOPO, and the sequence that encodes the ampicillin resistance gene (Fig. 10) Once the PCR product was obtained to the NS2A proteins of interest, a ligation reaction was setup with a molar ratio of 0.5: 1 to 2: 1 (PCR product: Vector). This ligation reaction was transformed in *Escherichia coli* DH5α. To do the transformation, DH5α was grown overnight in Luria Bertani medium (LB) without ampicillin and further was diluted 1:100 with fresh medium and allowed to grow until the optical density of 0.4 nm was reached. The bacteria were centrifuged at 2000 rpm at 4°C for 15 minutes; later the pellet was resuspended in 1 mL of fresh LB medium and 1 mL of the TSS 2X solution (1 g LB, 10 g polyethylene glycol, 40 mM MgCl<sub>2</sub>, pH 6.5) was added. 250 µl aliquots were then made, to which 3 µl of the ligation reaction was added and allowed to incubate on ice for 30 minutes, after the incubation time, a

thermal shock at 42°C was given for 45 seconds. They were then incubated on ice for 1 minute and 250 µl of fresh LB broth was added and allowed to stir for 1 hour, at 37°C. After this time, the bacteria were plated on LB agar plates with 120 µg of ampicillin, and incubated for 12 hours at 37°C. After 12 hours, colonies were picked to amplify the NS2A plasmid via Maxiprep (Qiagen Kit) according to manufacturer's protocol.

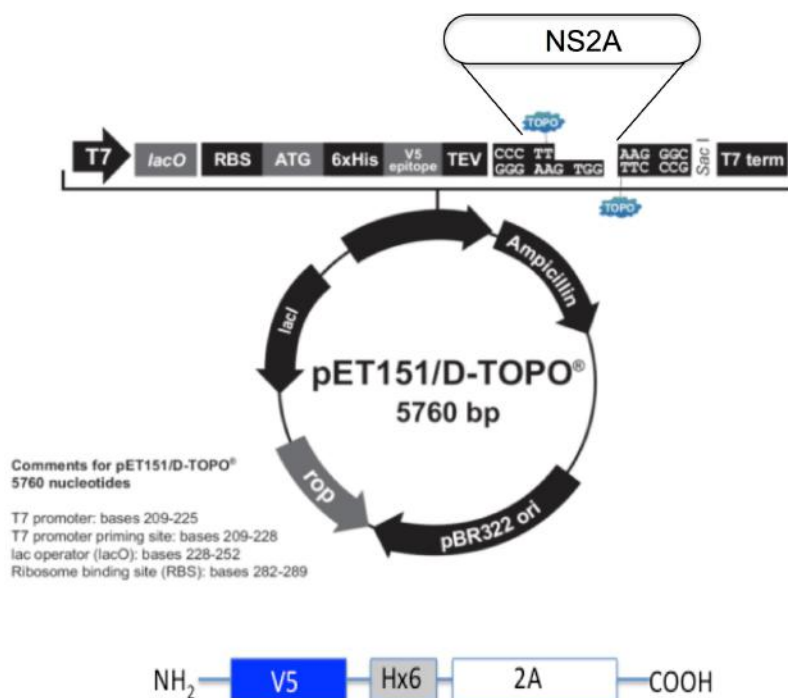


**Fig 10. Cloning of NS2A protein in prokaryote:** Schematic of pET151/D-TOPO vector and representation of the expression construct with sequence encoding the NS2A protein in frame with an N-terminal V5 epitope and 6X His tag.

## 6. Cloning and expression of NS2A in eukaryotic vector

To express the NS2A protein in eukaryotic cells, the vector pEGFPN1 (Clontech) was used (Fig. 11). This plasmid consists of the following elements: CMV (human cytomegalovirus) promoter; multiple cloning site; sequence encoding the green fluorescent protein (GFP); the Kozak consensus sequence SV40 Polyadenylation sequence; kanamycin Resistance gene. Oligonucleotides were designed to amplify the NS2A sequence (Table 4), these oligonucleotides contain the restriction sites for the enzymes XhoI and HindIII (New England Biolabs). The Cloning process was performed as described above.

**Table 4:** NS2A oligonucleotide for cloning in pEGFPN1 vector

OLIGONUCLEOTIDE	SEQUENCE	TM
NS2ApEGFPN1-F	ACGTAAGCTTCCTTTTCTTGTTGGT	56.4
NS2ApEGFPN1-R	TGCAAGCCTTTTCTTGTTGGTTCT	57.2

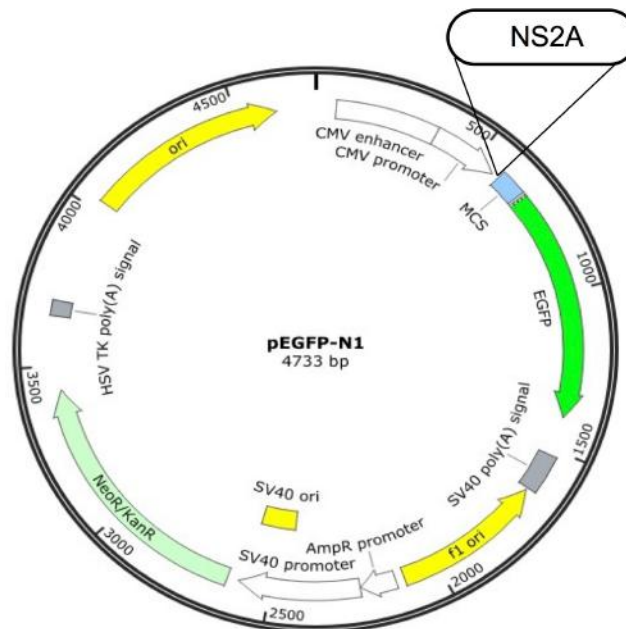


**Figure 11. Cloning of NS2A protein in eukaryote:** Schematic of pEGFPN1 vector with its components.

## **7. Analysis of recombinant clone**

### **7.1. Extraction of plasmid DNA**

The selected colonies were grown in LB medium with 120 µg / mL ampicillin on an orbital shaker at 37°C for 12 hours. Plasmid DNA was extracted from each colony on a small scale (miniprep). Briefly, 6 mL of the bacterial culture was transferred to an eppendorf tube and centrifuged at 6000 rpm for 1 minute, the supernatant was discarded, and subsequently the pellet was vortex and re-suspended in 300 µl of the TENS solution (10 mM Tris HCl pH 8.0, 1 mM EDTA pH 8.0, 0.1M NaOH and 0.5% SDS). The mixture was homogenized and 150 µl of 3 M sodium acetate pH 5.2 was added, resuspended by vortexing and the tubes were centrifuged at 13,000 rpm for 5 minutes. The supernatant was transferred to another tube and the DNA was precipitated with 900 µl of absolute ethanol, and saved at -20°C for 30 minutes to promote precipitation and then centrifuged at 13000 rpm for 5 minutes, the supernatant was removed and the DNA precipitate was washed twice with 900 µl of 70% ethanol and centrifuge at 13,000 rpm for 5 minutes. The supernatant was removed and the pellet was dried at 42 °C re-suspended in 20 µl of ddH<sub>2</sub>O.

### **7.2. Confirmation of NS2A DNA construct**

NS2A-GFP construct was by digesting the NS2A-GFP plasmid with restriction enzymes. To do this, a reaction mixture was prepared containing 3 µg NS2A-GFP plasmid, 0.2 µl of BSA, 2 µl of buffer B (10X), 3 units of RNase, 3 units of BamH1 and HindIII and volume was adjusted with injectable water to a final volume of 20 µl. The reactions were incubated at 37°C for 2 hours. The digested plasmid was analyzed on a 1% agarose gel.

## **8. Bulk preparation of NS2A plasmid by Maxiprep**

To generate the ample amount of pET-NS2A-Topo & NS2A-GFP plasmid, transformed colonies of respected construct were picked up and allowed to grow in LB medium overnight with ampicillin and kanamycin respectively. This primary culture was further diluted at 1:100 ratio in the 300 mL of fresh LB media broth containing antibiotics to grow overnight at shaker incubator at 37°C, 180 rpm. Overnight grown bacterial was poured broth plastic centrifuge bottle and centrifuged for 15 minutes at 5000 rpm. Supernatant was poured off and resuspended bacterial pellet in 10 mL Buffer P1 (this should already be cold, as its stored in

the refrigerator with RNase) and mixed properly. Further, 10 mL Buffer P2 was added and mixed gently and incubated at room temperature for 5 minutes and then 10 mL of cold Buffer P3 was added, mixed immediately but gently by inversion, and incubated on ice for 20 minutes. Centrifuged for 30 minutes on 12,000 rpm at 4°C. During the last 10 minutes of the spin, equilibrated the Qiagen-tip 500 column by adding 10 mL Buffer QBT and allowed column to drain. Decanted supernatant in Falcon 50 mL tubes and removed the remaining chunks with pipet. In the continuation, decanted supernatant was added to column and allowed to flow through. Column was washed 2 times with 30 mL Buffer QC. DNA was eluted by adding 15 mL Buffer QF and collected in fresh plastic centrifuge tube. DNA was precipitated with 10.5 mL isopropanol at room temperature. Centrifuged for 30 minutes on 12,000 rpm at 4°C. Supernatant was Poured off add DNA was washed 2 times with 1 mL 70% ethanol and centrifuged 5 minutes on 12, 000 rpm at 4°C. DNA pellet was air-dried for 5 minutes at 42°C and resuspended in 300 mL ddH<sub>2</sub>O and saved at -20°C.

## **9. Analysis of the expression of the recombinant proteins**

### **9.1. Induction of NS2A recombinant protein**

To analyze the expression of the NS2A recombinant protein of interest, kinetics of protein induction was performed. Initially, *Escherichia coli* bacteria from the BL21 STAR strain were transformed with each NS2A-topo construct under the protocol detailed above. Further, a colony was grown in LB medium with ampicillin overnight at 37°C in agitation. After the incubation time, a new culture of 30 mL of LB medium with ampicillin was inoculated from 1 mL of the overnight subculture. The cultures were grown at 37°C under agitation until optical density reached the logarithmic phase (0.4-0.6), then, original culture of NS2A construction was divided into 2 tubes. One of the NS2A protein growth culture (2mL) was induced with 1mM IPTG (Research Organic) and other culture was remained uninduced and further allowed to grow till 8 hours. Aliquots were taken at 0, 4, 6 and 8 hours and each of the aliquots were adjusted to a optical density of 0.4 with LB medium, then 1.5 mL of each aliquots were centrifuged at 13,000 rpm for 5 minutes and the pellet was resuspended in 35 µl buffer Laemmli 3X (2% SDS, 10% Glycerol, 100mM b-mercaptoethanol, 1mM Tris pH6.8, Bromophenol blue 0.001%), these samples were boiled for 10 minutes and subsequently analyzed on a SDS-PAGE gel 15 or 12% depending on the expected weight of the protein of



interest. Once electrophoretic run was completed, the gels were stained with Coomassie blue dye for 10 minutes, then gel was incubated with the de-staining solution composed of acetic acid 7.5%, 50% methanol. In addition, other gels were transferred to a hybond nitrocellulose membrane (Amersham Biosciences) for 1 hour and 20 minutes at 120 volts. After the protein transfer, the membrane was blocked for 1 hour at 37°C with 5% skim milk in PBS 1X 0.1% Tween. The membrane was washed three times with PBS 1X 0.1% Tween every 5 minutes and then incubated with the anti-V5 antibody coupled to HRP (Invitrogen) at a 1: 5000 dilutions in 1X PBS 0.1% Tween-5% gel or with the anti-Histidine antibody coupled to HRP (Invitrogen) to a 1: 5000 dilutions. Both antibodies were incubated for one hour at room temperature under stirring. Then the membrane was washed four times with PBS 1X Tween 0.1% and three times with PBS 1X. Finally, the detection of the proteins was done with the kit of chemiluminescence supersignal west femto (PIERCE) according to the Manufacturer's instructions.

## **9.2. Analysis of GFP-NS2A protein expression in HMEC-1 cells**

To assess whether the NS2A-GFP construct expressed the protein of interest, kinetics of transfection was performed at 4, 24 and 48 hours. To perform this experiment,  $1.2 \times 10^5$  HMEC-1 cells were seeded in 24-well plates under the culture conditions already mentioned. Subsequently, the cells were transfected with transfection mix that were prepared as manufacturer's protocol: In a eppendorf tube (A) 2 µg of the GFP (transfection control) or NS2A-GFP is resuspended with optimen (Gibco) to a final volume of 50 µl; Additionally, in eppendorf (B) 1 µl lipofectamine (Invitrogen) was added with 50 µl of optimen and was allowed to incubate for 5 minutes at room temperature. After this incubation time, a mixture was made of (A) and (B) and allowed to incubate for 30 minutes, subsequently the complexes were added dropwise over the cells, and then additionally 100 µl of optimen were added. These complexes were incubated for 4 hours at 37°C and then further cells were washed with 1X PBS and MDCD medium supplemented with 0.1% fetal bovine serum was added to the cells and incubated at 37°C for specific time. The cells were washed 3 times with 1X PBS and subsequently the cells were fixed with 4% paraformaldehyde (SIGMA) for 20 minutes, then coverslips were mounted on slides using vectashield H-100 and DAPI and the samples were analyzed in a Confocal Leica microscope (Leica TCS SP5).

## **10. Permeability assays using *E. coli* pLysS bacteria**

To check the lytic effect of NS2A on bacterial membrane, *E. coli* BL21 (DE3) pLysS bacteria were transformed with either NS2A-V5-H6 or PTB (control) or pET vector. The respective cultures were then incubated at 37°C in LB medium for their growth in the presence of two antibiotics: 100 µg/mL ampicillin and 34 µg/ml chloramphenicol depend on the antibiotic gene present on vectors. When cultures reached an absorbance of 0.4 at 600 nm, then 1 mM isopropyl-B-D thiogalactopyranoside (IPTG) was added for induced expression of the protein. The optical densities were measured, and culture aliquots were taken at intervals of 2-7 hours.

## **11. Purification of the NS2A protein by preparative gels**

*E. coli* bacteria from the BL21-STAR strain transformed with the V5-H6-NS2A plasmid with the protocol described above. A colony was used as seed in a 250 mL LB culture supplemented with 120 mg / mL ampicillin. Once it reached a density of 0.4 nm, 1mM of IPTG was added, this medium was incubated at 37°C for 12 hours. After the incubation time, the culture was centrifuged at 6000 rpm for 30 minutes to obtain the inclusion bodies. The pellet was resuspended in 12 mL of solution containing 15% Sucrose, 0.12% Triton X-100, 50 mM Tris-HCl pH 8.0, the mixture was Sonicated (3 cycles of one minute, 10 pulses with an amplitude of 40 volts), and further centrifuged at 6000 rpm for 4 minutes at 4°C. Pellet was resuspended in the 0.12% of Triton X-100, 10 mM EDTA and 50 mM Tris-HCl pH 8.0, and the mixture was sonicated under the same conditions and centrifuged at 6000 rpm for 30 minutes at 4°C. The pellet was resuspended in 6 mL of the Tris 50 mM pH 8.0, 10mM EDTA solution and the inclusion bodies were boiled 10 minutes with 2 mL of laemmli buffer and separated on a preparative SDS-PAGE gel (25 x 25 cm) at 17.5% gel. Once run is finished and markers are separately enough to cut the bands, the band was cut based on the expected molecular weight, this band was mashed with the aid of a 10-mL syringe. To this, 1 mL of 1X PBS was added and the protein was allowed to diffuse for overnight at 4°C. The next day the eluted protein was recovered and tested for purity by resolving on 15 % SDS-PAGE gel and further strain on a Coomassie-blue and detected by Western blot, as described above. Finally, the protein was quantified and stored at -20°C.

## **12. Generation of polyclonal anti-NS2A antibody**

Female wistar rats and rabbit were used to generate a polyclonal antibodies against the NS2A protein. For this, the animals were immunized intraperitoneally with 250 µg of recombinant NS2A protein; a mixture was made of protein and complete (first immunization) and incomplete Freud adjuvant and, in a final volume of 500 µl. The immunization schedule consisted of four doses at intervals of 15 days, serum of the animal was obtained in each immunization and this was evaluated by ELISA assay and western blot.

## **13. Cellular localization of NS2A protein by immunofluorescence assay**

$8 \times 10^4$  HMEC-1 cells were plated in 24-well plates on cover slips and incubated at 37°C for 24 hours in an incubator with 5% CO<sub>2</sub>. Cells were transfected with NS2A-GFP for 36 hours. Further, cells were incubated with 250 mM mitoTracker red CMXRox (Invitrogen) (mitochondria marker) or TOM22 (outer mitochondria membrane marker) and incubated at 37 °C for 45 minutes. For ER and Golgi localization, Cells were washed, fixed and permeabilized as described in standard protocol. The cells were then incubated with the following antibodies: A monoclonal mouse anti-calnexin antibody (Invitrogen) to detect endoplasmic reticulum with a 1:100 dilution; a mouse monoclonal anti-golgi (Invitrogen) was used to detect the Golgi complex with a 1: 100 dilutions. The cells were then incubated with the following secondary antibodies; Total mouse IgG coupled to CY3 (Invitrogen), rat IgG coupled to CY3 (Invitrogen) at a 1: 100 dilutions. These were incubated at room temperature for one hour, finally the cells washed 3 times with 0.1% PBS-Triton X-100. The coverslips were mounted on slides using vecta shield H-100 (vector) and DAPI and samples were analyzed under a microscope Confocal Leica (Leica TCS SP5).

## **14. Cross-linking test with Glutaraldehyde**

Seven micrograms of purified V5-H6-NS2A protein in HEPES buffer was incubated with increased concentrations (0.1– 0.5 %) of glutaraldehyde (Sigma). The mixture was incubated in the dark for 2 minutes at 25°C and subsequently quenched with 50 mM Tris– HCl, pH 8.0 for 15 -20 minutes. Cross-linked proteins were separated on a 12 % SDS-PAGE gel under reducing conditions, and complexes were detected in western blots with a HRP tagged anti-V5 antibody.

### **15. Purification of the membrane**

*E. coli* BL21 Star was transformed with V5-H6-NS2A construct and further transformed colony was grown in LB broth in the presence of 1mM IPTG for 8 hours. Culture that expressed NS2A proteins was harvested by centrifugation (11,000 g for 10 minutes at 4°C). The cellular pellets were subsequently suspended in the lysis buffer, which constitutes of 20 mM Tris– HCl, pH 7.8, 300 mM NaCl, and 2 mM  $\beta$  –mercaptoethanol. This cellular pellet was then sonicated on ice. Consequently, the cell debris was removed by centrifugation at 5000 g for 20 minutes. The supernatant was then added to an ultra-centrifuge tube containing 4 mL of 30 % and 4 mL of 60 % sucrose solution. The cellular membrane was drawn from the interface after ultracentrifugation at 125,000 g for 1 hour. and then used to perform western blot experiments. A hyperimmune mouse antibody specific for OMPC was used to re-probe the membrane where NS2A protein was detected in the bacterial membrane fraction.

### **16. Preparation of liposomes and encapsulation of FITC**

Liposomes were prepared using a Liposome encapsulation kit (composition of Liposomes- L-phosphatidylcholine egg yolk, stearylamine and Cholesterol; Sigma-Aldrich, catalogue no L4395). This kit was used to encapsulate FITC (25  $\mu$ M), dissolved in HEPES buffer (pH 7.4), 100 mM NaCl (HBS), overlay the liposomes mixture with argon and cap it with a Teflon lining. The mixture was incubated in a shaker for 16–18 hours at room temperature, to ensure efficient encapsulation of FITC. Liposomes were then washed with 1 mL HBS, resuspended by repeated centrifugation (100,000 X g, 10°C, 20 minutes) and then the encapsulated liposomes were recovered in the pellet. Pelleted liposomes resuspended in 1 mL HBS solution were stored at 4°C. The integrity of liposomes was checked by comparison of fluorescent signals under different permeability conditions, with respect to the signal generated in the presence of 0.5% Triton X- 100, which completely disrupts liposomal integrity (100% signal).

## **17. SDS-PAGE and immunoblotting**

Protein lysates were mixed with 3X Laemmli loading buffer and then heated at 95°C for 10 minutes. Sample proteins were resolved by SDS-PAGE using 12% Tris-HCl gels for 80 minutes at 160 V (Mini-Protean Cell; Amersham Biosciences, Piscataway, NJ, USA) and then electro transferred (120 V for 2 hours) onto nitrocellulose membranes (Hybond ECL; GE Healthcare, Little Chalfont, UK). Air-dried membranes were blocked and then incubated with the appropriate primary antibody, followed by the appropriate horseradish peroxidase (HRP)-conjugated secondary antibody (1:3000) in PBS-Tween-20. The membranes were stripped if necessary. After further washing with PBS-Tween-20, the membranes were treated with western lightning enhanced chemiluminescence reagent (Pearce, Rockford, IL, USA), and immunoreactive proteins were detected by exposure to film (Kodak, Rochester, NY, USA).

## **18. Mitochondrial membrane potential Assay**

TMRE-Mitochondrial Membrane Potential Assay Kit (ab113852) was used to quantify the changes in mitochondrial membrane potential in live HMEC-1 cells due to NS2A and NS2B.  $1 \times 10^5$  HMEC-1 were plated in the cell plate and transfected with either GFP, NS2A-GFP, NS2B-GFP as described before. 36 hours post transfection, HMEC-1 cells were stained with 175nM TMRE in MCDB base medium and incubate for 30 minutes at 37°C (tetramethylrhodamine, ethyl ester) to label active mitochondria. TMRE is a cell permeant, positively-charged, red-orange dye that readily accumulates in active mitochondria due to their relative negative charge. Depolarized or inactive mitochondria have decreased membrane potential and fail to sequester TMRE. Positive control cells were treated with 20 $\mu$ M FCCP in MCDB base medium for 10 minutes (carbonyl cyanide 4-(trifluoromethoxy) phenylhydrazone) is a ionophore uncoupler of oxidative phosphorylation. Treating cells with FCCP eliminates mitochondrial membrane potential and TMRE staining. After the incubation, FCCP solution was removed and replaced with TMRE solution and incubate for 37°C for 20 minutes. After the incubation period, TMRE solution was discarded and the cells were washed with 1X PBS. Cells were trypsinized with trypsin-EDTA (0.05%) and detached and washed with 2 times with 1X PBS and put in 15 mL falcon. Cells were centrifuged at 12,000 rpm, for 5 minutes at 4°C, and further resuspended in 0.2% BSA in 1X PBS. Read in the flowcytometry at 488nm (excitation peak- 595nm, emission-575nm).

## **19. Knockout of Inflammasome gene by CRISPR-CAS9 Technology**

**19.1 CRISPR** (Clustered Regularly Interspaced Short Palindromic Repeats) is a microbial nuclease system involved in defense against invading phages and plasmids. CRISPR loci in microbial hosts contain a combination of CRISPR associated (Cas) genes, non-coding RNA elements and a distinctive array of repetitive elements (direct repeats). These repeats are interspaced by short variable sequences derived from exogenous DNA targets known as protospacers, and together they constitute the CRISPR RNA (crRNA) array. Within the DNA target, each protospacer is always associated with a protospacer adjacent motif (PAM), which can vary depending on the specific CRISPR system. The Type II CRISPR system is consisting of the nuclease Cas9, the crRNA array that encodes the guide RNAs and a required auxiliary trans-activating crRNA (tracrRNA) that facilitates the processing of the crRNA array into discrete units. Each crRNA unit then contains a 20-nt guide sequence and a partial direct repeat, where the former directs Cas9 to a 20-bp DNA target via Watson-Crick base pairing (Fig 12). In the CRISPR-CAS system derived from *Streptococcus pyogenes* (which is the system used in this protocol), the target DNA must immediately precede a 5'-NGG PAM. The RNA-guided nuclease function of CRISPR-Cas is reconstituted in mammalian cells through the heterologous expression of human codon-optimized Cas9 and the requisite RNA components. Furthermore, the crRNA and tracer RNA can be fused together to create a chimeric, single-guide RNA (sgRNA) (Fig 12) Cas9 can thus be re-directed toward almost any target of interest in immediate vicinity of the PAM sequence by altering the 20-nt guide sequence within the sgRNA. In this protocol we use Lenti-CRISPRV2 plasmid (195).

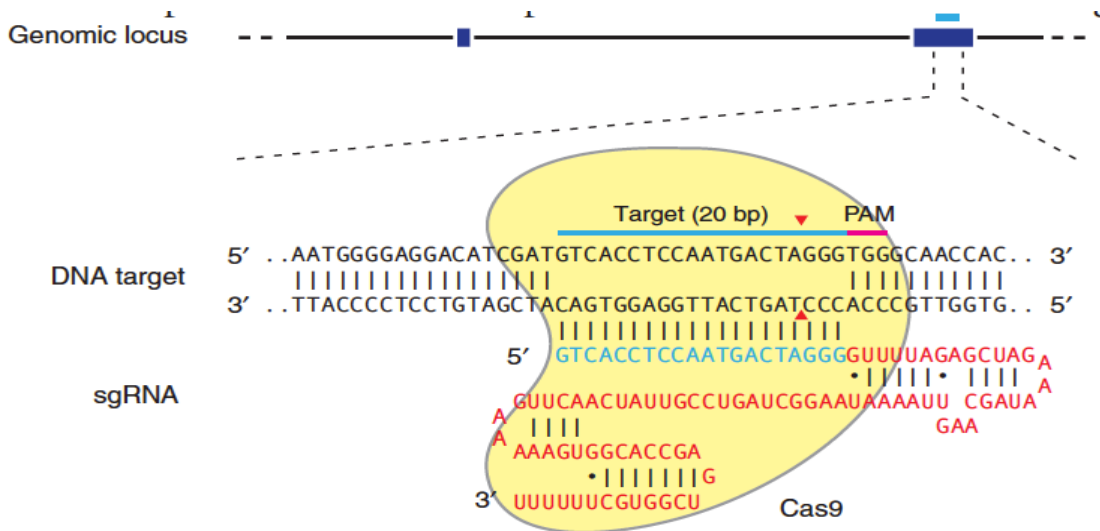


**Fig 12. Schematic of the RNA-guided Cas9 nuclease.** The Cas9 nuclease from *S. pyogenes* (in yellow) is targeted to genomic DNA (shown for example is the human EMX1 locus) by an sgRNA consisting of a 20-nt guide sequence (blue) and a scaffold (red). The guide sequence pairs with the DNA target (blue bar on top strand), directly upstream of a requisite 5'-NGG adjacent motif (PAM; pink). Cas9 mediates a DSB ~3 bp upstream of the PAM (red triangle)(195).

**19.2 lentiCRISPRv2 (one vector system):** This plasmid contains two expression cassettes, hSpCas9 and the chimeric guide RNA. The vector can be digested using BsmBI, and a pair of annealed oligos can be cloned into the single guide RNA scaffold. The oligos are designed based on the target site sequence (20bp) and needs to be flanked on the 3' end by a 3bp NGG PAM sequence(196)(15).

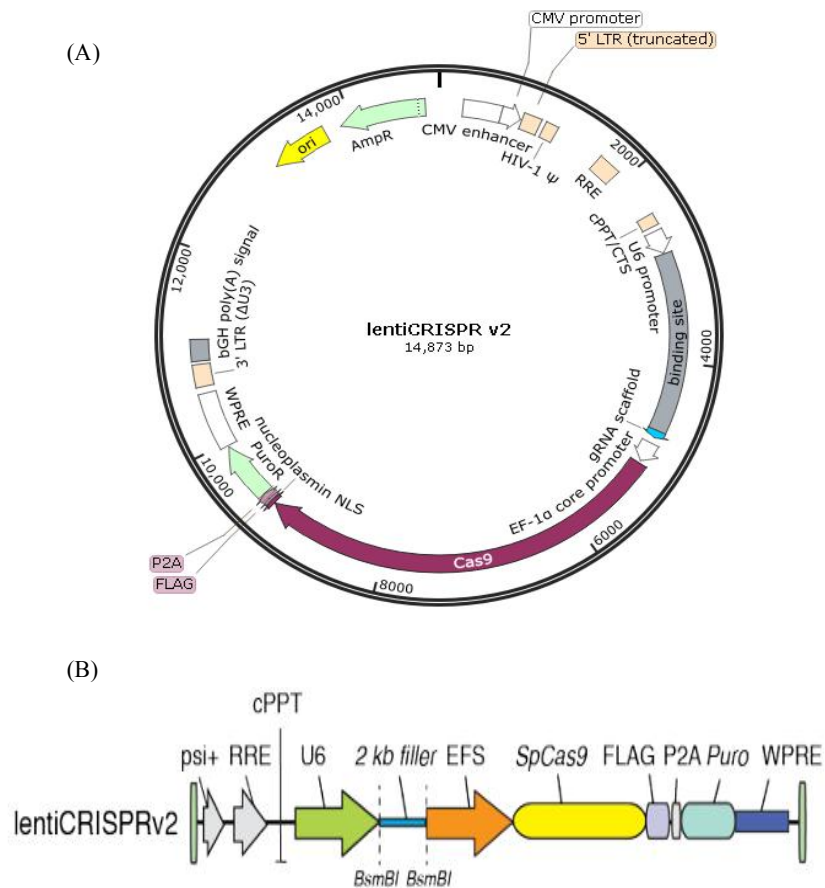


**Fig 13. Cloning of sgRNA of NLRP3, ASC and Caspase 1:** (A) Schematic of lentiCRISPRv2 vector (B) expression cassettes of lentiCRISPRv2 vector

### 19.3 Designing of guide RNA targeting NLRP3, CASPASE-1, ASC

The specificity of the Cas9 nuclease is determined by the 20-nt guide sequence within the sgRNA. For the *S. pyogenes* system, the target sequence (e.g., 5'-GTCACCTCCAATGACTAGGG-3') must immediately precede (i.e., be 5' \_to) a 5'-NGG PAM, and the 20-nt guide sequence base pairs with the opposite strand to mediate Cas9 cleavage at ~3 bp upstream of the PAM. 5'-NGG PAM is required for the specific recognition and further for cleavage (Fig. 15). Thus, there are two main considerations in the selection of the 20-nt guide sequence for gene targeting: (i) the 5'-NGG PAM for *S. pyogenes* Cas9 and (ii) the minimization of off-target activity. Off target activity is required to avoid the non-targeted, nonspecific binding and cleavage. Several CRISPR sgRNA design tool are available such as “[Broad Institute guide RNA design tool](#)” “[crispr.dbcls.jp](#)” “[crispr.mit.edu](#)” that takes a



genomic sequence of interest and identifies suitable target sites and provide specific guideRNA. The tool assess off-target genomic modifications for each sgRNA, targets on target sites and corresponding sgRNA, ranked according to the quantitative specificity analysis on the effects of base-pairing mismatch identity, position and distribution. The CRISPR Design Tool provides the sequences for all oligos and primers necessary for (i) preparing the sgRNA constructs, (ii) assaying target modification efficiency and (iii) assessing cleavage at potential off-target sites.

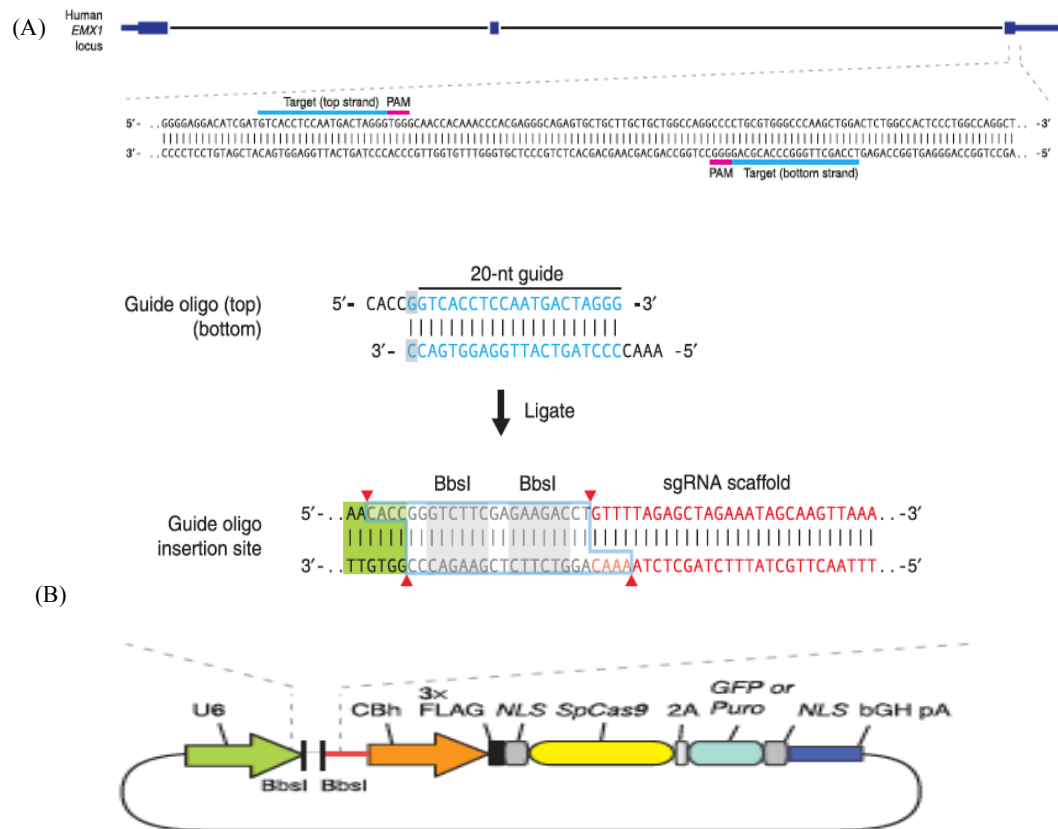


**Fig 14. Target selection and reagent preparation.** (A) For *S. pyogenes* Cas9, 20-bp targets (highlighted in blue) must be followed at their 3'ends by 5'-NGG, which can occur in either the top or the bottom strand of genomic DNA, as in the example from the human *EMX1* gene. (B) Schematic for scarless cloning of the guide sequence oligos into a plasmid containing Cas9 and the sgRNA scaffold (pSpCas9(BB)). The guide oligos for the top strand example (blue) contain overhangs for ligation into the pair of BbsI sites in pSpCas9(BB), with the top and bottom strand orientations matching those of the genomic target (i.e., the top oligo is the 20-bp sequence preceding 5'-NGG in genomic DNA). Digestion of pSpCas9 (BB) with BbsI allows the replacement of the Type II restriction sites (blue outline) with direct insertion of annealed oligos. Likewise, a G-C base pair (gray rectangle) is added at the 5' \_end of the guide sequence for U6 transcription, which does not adversely affect targeting efficiency.

Using the Broad institute and MIT webserver of guide RNA designing tool, guide RNA of NLRP3, ASC and Caspase-1 were selected and further specific nucleotide sequence in 5' and 3' end of the guide RNA was added according to the backbone and restriction enzyme site of BsmB1 in the LentiCRISPRV2 plasmid (Table 5). As example: in order to clone the target sequence into the lentiCRISPR backbone, synthesize two oligos of the form:



Example oligo design : Note that the NGG PAM is not included in the designed oligos.

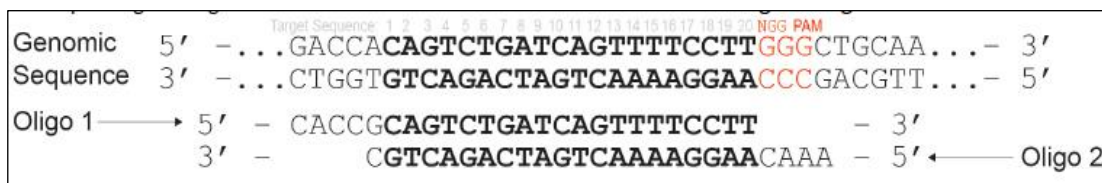


**Table 5:** Guide RNA specific for NLRP3, Caspase-1, ASC

<b>hCasp1 gRNA 1F</b>	caccgATTGACTCCGTTATTCCGAA
<b>hCasp1 gRNA 1R</b>	AaacTTCGGAATAACGGAGTCAATc
<b>hASC gRNA 1F</b>	caccgGCTGGAGAACCTGACCGCCG
<b>hASC gRNA 1R</b>	AaacCGGCGGTCAGGTTCTCCAGCc
<b>hNLRP3 gRNA 1F</b>	caccgGCTAATGATCGACTTCAATG
<b>hNLRP3 gRNA 2R</b>	AaacCATTGAAGTCGATCATTAGCc

#### **19.4 Cloning of guide RNA in lentiCRISPRv2 plasmid**

To clone the guide RNA specific to vector, 5 $\mu$ g of the lentiviral CRISPR plasmid were digested with BsmBI for 30 minutes at 37°C. The digestion reaction mixture contained 5  $\mu$ g lentiCRISPR plasmid, 3  $\mu$ l FastDigest BsmBI (Fermentas), 3  $\mu$ l FastAP (Fermentas) 6  $\mu$ l 10X FastDigest Buffer and volume was made up 60  $\mu$ l with ddH<sub>2</sub>O. Further, digested plasmid was analyzed in 8% agarose gel electrophoresis and gel was purified using QIAquick Gel Extraction Kit and elute in EB. If BsmBI digested, a ~2 kb filler piece should be present on the gel. Only the large fragment (~11 kb) band was purified. In parallel, guide RNA was phosphorylated and annealed with each pair of oligos. The reaction mixture contained 1  $\mu$ l Oligo Forward (100 $\mu$ M), 1  $\mu$ l Oligo Reverse (100 $\mu$ M), 1  $\mu$ l 10X T4 Ligation Buffer (NEB), 6.5  $\mu$ l ddH<sub>2</sub>O, 0.5  $\mu$ l T4 PNK (NEB M0201S). The phosphorylation/annealing reaction were put in a thermocycler using the following parameters: 37°C for 30 minutes, 95°C for 5 minutes and then ramp down to 25°C at 5°C/min. The annealed oligos were diluted at a 1:200 dilution with sterile water or EB. Further, ligation reaction was set up and incubate at room temperature for 10 minutes. Ligation reaction contained 50 ng BsmBI digested plasmid, 1  $\mu$ l diluted oligo duplex, 5  $\mu$ l 2X Quick Ligase Buffer (NEB), 1  $\mu$ l Quick Ligase (NEB M2200S) and volume were made up 11 $\mu$ l with ddH<sub>2</sub>O.

#### **19.5 Transformation**

1.5  $\mu$ l ligated vector DNA was mixed very gently with 20  $\mu$ l competent Stbl3 bacterial cell, and incubated in ice for 30 minutes. After the incubation, heat shock at 42°C for 45 seconds was given and further tubes were put again on ice for 2 minutes. 50 $\mu$ l of SOC media was added and allowed to grow the bacteria at 37°C shaker for 60 minutes. Grown bacteria were plated on LB-Agar plates and allowed to grow on plates for 12 hours.

#### **19.6 Confirmation of the clones by colony PCR**

3 colonies per plasmid were picked up and set up the colony PCR reaction using forward primer from the vector plasmid and reverse primer from reverse guide RNA (Table 6). PCR condition were used: 94°C, 2 minutes, 94°C, 20 sec, 58°C, 20 sec, 68°C, 2 minutes, 72°C, 5 minutes, hold to 4°C. Further the amplified DNA will be resolved in 2% agarose gel and positive expected band size (125bp) were observed. Further, positive clones were selected and

amplified by Maxiprep as described above

**Table 6:** Reagent cocktail for colony PCR

<b>Forward Primer (100mM)</b> AATGGACTATCATATGCTTACC	1µl
<b>Reverse Primer (reverse guide RNA) (100mM)</b>	1µl
<b>Master Mix</b>	9µl
<b>Nuclease Free Water</b>	9µl
<b>Bacterial Colony</b>	---
<b>TOTAL</b>	20µl

### **19.7 Transfection, Transduction & Selection:**

3X10<sup>6</sup> HEK 293T cells were plated in 10cm dish with 10ml cDMEM (2plates/plasmid). HEK 293T cells with tranfected with 4 µg of pLentiCRISPR v2 encoding sgRNA against GFP (control) or human NLRP3, Caspase-1 and ASC and packaging plasmids pVSVg and psPAX2 (1 µg each). The reaction mixture detail is provided in Table 7. GFP plasmid were transfected as a control. After 6 hours transfection, 10 mL growth medium (cDMEM with 20% FBS) were replaced. After 48 hours post transfection, cell supernatant was collected and saved at 4°C and again 10 mL cDMEM medium will be added and then cell supernatant were collected at 72hrs post transfection and pool with the old medium. Therefore after 72 hours post transfection, 40 mL cell supernatant were observed. 1X10<sup>6</sup> HMEC-1 cells were plated in 6 well plate for transduction. Once all the viral supernatant (40 mL) were collected in 50 mL falcon tube, spin at 400g for 5 minutes. The supernatant was filtered using 0.22-micron filter with 60 mL syringe. The supernatants were balanced up to 1mg of the difference using the base cDMEM media and further centrifuged at 20,000g for 2 hours at 4°C to pellet the virus particle. Supernatants were thrown and resuspend the small virus pellet in 5 mL HMEC-1 growth media in the presence of polybrene (1:1000) and replaced the 6 well plated HMEC-1 media. Centrifuge the plates for 45 minutes at 2,000 g at 37°C. After centrifuge, plate was saved in CO<sub>2</sub> incubator. After 12 hours/overnight incubation, cells were tripsinized, washed and transferred to T75 culture flask with HMEC-1 media containing puromycin (1µg/mL) as

a starting antibiotic selection. Check the cells every 3 days and change the medium with puromycin.

**Table 7:** Transfection reaction cocktail

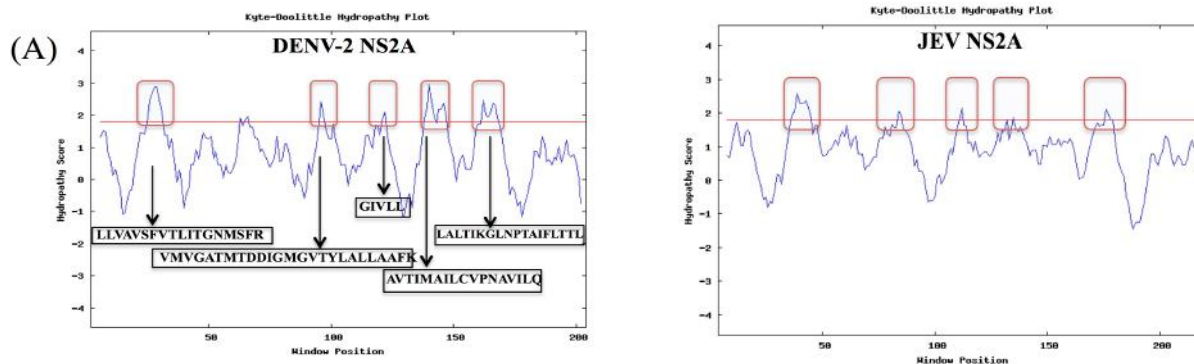
<b>Optimem</b>	200µl
<b>Lipofectamine 2000</b>	20µl
<b>pVSVg (AddGene 8454)</b>	1µg
<b>psPAX2 (AddGene 12260)</b>	3µg
<b>Plasmid DNA</b>	4µg

## RESULTS

### 1. *In silico* analysis of NS2A sequence of DENV-2 and Japanese encephalitis virus

#### ***In silico* analysis of DENV NS2A protein indicates that NS2A has pore-forming properties**

The main objective of the present study was to determine whether the full length NS2A protein possesses viroporin activity. To address this question, we performed an *in silico* analysis of the DENV NS2A protein to determine whether it exhibits the properties consistent with a role as a viroporin. NS2A of JEV, which possesses membrane-destabilising ability and behaves as a viroporin, was used for comparison. First, we generated hydropathy plots of the protein and analysis clearly revealed six putative membrane-interacting motifs with value more than 1.8 that further exhibited sequence similarity with JEV NS2A (Fig. 15A). Moreover, these six transmembrane regions were observed in the same positions along with the amino acid sequence similarity with JEV NS2A protein. Since the NS2A protein of JEV is known to modify the membrane permeability in different systems, we compared the protein sequences of the JEV and DENV NS2A proteins, revealing that they exhibited 26% identity and more than 50% similarity between them (Table 8). In addition, this analysis identified a number of amino acids in the transmembrane domains that were identical, or showed strong similarity, suggesting that the physicochemical properties of JEV and DENV are comparable thus, indicating that both the viral NS2A proteins have membrane-altering properties. Moreover, aromatic and basic residues, which are an important characteristic of viral proteins with membrane destabilising ability, were identified in both sequences (Fig. 15B). Subsequently, a topological representation of the DENV NS2A protein was generated which identified seven potential transmembrane regions. Furthermore, this analysis indicated that the amino and carboxyl-terminal domains of DENV NS2A orient towards the lumen of the endoplasmic reticulum and the cytoplasm, respectively (Fig. 15C). Notably, these findings are consistent with the topology of flavivirus NS2A proteins generated via various bioinformatics algorithms and corroborated by biochemical approaches. These *in silico* data suggest that the DENV NS2A protein possesses properties of pore-forming proteins.



(B)

```

# Length: 219
# Identity: 58/219 (26.5%)
# Similarity: 111/219 (50.7%)
# Gaps: 14/219 (6.4%)
# Score: 171.0
#
#-----

```

```

JEVNS2A      1  GLLVMPFLATQEVLRKRWTARLTIPAVLGALLVLMGGITYTDLARYVVLV      50
DENV2NS2A    1  GVLGMALFLEEMLRTRVGTKRHAILLVAVSFVTLITGNMSFRDLGRVMVMV      50
JEVNS2A     51  AAFAEANSGCCVHLHALIAVFKIQPNFLVMNMLSTRWTNGENVVLVGA     100
DENV2NS2A   51  GATMTD-DIGMGVTYLALLAAFKVRPTF-AAGLLLRKLTSKELMNTTIGI     98
JEVNS2A    101  ALFQASVDLQIGVHGELNAAAIAMWIVRAITFPPTSSVTPMLVALLTPG     150
DENV2NS2A   99  VLSQSTIPETI--LELTDALALGMMVLRKMKVQKMEKYQLAVTMAILCVP     146
JEVNS2A    151  MRALYLDTYRI---LLVIGICSLLOERKKTMAKKGAVLEGLAETSTGW     197
DENV2NS2A  147  NAVILQNAWKVSCITLAVSVSPLF----LTSSQOK-ADWIPALTIKG-     190
JEVNS2A    198  FSPTTIAAGLMVCNPNKKR      216
DENV2NS2A  191  LNPTAIFL--TTLRSTNKKR      208

```

(C)

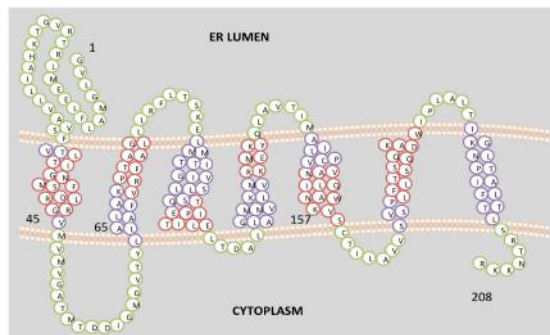


**TABLE 8:** Percent similarity and identity between JEV and DENV NS2A

SEQ	NAME	LENGTH	SEQ	NAME	LENGTH	SIMILARITY	IDENTITY
1	DENV-2 NS2A	218	2	JEV NS2A	227	50.7%	26.5%

**Fig 15. *In silico* analysis of the amino acid sequence of NS2A.** A. Hydropathy plots of the NS2A protein of Dengue virus (DENV), as generated via the Kyte-Doolittle method and DAS TM prediction algorithm using SOSUI software. Red boxes indicate the highly hydrophobic transmembrane regions of NS2A. B) Alignment of the amino acid sequences of NS2A from DENV and Japanese encephalitis virus (JEV), as generated using ClustalW software. Identical (\*), similar (.), and low-similarity (: ) amino acids were observed. C. Proposed model of NS2A topology generated using SOCS MEMSAT software. Trans-membrane segments are shown in purple, while the green colour indicates inter-transmembrane regions of NS2A. Regions highlighted in red denote highly hydrophobic, possible membrane interacting, transmembrane segments.

## 2. Cloning of NS2A protein in prokaryotic and eukaryotic system

Once we have determined *in silico* that NS2A protein could be possible viroporin, we cloned the NS2A in the above described plasmids. PCR amplified DENV-2 NS2A was resolved in 1% agarose gel as shown (Fig 16A). Further, amplified NS2A amplicon was cloned in pET151/D-TOPO vector as described in materials and methods. Additionally, NS2A sequence was subjected to clone in eukaryotic expression system vector with GFP tagged i.e pGFPN1 (Fig. 16B). The resultant clones were analyzed by restriction digestion with BamHI and Hind III and 650 bp segment was released as the NS2A in clone 6. The sequence was flanked with these two restriction enzyme sites as shown in the figure (Fig 16C). Later the verified clone was also verified via sequencing to check if the sequences were cloned in frame with the plasmid.

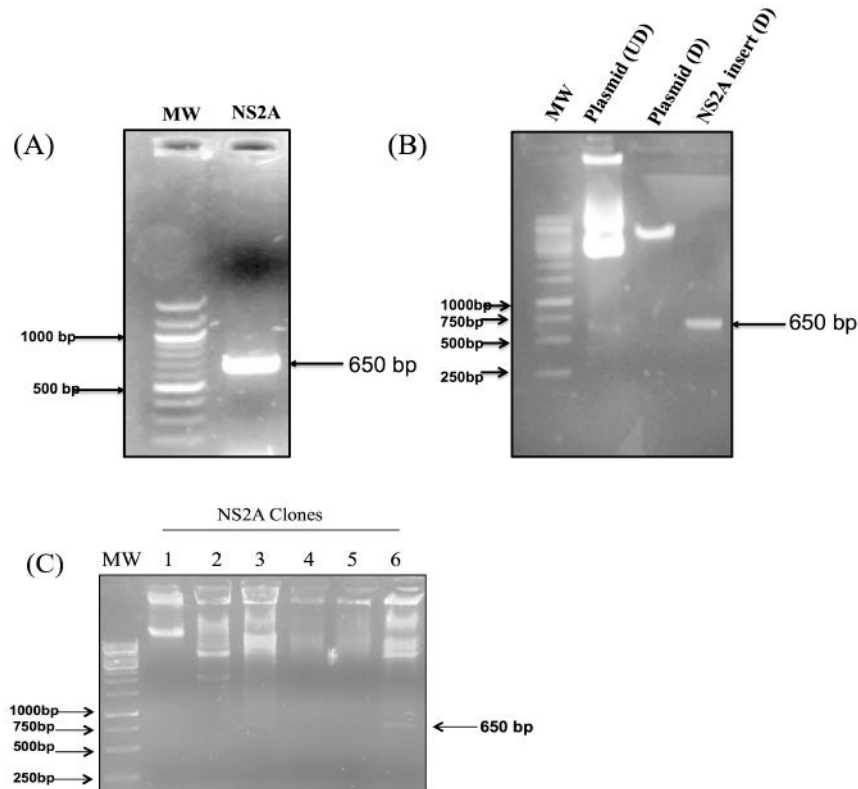


**Figure 16. Cloning of NS2A protein:** (A) PCR amplification of NS2A sequence (650bp) from cDNA clone of Dengue virus serotype 2 (B) Digestion and purification of pEGFPN1 Plasmid and insert (NS2A) (C) Restriction pattern obtained with HindIII and BamHI enzymes from transformed plasmid DNA clones of pGFPN1-NS2A, a fragment of 650bp was obtained.



### 3. Bacterial expression and purification of the DENV NS2A protein

To obtain sufficient recombinant DENV NS2A protein to evaluate its membrane-altering activity was transformed in *Escherichia coli* BL21 Star cells. Then the bacteria were transformed with NS2A-pET151/D-TOPO and induced with IPTG for a further 0, 4, 6, and 8 h post induction to check the optimal time of expression (Fig 17 A). These kinetic bacterial samples were analyzed in 15% SDS-PAGE to analyze the protein profile. We could not observe the clear band of 25kDa corresponding to NS2A in coomassie staining. Further, protein profile was analyzed by western blot, detected by anti-V5 antibody. The peak NS2A expression was found at 4 and 6 hours post induction as shown in figure (Fig 17 B). Thus, NS2A expression was purified at 6h post induction from a preparative gel by the elution of a band with the predicted molecular mass (25 kDa) (Fig 17 C). NS2A was further purified with nickel resin via its N-terminal 6 $\times$ His tag then analyzed by staining using coomassie blue, the presence of the 25-kDa band in the last recovered fraction confirm the presence of NS2A. The optimum time of NS2A expression were further used to obtain large quantity of proteins for further experiments. To address whether the NS2A protein is associated with bacterial membranes, we extracted membrane proteins using TDPC detergent. Further, to evaluate the presence of NS2A protein in the membrane fractions of inclusion bodies, western blots were then performed using an anti-V5 antibody to detect the presence of the NS2A protein in bacterial membranes (Fig 17 D). Subsequently, membranes were washed, stripped, and assessed by re-probing with a mouse polyclonal antibody against the *E. coli* OmpC membrane protein which detected a band of the predicted molecular weight (40 kDa), confirming that the NS2A protein is found in the membrane fraction, along with OmpC (Fig 17 E).

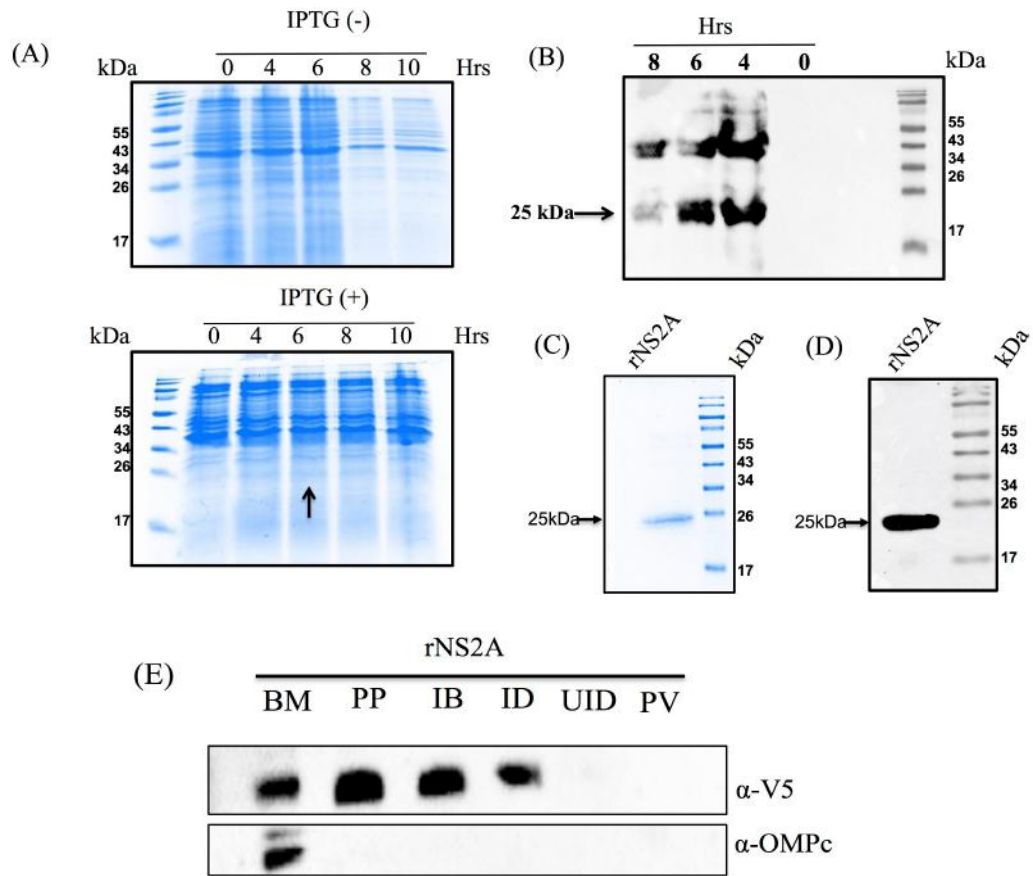


**Figure 17. Expression and purification of NS2A protein from bacteria and confirmation of NS2A association with bacterial membranes.** Cells were induced with IPTG or uninduced at different time points and analyzed at the indicated times postinduction by (A) SDS-PAGE (B) western blot analysis. The NS2A protein was detected using an anti-V5 antibody (dilution, 1:5000) (C). Analysis of recombinant NS2A protein (rNS2A) purification following different isolation steps by SDS-PAGE and Coomassie blue staining. Preparative gel electrophoresis was used for purification. Lane 1: purified fraction of NS2A obtained from preparative gels (molecular weight, approximately 25 kDa). (D) Recombinant NS2A protein (rNS2A) purification was analyzed by western blot. The NS2A protein was detected using an anti-V5 antibody (dilution, 1:5000) (E) Presence of the NS2A protein in bacterial membrane. Western blot analysis of NS2A protein expressed in *E. coli* using an anti-V5 antibody and a mouse polyclonal antibodies specific for OmpC (a protein resident in bacterial membranes). Lane 1 (BM): purified bacterial membranes Lane 2 (PP): purified NS2A protein Lane 3 (IB): Inclusion bodies of bacteria transformed with NS2A Lane 4 (ID): NS2A clone, induced with IPTG. Lane 5 (UID): NS2A clone, uninduced Lane 6 (PV): bacteria transformed with the parental vector.

#### 4. Production of polyclonal antibody against NS2A protein

Polyclonal antibody against NS2A was created to investigate the cellular localization of NS2A during the Dengue viral infection. To do this, rats and rabbits were immunized 4 times with 150  $\mu\text{g}$  of NS2A recombinant proteins in interval of 15 days with Freund adjuvant. Antibody response against NS2A were analyzed and shown in figure (Fig 18 A, B). We evaluated the antibody response against the NS2A in the serum after 3rd immunization. To evaluate whether polyclonal serum recognize the NS2A viral protein, HMEC-1 and Vero cells were infected with DENV-2 and cell lysates were resolved in 15% SDS gel and western blot was performed utilizing hyper immune serum described above. A band size of  $\sim 34$  kDa was observed in both HMEC-1 and Vero cells infected with DENV-2 instead of 25 kDa NS2A band expected (Fig 18 C). Data suggest that the band of  $\sim 34$  kDa could be due to incomplete processing of NS2A. As a positive control, recombinant protein was resolved in SDS PAGE and in western blot  $\sim 25$  kDa band was observed suggested that polyclonal antibody is functional and detects the NS2A protein.

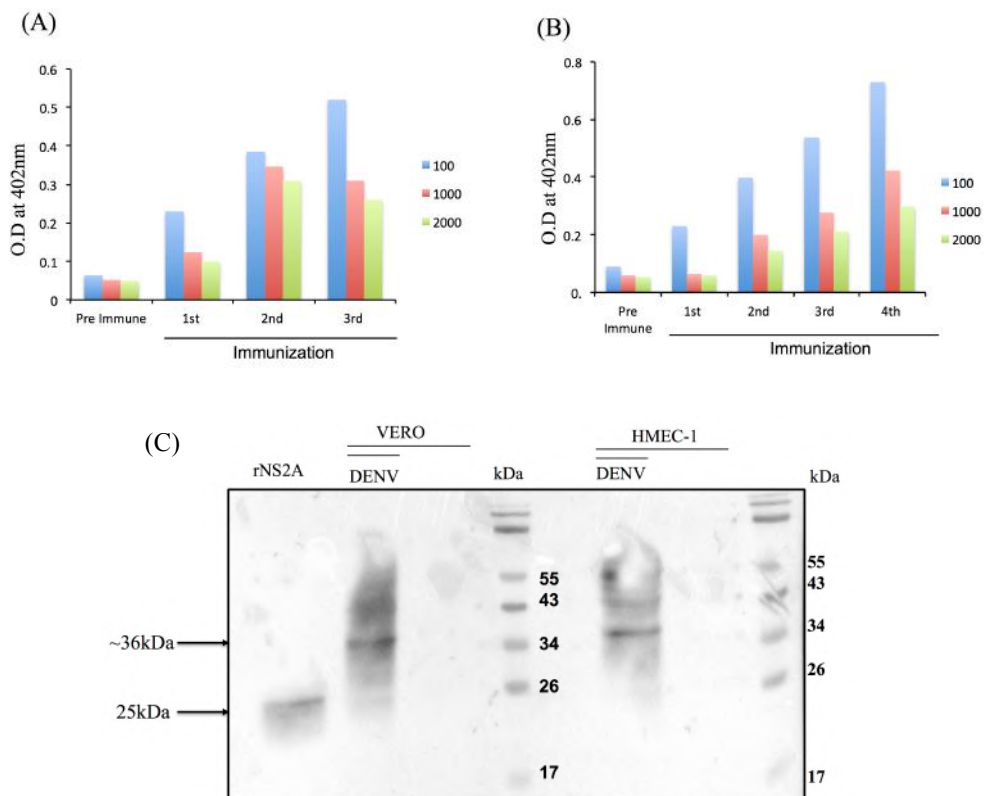


**Fig 18. Production of a polyclonal antibody against the NS2A protein.** Evaluation of polyclonal serum during the immunization by an ELISA assay (A) Rat (B) Rabbit. Different dilutions of this serum were evaluated (1:00, 1:1000, 1:2000). (B) Evaluation of NS2A rabbit polyclonal serum (1:1000) in DENV-2 infected HMEC-1 cells or VERO cells lysates, the serum recognized the viral protein NS2A, and the recombinant protein NS2A-V5 as a positive control.

## 5. Evaluation of lytic activity of NS2A in E.Coli

In prokaryotic systems such as *E. coli*, bacterial growth can be altered directly by the expression and subsequent incorporation of viroporins within bacterial membranes, leading to a loss of membrane integrity. As first approach we analyze the homology between DENV and JEV NS2A. We therefore evaluated whether DENV NS2A also possesses membrane-destabilising activity, by transforming *E. coli* BL21 (DE3) pLysS cells, which express bacteriophage T7 lysozyme, with a plasmid encoding NS2A protein or control plasmids (Fig 19 A). In this system, disruption of the inner bacterial membrane triggers lysozyme release resulting in cell lysis. As expected, transformation of *E. coli* with the parental vector (pET) or with a vector expressing a soluble polypyrimidine-tract binding (PTB) protein (RNA-binding protein found only in the cytosol; negative control) had no effect on bacterial cell growth (Figure 19 B). Likewise, cells harbouring the NS2A expression vector showed no significant defect in cell growth rates when cultivated in the absence of the inducing agent IPTG. In contrast, the growth rates of cells expressing NS2A were markedly lower than those of the PTB and pET controls when culture was induced with IPTG, indicating that this protein is capable of permeabilising intracellular membrane (Fig 19 B). This data provide the first evidence that NS2A shows pore-forming activity when expressed in a bacterial system.

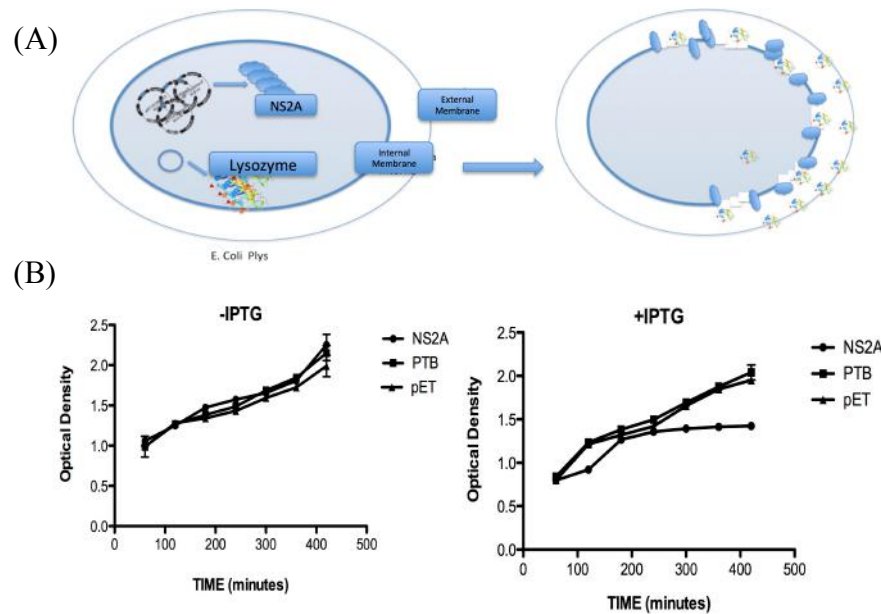


**Figure 19: NS2A protein expression arrests the growth of *E. coli* and affects the permeability of bacterial membranes.** (A) NS2A membrane permeability model (B) Growth curves of engineered *E. coli* BL21 pLys transformed with NS2A, pET, and PTB constructs in the absence (left) or presence (right) of IPTG. The cellular density of bacterial cultures was determined every 100 min after induction by measuring optical density at 660 nm.

## 6. Oligomerization of NS2A Protein

Conserved characteristics of viroporins include the presence of hydrophobic domains that interact with lipid membranes and the ability to oligomerize once inserted into cell membranes to form a structure in the form of pores. There are several reports of viroporin oligomer stabilization in the presence of glutaraldehyde crosslinking. To determine whether NS2A resembles a viroporin, we evaluated whether increasing concentrations of glutaraldehyde stabilizes NS2A concatamers. Western blots for NS2A treated with different concentration of glutaraldehyde revealed two or three bands (Figure 3B, lanes 1–3), which migrated as expected for monomers (25 kDa), dimers (50 kDa), and pentamers (~125 kDa) of the protein. In addition, it is important to make clear that NS2A dimer is observed without the treatment of glutaraldehyde crosslinking suggest that NS2A protein forms oligomers spontaneously and its the nature of NS2A protein. This result indicates that the NS2A protein oligomerizes in association with cellular membranes (Fig 20 A).

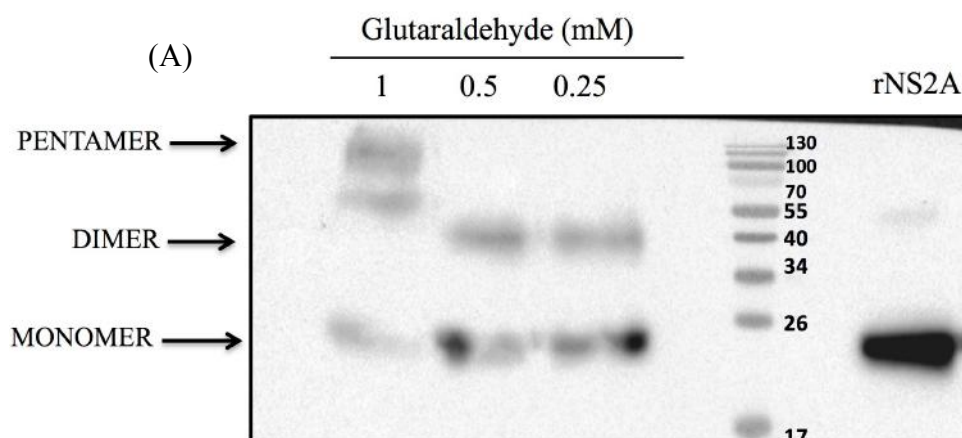


**Fig 20: Oligomerization of NS2A protein.** (A) Purified NS2A protein was incubated with different concentrations of glutaraldehyde (0.25, 0.5, and 1 mM). The samples were resolved in SDS-PAGE under reducing conditions, and protein expression analysed by western blotting. Then, oligomeric structures (dimers and pentamers) were detected using anti-V5 antibody at a dilution of 1:5000.

## 7. Evaluation of Lytic activity of NS2A in eukaryotic membrane

Pertaining to the above results, which demonstrated that the NS2A protein forms at least pentameric structures, we produced liposomes (artificial membranes) that mimics the eukaryotic plasma membrane (Fig 21 A). Therefore, we examined the ability of NS2A to induce membrane permeability in liposomes, charged with FITC. After purification, NS2A protein was first subjected to treatment with different solvents; the protein dissolved well in methanol and was active in liposomal mixtures. NS2A (119–714 nM) was then incubated with liposome-encapsulated FITC (25  $\mu$ M). For these analysis, untreated liposomes were utilised as a control for auto-fluorescence, while FITC-labelled liposomes treated with PTB (98.25 nM) or Triton-X 100 were utilised as negative and positive controls, respectively. The maximum signal derived was compared with the fluorescence signals obtained from liposomes incubated with the different concentrations of NS2A protein and was expressed as a percentage of the maximum signal derived from the positive control sample. There was a protein concentration-dependent increase in fluorescence signal obtained from liposomes incubated with NS2A, with the highest level of FITC leakage (75%) being observed in those incubated with 714.29 nM NS2A (Fig 21 B). The NS2A-dependent release of FITC was also time-dependent, reaching a

plateau within 10 min. Thus, these data provide further evidence that NS2A acts as a membrane permeability virulence factor.

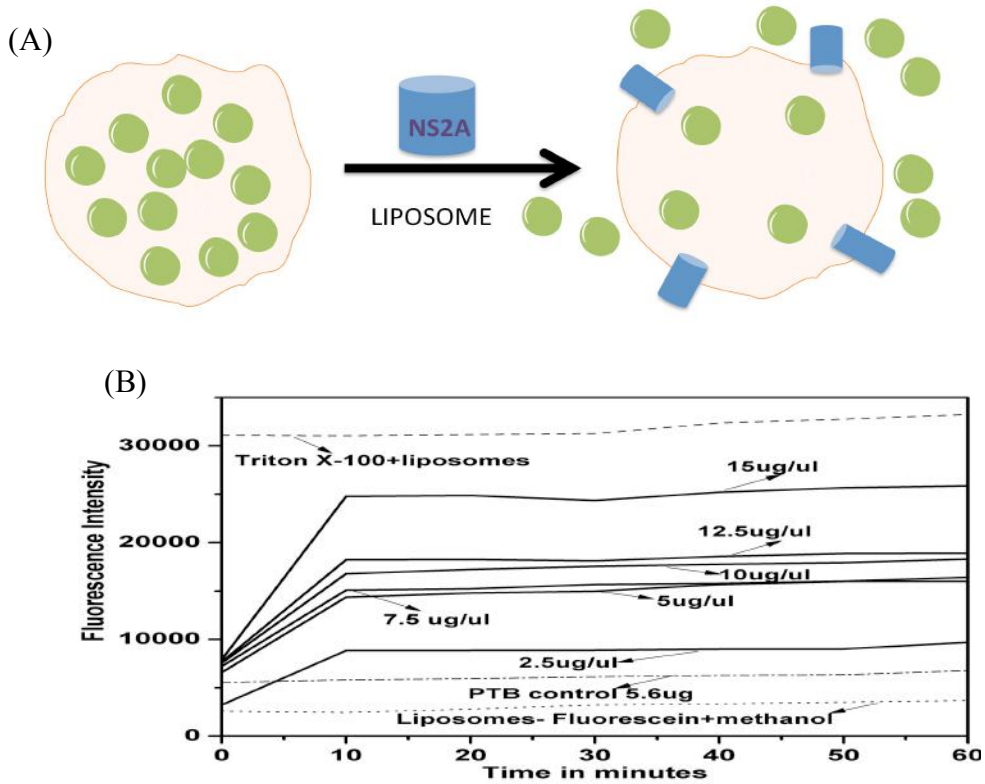
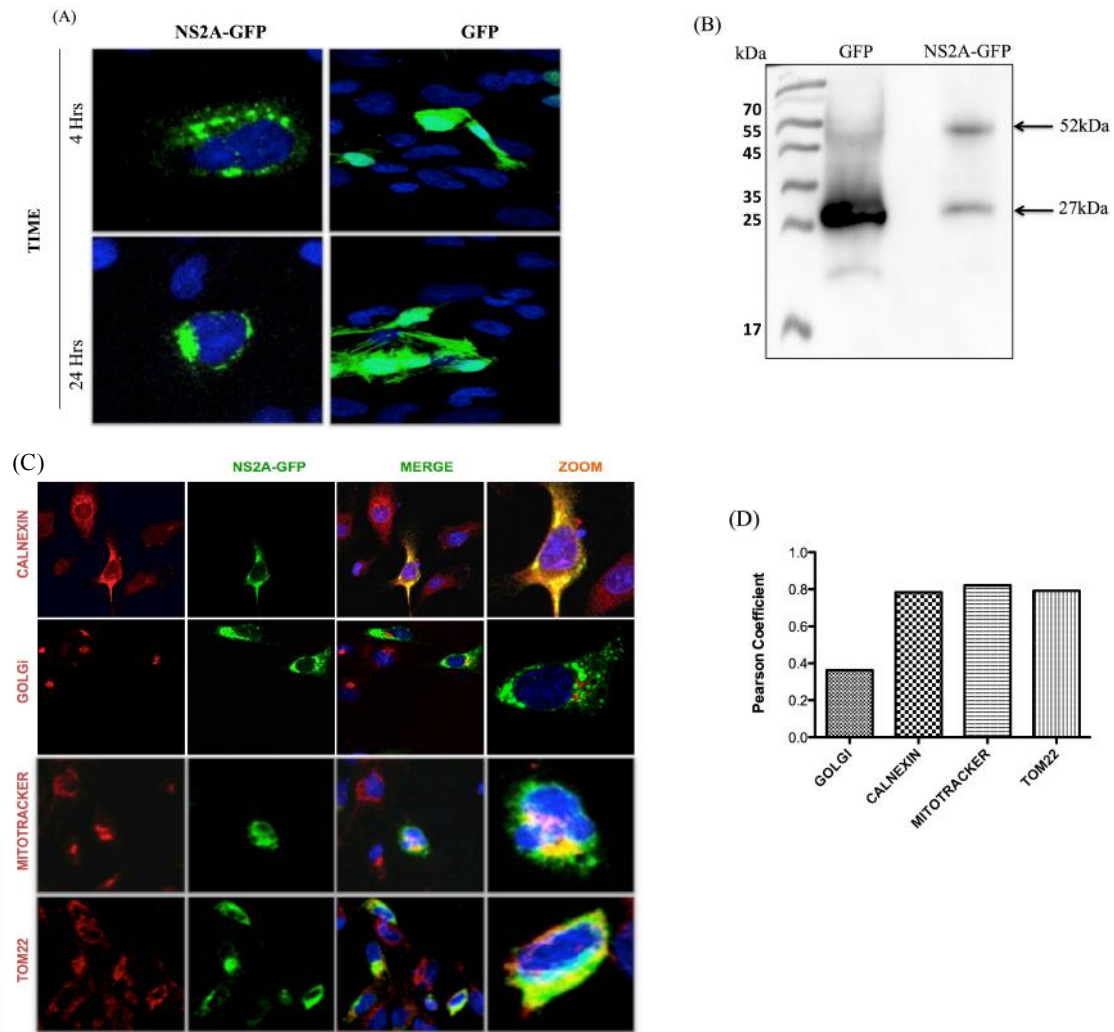


**Fig 21: NS2A lytic effect on Liposome:** Membrane disruption was examined by encapsulating FITC in liposomes (a model for eukaryotic cell membranes). FITC encapsulated liposomes were incubated in solutions containing either Triton X-100 (positive control), different concentrations of NS2A (2.5–15  $\mu\text{g}/\mu\text{l}$ ), or PTB protein (5.7  $\mu\text{g}/\mu\text{l}$ ; negative control). Protein mediated disruption was monitored every 10 min by measuring the fluorescence emission. Protein disruption studies were performed using 5  $\mu\text{L}$  of FITC encapsulated liposomes to determine baseline fluorescence intensity. Fluorescence was monitored using a Synergy H4 Fluorescence reader, equipped with a FITC 485 excitation filter, a FITC 535 emission filter, and a 50/50 beam splitter. Fluorescence values were read every 30 s for 1 h at 37°C.

## 8. Expression and localization of NS2A-GFP in HMEC-1 cells

The expression of NS2A-eGFPN1 construct (NS2A-GFP) was addressed in HMEC-1 cells using immunofluorescence and western blot. To do this, NS2A-GFP and eGFPN1 plasmids were transfected in HMEC-1 cells and analyzed at different times (4 hrs and 8 hrs ) using fluorescence microscope. The expression of NS2A-GFP was observed in perinuclear space in HMEC-1 cells at both time points demonstrate its functional expression in cytoplasmic region (Fig 22 A). In addition, NS2A-GFP, eGFPN1 transfected cells were lysed, resolved in 15% SDS PAGE and analyzed by western blot using anti GFP antibody. A sharp band with expected 27 kDa was observed in eGFPN1-transfected cells showing the expression of GFP protein in contrast to 2 bands one of the 27 kDa and other 53 kDa band was observed in NS2A-GFP transfected cells. This data suggest the expression of fusion NS2A-GFP protein (Fig 22 B). As DENV NS2A protein was predicted to associate with the membranes of various organelles. Owing to the difficulties in obtaining specific antibodies against hydrophobic antigens such as the NS2A protein, we utilized the NS2A-GFP plasmid to determine its subcellular localization by transfection into HMEC-1 cells Thus, we used different organelle marker for endoplasmic reticulum, golgi and mitochondria. The immunofluorescence signal representing NS2A exhibited significant overlap with that of calnexin A, which is a transmembrane protein that resides in the ER membrane that serve as a marker of ER membrane, indicating that NS2A partially locates to the ER network. Interestingly, NS2A also co-localised with a marker associated with mitochondria (MitoTracker) and Tom22, an outer mitochondrial membrane protein. In contrast, NS2A did not co-localize with a Golgi apparatus marker (GOLGI) (Fig 22 C). Hence, our co-localization studies indicated that the NS2A protein localizes to both the ER and mitochondria organelles with Pearson's coefficient values of 0.79 and 0.81 respectively (Fig 22 D); this localization is similar to previously reported observations for other viroporins. The Pearson's coefficients between NS2A and the different markers analysed was calculated as an average value from 20 individual cells. Taken together all the experiments suggested that NS2A is a viroporin.

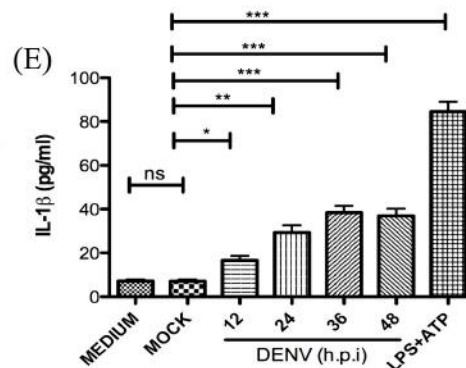
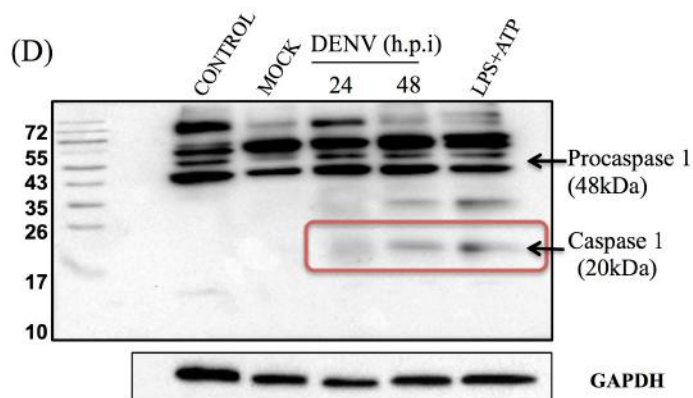
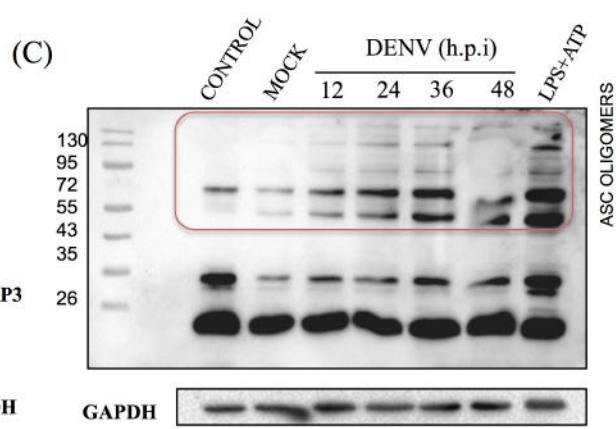
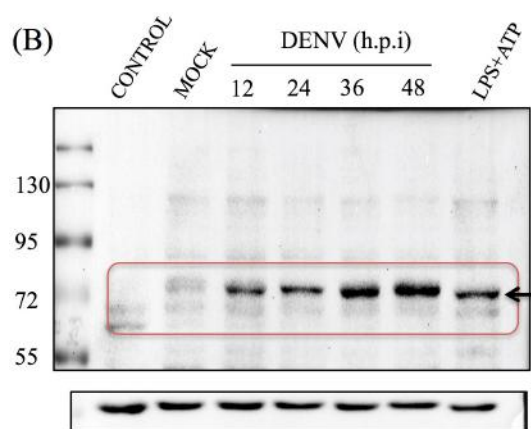
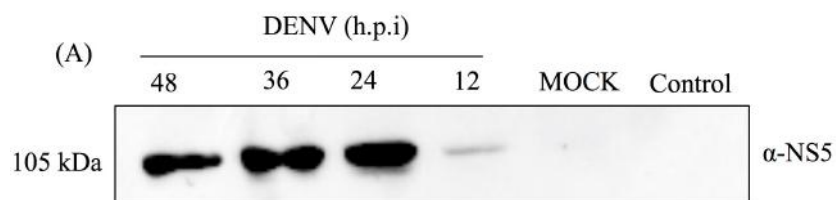




**Fig 22: Expression and localization of NS2A protein in HMEC-1 cells.** (A) HMEC-1 cells were transiently transfected with the plasmids coding for the NS2A-GFP and GFP protein (control) for 4 and 24 hours. Cells were fixed and analyzed by confocal microscopy. (B) HMEC-1 cells were transiently transfected with the plasmids coding for the NS2A-GFP and GFP protein and lysates were analyzed by western blot using anti-GFP antibody (1:1000). Lane 1: molecular weight (MW), Lane 2: GFP transfected lysate, Lane 3: NS2A-GFP transfected Lysate showing band of GFP (27 kDa) as well as NS2A-GFP (52 kDa). (C) To evaluate the localization of the NS2A protein, HMEC-1 cells were transfected with a plasmid encoding GFP-tagged DENV-2 NS2A and stained with either anti-calnexin (ER Marker; red), anti-GM (Golgi marker; red), mitotracker (mitochondrial marker; red) or TOM22 (mitochondrial outer membrane marker) and observed with a confocal microscope 24 h after transfection. (D) Pearson Coefficient of the NS2A-GFP localization in different membrane organelles.

## 9. Dengue activates the NLRP3 inflammasome:

In order to characterize the experimental conditions, microvascular endothelial cells (HMEC-1) cells were infected with Dengue virus serotype 2 (DENV-2) at different time frames. Cell lysates from infected cells were resolved in 10% SDS gel and further western blot was analysed using monoclonal antibody against NS5 demonstrated the presence of infection as NS5 band was observed after 12 hrs of infections (Fig 23 A). Further, to determine whether DENV-2 activates the NLRP3 Inflammasome, HMEC-1 was infected with DENV-2 and mock at different time point and cell lysates were resolved in 10% SDS gel and western blot was analyzed using anti-NLRP3 antibody. During the infection of DENV-2, high expression of NLRP3 was observed at late phase (36hrs, 48hrs) of virus life cycle, in contrast to HMEC-1 cell and mock-infected cell where no/low expression of NLRP3 was observed. In the positive control, high expression of NLRP3 was observed in HMEC-1, treated with LPS (2 $\mu$ g/ml) followed by ATP that provides signal 1 and signal 2 respectively to induce the formation of inflammasome complex (Fig 23 B). In continuation, to analyze the oligomerization of ASC adapter protein, cell lysates were resolved in 15% SDS gel and western blot was analyzed using anti ASC antibody. We observed the ASC oligomerization in the cell lysates infected with DENV-2 at 24 hrs, 36hrs and 48hrs post infection as well as in the cells treated with LPS and ATP, in contrast to HMEC-1 and mock-infected cells where ASC oligomerization was not observed (Fig 23 C). Additionally, the detection of active caspase 1 (~20kDa) was observed at 24 hrs and more prominent band was observed at 48 hrs post infection with dengue virus (Fig 23 D). Once caspase-1 is activated, caspase-1 further process pro-1L-1 $\beta$  to 1L-1 $\beta$ . Therefore to check the activation of pro-1L-1b to active 1L-1 $\beta$  by caspase 1, we measured 1L-1 $\beta$  secretion in cell supernatant and we observed significant increase in 1L-1 $\beta$  at 36 and 48 hrs post infection in cell supernatant of DV-2 infected cells when compared with mock infected cell supernatant (Fig 23 E). ASC punctate structures have been shown in several studies as a marker of “Inflammasome complex” formation. Therefore to confirm the above results, HMEC-1 cells were infected with mock or DENV-2 at different time points and demonstrated the ASC punctate structures in the cells infected with DENV-2 at 36 hrs and 48 hrs in contrast to mock infected cells (Fig 23 F). Number of ASC per cell was counted (Fig 23 G). Together these results demonstrated the role of DENV-2 in the activation of NLRP3 inflammasome in endothelial cells.



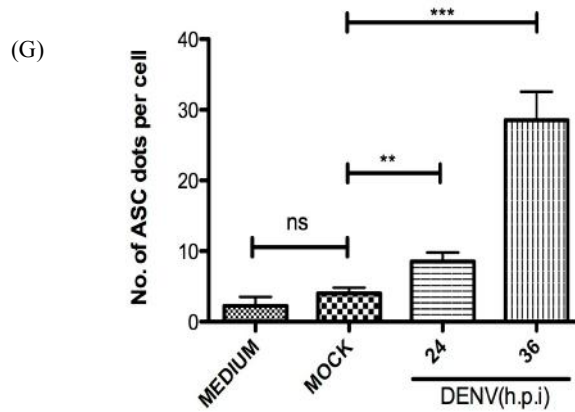
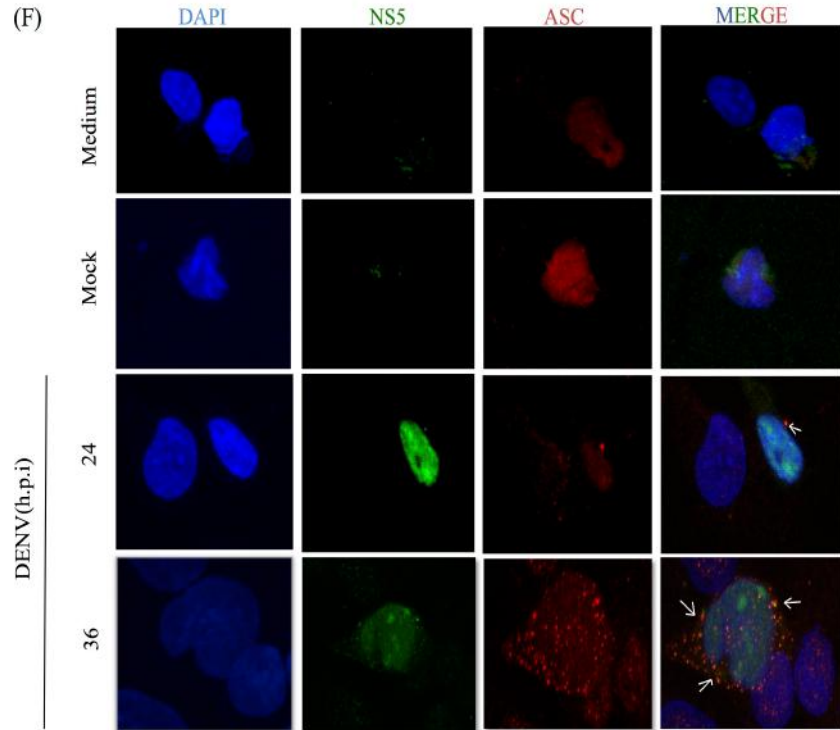
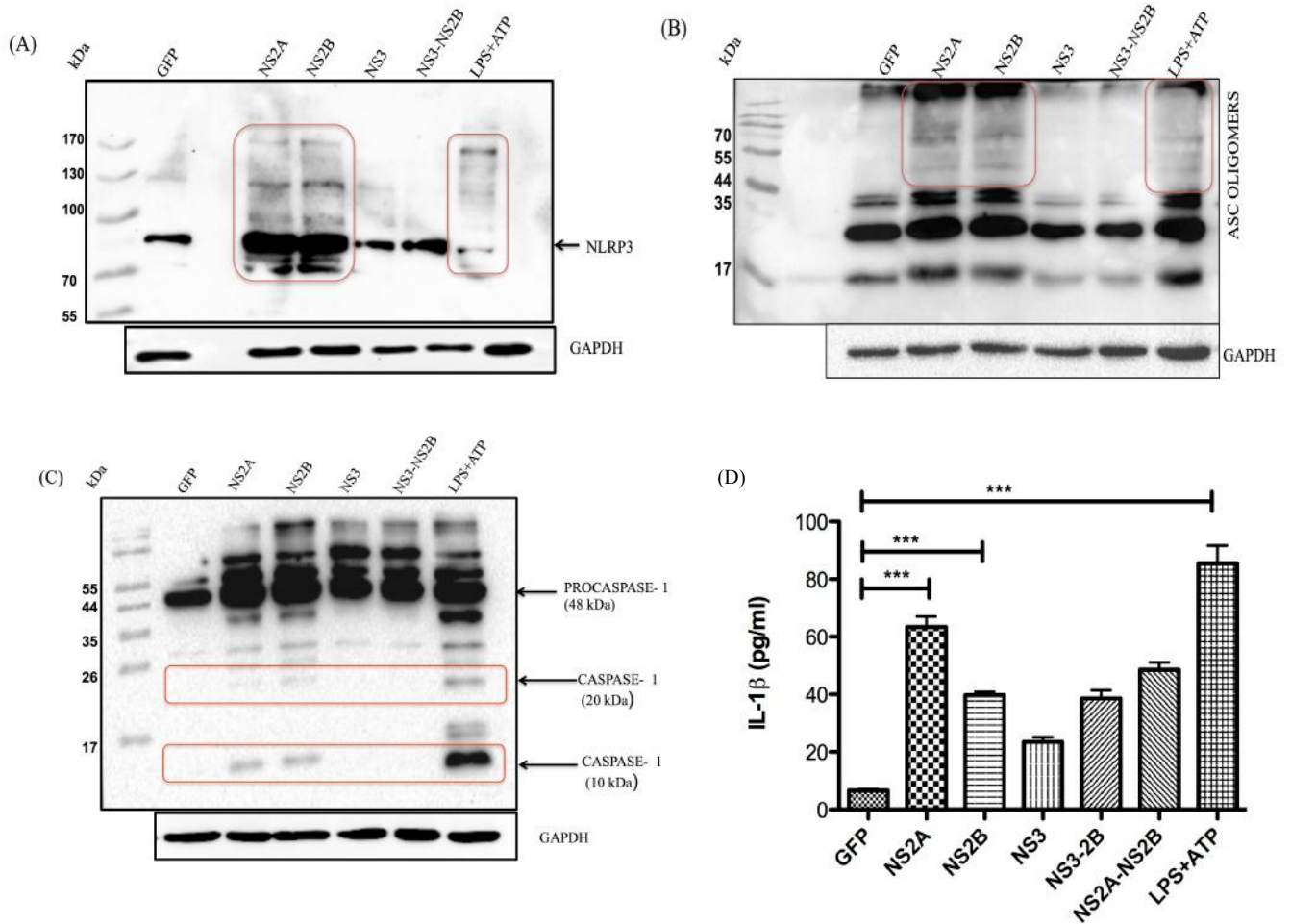


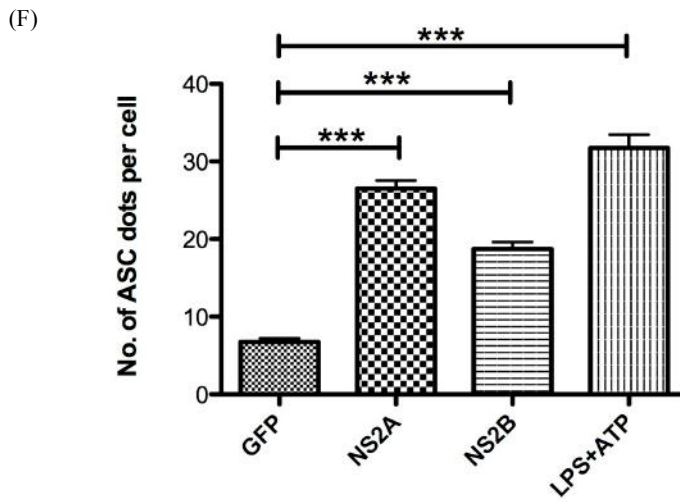
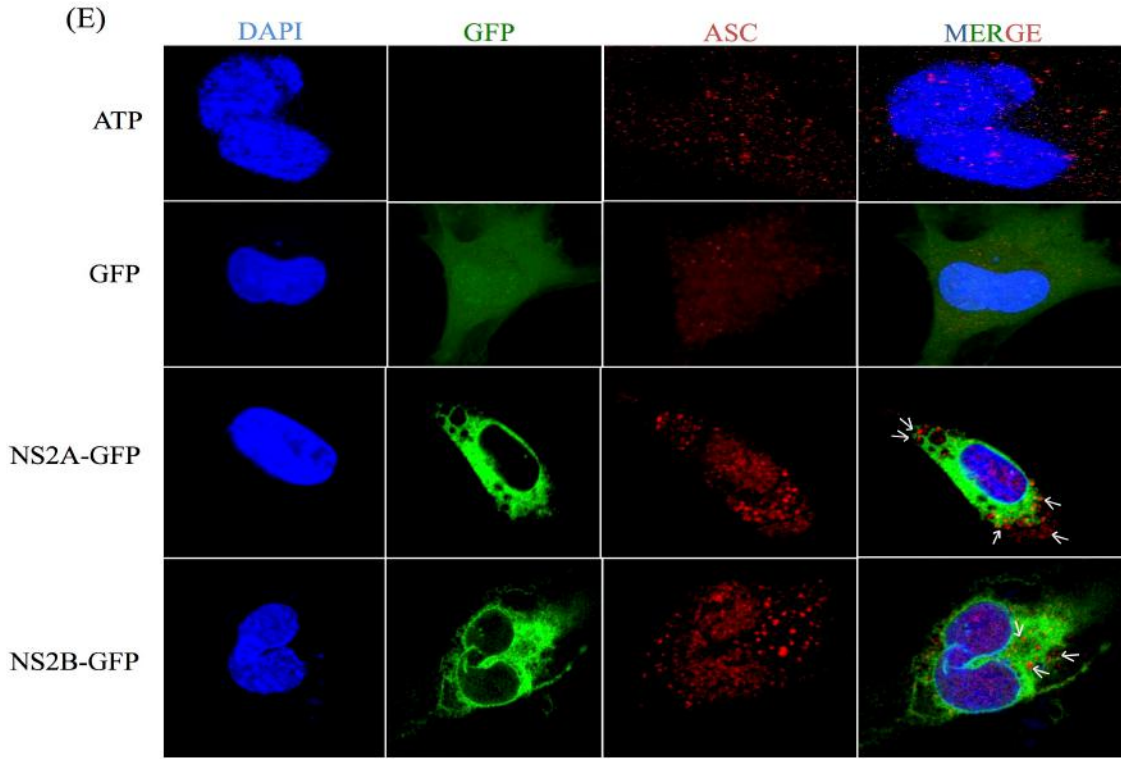
**Fig 23: NLRP3 inflammasome activation by DENV-2** (A) HMEC-1 were infected with DENV-2 at the MOI of 5 and the cell lysates were analyzed by anti-NS5 antibody (B) HMEC-1 were infected with DENV-2 at MOI of 5 at different time point or mock infected or treated with LPS (5µg/ml) and ATP (5mM) as a positive control and the cell lysates were analyzed by western blot using anti-NLRP3 antibody (1:500) (C) anti-ASC antibody (1:1000) (D) anti-caspase-1 antibody (1:1000). (E) HMEC-1 were infected with DENV-2 at the MOI of 5 at different time point or mock infected or treated with LPS (5µg/ml) and ATP (5mM) as a positive control and cell-free supernatants were collected at 12 hrs, 24hrs, 36hrs, 48 hrs after infection and analyzed for 1L-1β by ELISA. (F) HMEC-1 were infected with DENV-2 at the MOI of 5 at 24hrs and 36hrs or mock infected. Cells were stained with anti-NS5 (green) and anti-ASC (red) and analyzed by a confocal microscopy. Mock-treated cells were also examined. Nuclei were visualized by staining with DAPI. (G) Number of ASC dots per cell was calculated by a confocal microscopy. Data are representative of at least three independent experiments, and indicate the mean ± S.D.(E,F). \*, P<0.05; \*\*, P<0.01; \*\*\*, P<0.001.

## 10. NS2A and NS2B proteins activate NLRP3 inflammasome

In our previous articles, we have reported that dengue NS2A and NS2B protein act as viroporin (197) (50) and several viroporins have been demonstrated to activate inflammasome during viral infection. Thus, we hypothesized that dengue virus viroporin NS2A and NS2B may trigger inflammasome activation either by altering intracellular ionic concentration or by inducing ROS from mitochondria. To evaluate this hypothesis, HMEC-1 were primed with LPS (signal 1) followed by the transfection with several GFP tagged plasmid expressing dengue NS2A, NS2B, NS3, NS32B, NS2A-NS2B proteins. Western blot analysis demonstrated the higher expression of NLRP3, oligomerization of ASC, and activation of caspase-1 from LPS primed HMEC-1 cells transfected for 36 hrs with NS2A or NS2B expressing vectors, but not from transfected with other GFP tagged protein vectors. ATP (5 mM) was used as a positive control as a inducer of NLRP3 inflammasome (Fig 24 A, B, C). Cell free supernatants were collected at 36 h post-transfection and analyzed for the presence of IL-1 $\beta$  using an enzyme-linked immunosorbent assay (ELISA). A standard curve was constructed using a serial dilution of IL-1 $\beta$  standards and used to calculate IL-1 $\beta$  concentrations in the collected samples. Significant IL-1 $\beta$  was released from LPS primed HMEC-1 cells transfected with NS2A or NS2B expressing vectors, in contrast with HMEC-1 cells transfected with other GFP tagged protein vectors (Fig 24 D). This data suggest the role of viroporins NS2A and NS2B in activating inflammasome components (NLRP3, ASC, Caspase-1) and subsequently release of IL-1 $\beta$ . To support the above results we also examined the oligomerization of ASC, caspase-1 activation and inflammasome complex activation by NS2A and NS2B. To do this, HMEC-1 were first primed with LPS for 6 hours followed by either transfection with GFP-plasmid or GFP tagged NS2A and NS2B. We have shown that ASC punctate structures were formed in the cytoplasm of HMEC-1 cells transfected with the plasmid expressing the NS2A-GFP and NS2B-GFP in contrast to the cells transfected with GFP expressing cells, did not express ASC punctate structure (Fig 24 E). As a positive control, HMEC-1 were treated with ATP for the 45 mins for the presence of ASC punctate structures. Number of ASC per cell was counted (Fig 24 F). We also examined the intracellular localization of NLRP3. In HMEC-1 cells, NLRP3 expression was observed in the cytosol, however in cells transfected with dengue NS2A for 36 hours, NLRP3 was redistributed to the perinuclear region or cytoplasmic granular structures,

which are considered as a hallmark of NLRP3 activation. Further, we have demonstrated that NLRP3 was colocalized with NS2A-GFP in HMEC-1 cells with in contrast to either GFP or NS2B-GFP. 60% cells expressing the NS2A-GFP showed the colocalization with NLRP3 and the co-localization between NS2A-GFP was found to very strong as strong (0.8427) pearson coefficient was observed (Fig 24 G). Together, these data provide the evidence that the dengue virus viroporin NS2A and NS2B are able to trigger NLRP3 inflammasome activation and secretion of 1L-1 $\beta$  from LPS-primed HMEC-1.





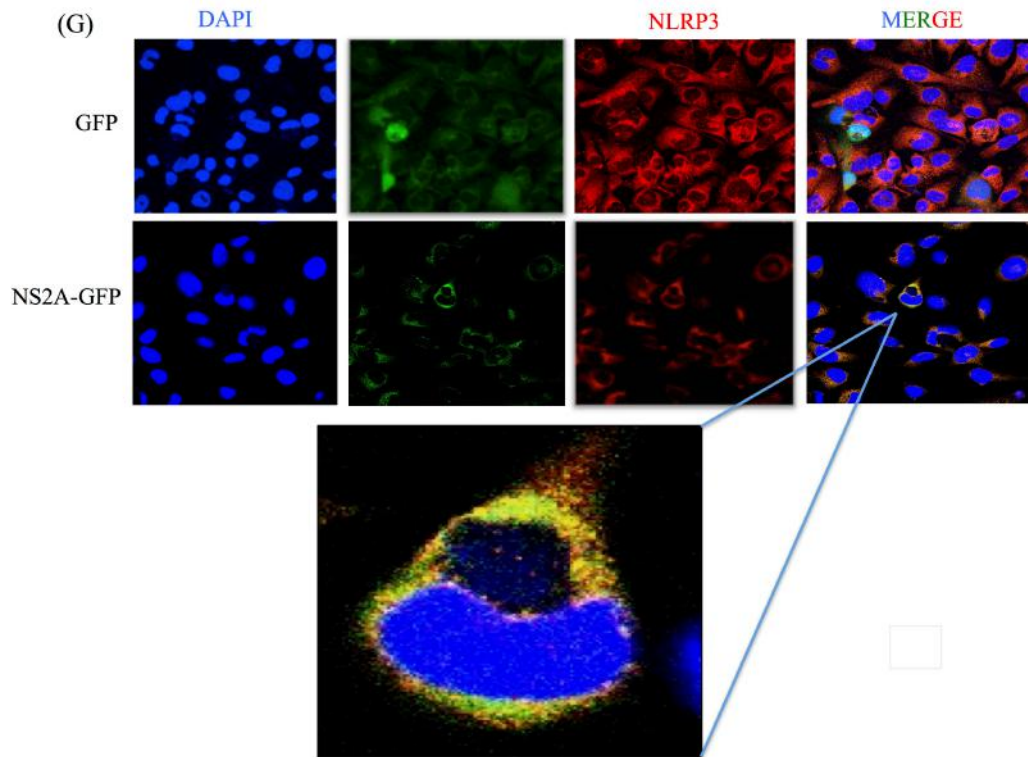
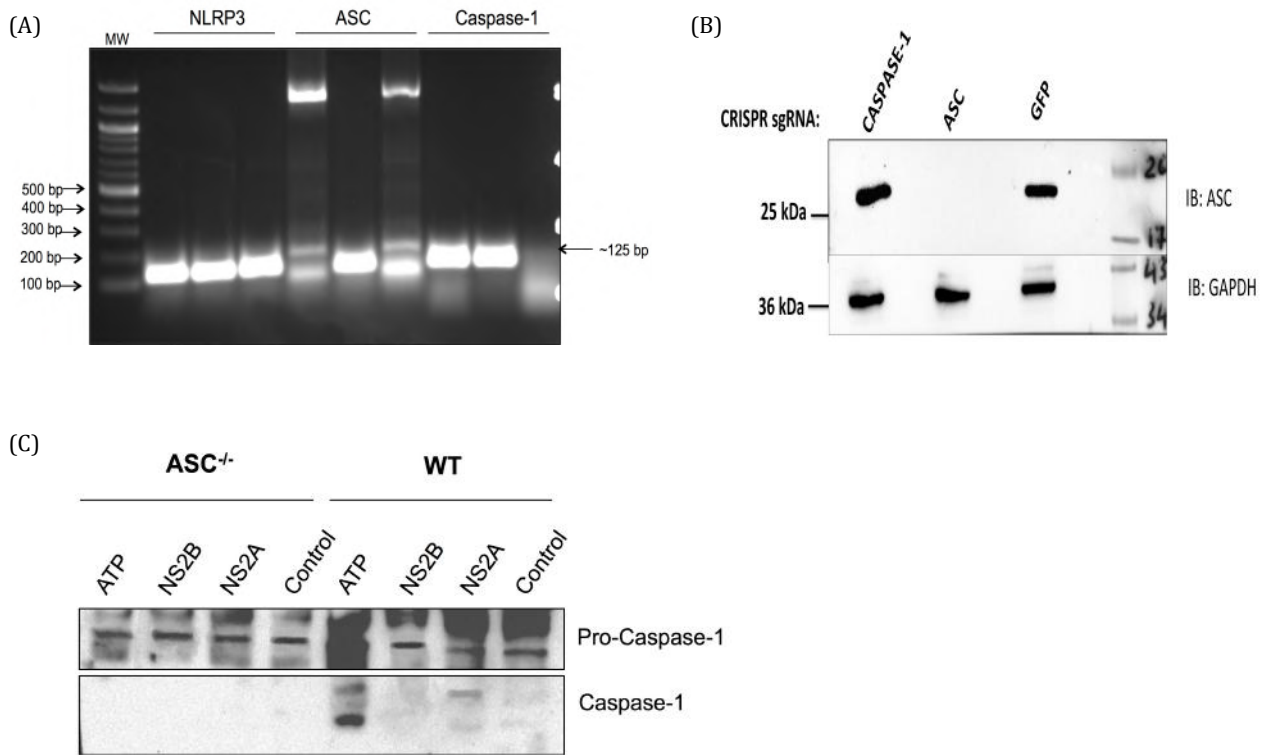


**Fig 24: NLRP3 inflammasome activation by DENV viroporin NS2A and NS2B** (A) HMEC-1 cells were transfected with the expression plasmid encoding GFP-tagged DENV-2 NS2A, NS2B, NS3, NS3-NS2B or or pEGFPN1 empty vector for 36 hrs or treated with LPS (5 $\mu$ g/ml) and ATP (5mM) as a positive control and the cell lysates were analyzed by western blot using (A) anti-NLRP3 antibody (1:500) (B) anti-ASC antibody (1:1000) (C) anti-caspase-1 antibody (1:1000). (D) HMEC-1 cells were transfected with the expression plasmid encoding GFP-tagged DENV-2 NS2A, NS2B, NS3, NS3-NS2B or or pEGFPN1 empty vector for 36 hrs or treated with LPS (5 $\mu$ g/ml) and ATP (5mM) as a positive control and the cell free supernatant was analyzed for 1L-1 $\beta$  by Elisa. (E) HMEC-1 cells were transfected with the expression plasmid encoding GFP-tagged DENV-2 NS2A, NS2B or pEGFPN1 empty vector for 36 hrs or treated with LPS (5 $\mu$ g/ml) and ATP (5mM) as a positive control and the cells were stained with anti-ASC (Red) and analyzed by a confocal microscope. (F) Number of ASC dots per cell was calculated by a confocal microscopy. (G) HMEC-1 cells were transfected with the expression plasmid encoding NS2A-GFP or GFP for 36 hrs. Cells were stained with anti-NLRP3 (Red) and analyzed by confocal microscope. Nuclei were visualized by staining with DAPI. Data are representative of at least three independent experiments, and indicate the mean  $\pm$  S.D. (D,F). \*, P<0.05; \*\*, P<0.01; \*\*\*, P<0.001.



## 11. Confirmation of viroporin effect in activating inflammasome by CRISPR-CAS9

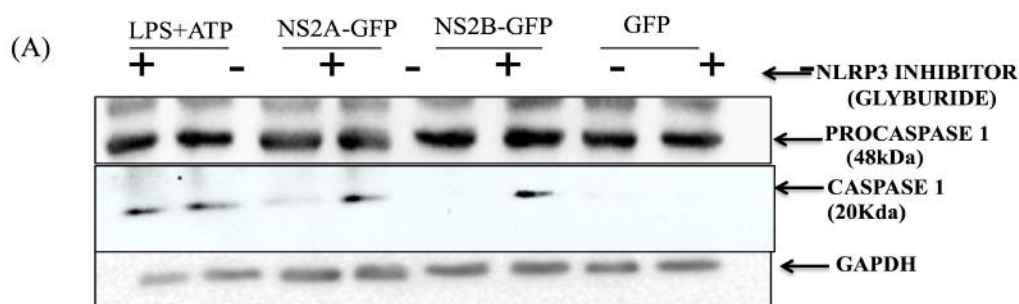
To confirm the effect of NS2A and NS2B in inducing NLRP3 inflammasome, HMEC-1 cells were knocked out with human NLRP3, Caspase-1 and ASC gene. To do this, guide RNA specific to NLRP3, Caspase-1 or ASC were cloned in lentiCRISPRv2 plasmid according to the protocol discussed above. To confirm the positive clones, 3 random transformed bacterial colonies per gene were taken and colony PCR was done using forward primer of lentiCRISPRv2 vector and reverse primer of the specific gene of interest (NLRP3, Caspase-1, ASC). We have obtained the band of ~125bp showing the positive clones of the NLRP3, Caspase-1 and ASC (Fig 25 A). Further, positive clones were picked up and plasmid was made according to protocol. The lentiCRISPRv2 plasmid containing sgRNA of NLRP3, caspase-1 and ASC were transfected and further transduced in HMEC-1 cells. To confirm the knockout of NLRP3, Caspase-1, ASC, lysates of HMEC-1 cell expressing NLRP3, Caspase-1, ASC were analyzed by western blot and observed that HMEC-1 cells transduced with lentiCRISPRv2-ASC were completely knocked out with ASC gene (Fig 25 B). ASC<sup>-/-</sup> HMEC-1 cells were selected to analyze the inflammasome activation due to NS2A and NS2B. To do this, ASC<sup>-/-</sup> HMEC-1 cells or WT HMEC-1 cells were primed with LPS 2µg/ml for 6 hours followed by transfection with GFP, NS2A-GFP and NS2B-GFP for 36 hours. As positive control cells were primed with LPS 2µg/ml for 6 hours followed by 5mM ATP for 45 mins. Lysates were analyzed in western blot and demonstrated the activation of caspase-1 due to NS2A and ATP in WT HMEC-1 cells in contrast to ASC<sup>-/-</sup> HMEC-1 cells (Fig 25 C). This result confirms the effect of NS2A in activating the inflammasome and activation of caspase-1.



**Fig 25: Confirmation of inflammasome activation by viroporin by CRISPR-CAS 9.** (A) Colony PCR of transformed clone of lentiCRISPRv2 with NLRP3, Caspase-1, ASC. Amplified PCR were resolved at 0.8% agarose gel. (B) HMEC-1 lysates expressing lentiCRISPRv2-GFP/Caspase/ASC were resolved in western blot. Primary antibody against ASC was used at dilution (1:1000). HRP-anti rabbit was used for secondary antibody (1:5000) (C) ASC<sup>-/-</sup> HMEC-1 cells or WT HMEC-1 cells were primed with LPS 2 $\mu$ g/ml for 6 hours followed by transfected with GFP, NS2A-GFP and NS2B-GFP for 36 hours. As positive control cells were primed LPS 2 $\mu$ g/ml for 6 hours followed by 5mM ATP for 45 mins. Lysates were analyzed in western blot. Primary antibody against aaspase-1 primary antibody was used. HRP-anti rabbit was used for secondary antibody (1:5000).

## 12. NS2A & NS2B mediated inflammasome is dependent of NLRP3 and Caspase-1

To determine whether inflammasome activation by viroporins (NS2A, NS2B) of dengue virus is dependent of NLRP3 and caspase-1, HMEC-1 cells were primed with LPS (2 $\mu$ g/ml) for 6 hrs followed by the treatment with glyburide (NLRP3 inhibitor) for 1 hr prior to transfection with GFP, NS2A-GFP or NS2B-GFP for 36 hrs. Immunoblot assay showed that no activation of caspase-1 was observed in the presence of NLRP3 inhibitors in contrast to the cell only transfected with GFP-NS2A or GFP-NS2B where activation of caspase-1 was observed (Fig 26 A). In addition, cell supernatant was obtained to determine the secretion of 1L-1 $\beta$  in the presence or absence of NLRP3 inhibitor. The results has shown the reduced secretion of 1L-1 $\beta$  in the presence of NLRP3 inhibitor depicting that NS2A and NS2B activates caspase-1 and secrete 1L-1 $\beta$ , which is dependent on NLRP3 (Fig 26 B). Studies also suggest the existence of other pathways through which 1L-1 $\beta$  is secreted. Therefore, to check whether secretion of 1L-1 $\beta$  is dependent on caspase-1 due to the GFP-NS2A and GFP-NS2B, HMEC-1 cells were primed with LPS (2  $\mu$ g/ml) for 6 hrs followed by the treatment with YVAD (caspase-1 inhibitor) for 1 hr prior to transfection with GFP, NS2A-GFP or NS2B-GFP for 36 hrs. Then cell supernatant were collected and the results has shown the reduced secretion of 1L-1 $\beta$  in the presence of caspase-1 inhibitor (YVAD) inhibitor depicting that NS2A and NS2B depend secretion of 1L-1 $\beta$  is specific to caspase-1 (Fig 26 C). As a positive control ATP was used, however NLRP3 inhibitor has no or less effect on ATP to secrete 1L-1 $\beta$  in cell supernatant as well as caspase-1 activation in immunoblot. However, in the presence of caspase-1 inhibitor, secretion of 1L-1 $\beta$  was found reduced to 50% due to ATP. These observations suggest that activation of inflammasome and subsequently secretion of 1L-1 $\beta$  in cell supernatant by dengue viroporins NS2A and NS2B is specific to NLRP3 and Caspase-1.



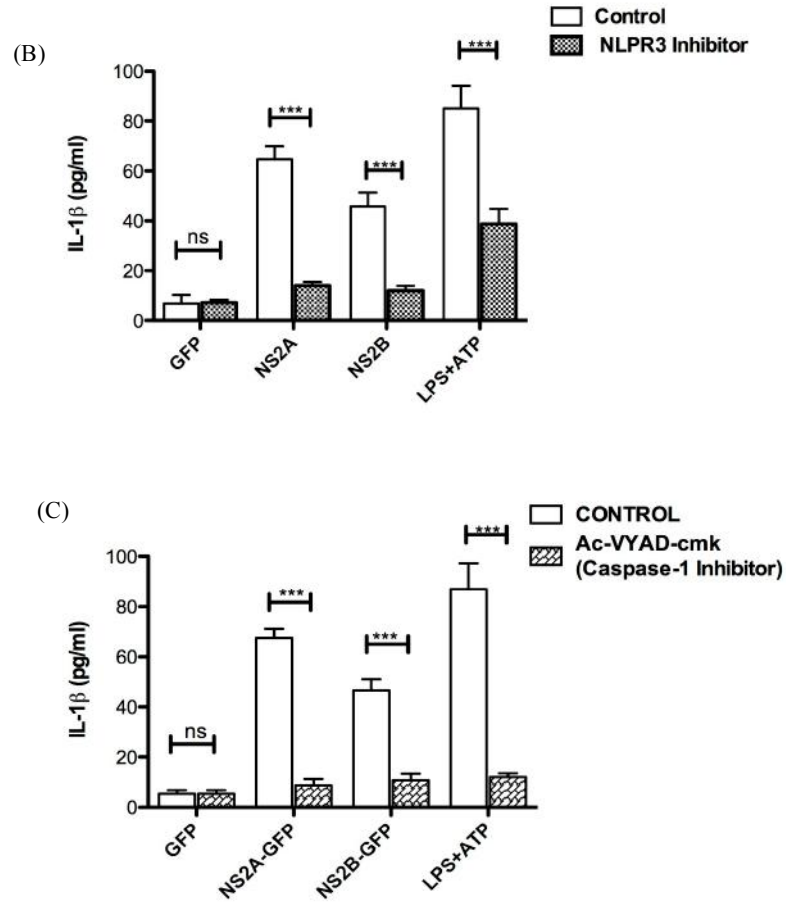


**Fig 26: NLRP3 and caspase-1 specific activation of Inflammasome by NS2A and NS2B:** HMEC-1 cells were transfected with the expression plasmid encoding GFP, NS2A-GFP, NS2B-GFP (green) for 36 hours or treated with LPS(5ug/ml) and ATP (5mM) as a positive control in the presence or absence of Glyburide (200uM) (A) the cell lysates were analyzed by western blot using anti-Caspase 1 antibody (1:1000) (B) the cell free supernatant was analyzed for 1L-1B by Elisa (C) HMEC-1 cells were transfected with the expression plasmid encoding GFP, NS2A-GFP, NS2B-GFP (green) for 36 hours or treated with LPS(5ug/ml) and ATP (5mM) as a positive control in the presence or absence of Ac-VYAD-cmk (50uM) and the cell free supernatant was analyzed for 1L-1B by Elisa. Data are representative of at least three independent experiments, and indicate the mean  $\pm$  S.D. (B,C). \*, P<0.05; \*\*, P<0.01; \*\*\*, P<0.001.

### 13. Regulation of Ca<sup>++</sup> impairs Inflammasome activation

It has been demonstrated that DENV NS2A and NS2B proteins are mainly localized to the endoplasmic reticulum (ER) and as a viroporin they could reduce the Ca<sup>++</sup> levels in those organelles thereby presumably elevating the local concentration of cytoplasmic Ca<sup>++</sup>. We evaluate whether the cell-permeable Ca<sup>++</sup>-chelator BAPTA-AM inhibits the inflammasome activation due to DENV NS2A and NS2B. Treatment with BAPTA-AM (10mM) inhibits the activation of caspase-1 due to DENV NS2A and ATP as shown in western blots. In addition treatment with BAPTA-AM (10mM) significantly reduced the expression of NLRP3 due to DENV NS2A, NS2B as well as ATP (Fig 27 A). Furthermore, treatment of HMEC-1 with 10 mM of BAPTA-AM significantly blocked 1L-1 $\beta$  secretion by DENV NS2A and NS2B protein (Fig 27 B). These results indicate that viroporins might induce Ca<sup>++</sup> flux from intracellular storages and are prerequisite in DENV-induced inflammasome activation. These data indicate that DENV infection increases [Ca<sup>++</sup>] cyt via the flux from intracellular storages and thereby activates NLRP3 inflammasome.

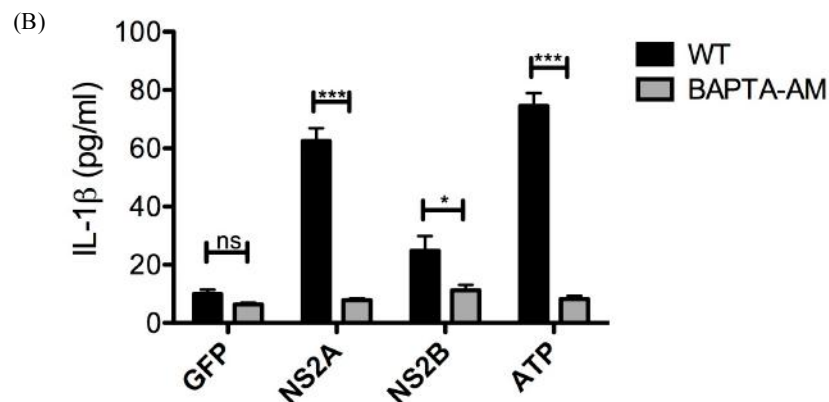
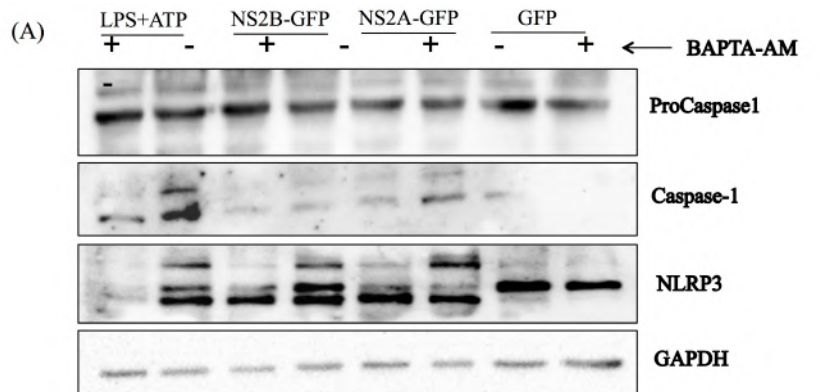
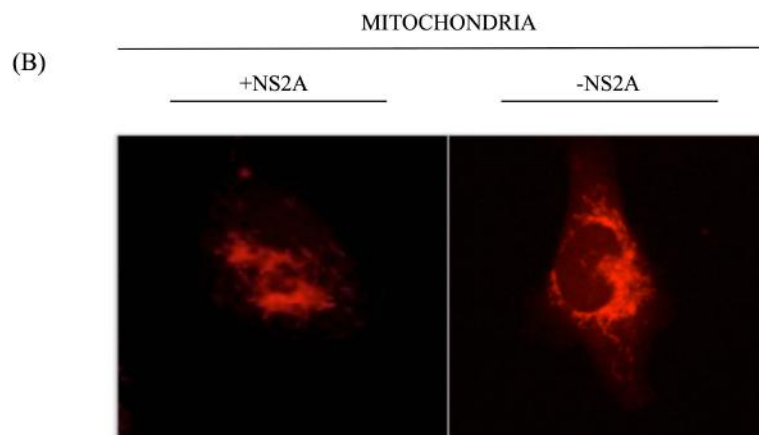
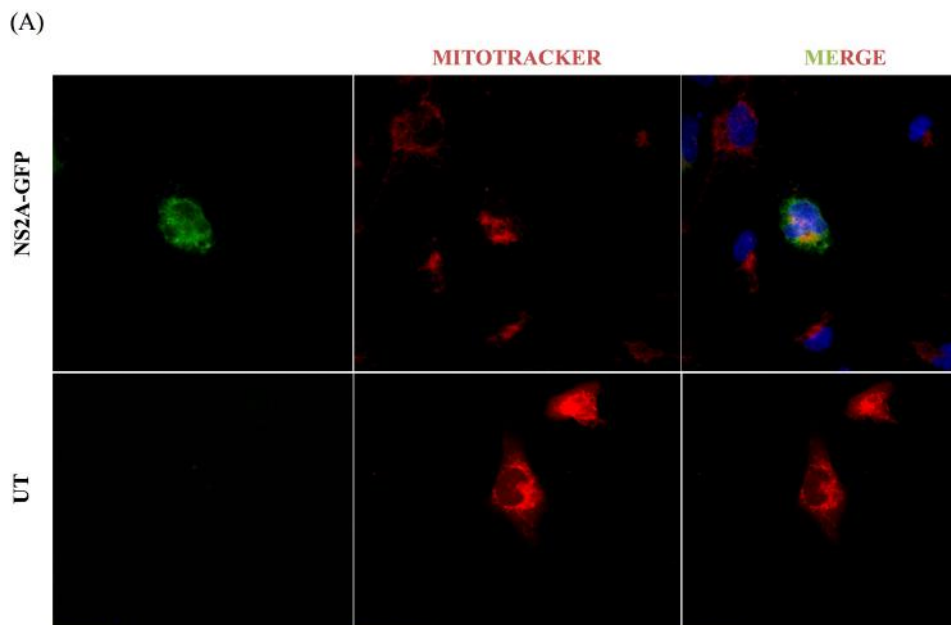


**Fig 27: Requirement of increased intracellular  $Ca^{++}$  concentration for NLRP3 inflammasome activation by NS2A and NS2B:** HMEC-1 cells were transfected with the expression plasmid encoding GFP, NS2A-GFP, NS2B-GFP for 36 hours or treated with LPS (5  $\mu$ g/ml) and ATP (5mM) as a positive control in the presence or absence of BAPTA-AM (10mM) and (A) the cell lysates were analyzed by western blot using anti-caspase 1 antibody (1:1000) and anti-NLRP3 (1:500) (B) the cell free supernatant was analyzed for IL-1 $\beta$  by Elisa. Data are representative of at least three independent experiments, and indicate the mean  $\pm$  S.D. (B,C). \*, P<0.05; \*\*, P<0.01; \*\*\*, P<0.001.

#### **14. DENV activates NLRP3 inflammasome is dependent of mitochondrial ROS**

We finally tested the role of previously identified factors that can activate the NLRP3 inflammasome. We have already shown that NS2A and NS2B found to be localized in mitochondria as viroporin, they could cause damage or membrane permeability of the mitochondria membrane. HMEC-1 cells were transfected with NS2A-GFP for 36 hrs and using immunofluorescence assay, we have observed that NS2A changes the morphology of the mitochondria (Fig 27 A, B). Therefore to analyze the effects of DENV viroporin in mitochondria, we have tested whether DENV viroporins could change the mitochondria membrane potential by permeabilizing the mitochondria. Mitochondrial transmembrane potential is an important parameter of mitochondrial function used as an indicator of cell death. The collapse of the mitochondrial transmembrane potential coincides with the opening of the mitochondrial permeability transition pores, leading to the release of cytochrome c into the cytosol, which in turn triggers other downstream events in the apoptotic cascade. We have performed the experiment to evaluate the membrane potential and the results shown that 41.2 % and 25.5% cells transfected with NS2A-GFP and NS2B-GFP respectively diminished mitochondria membrane potential in contrast to HMEC-1 cells transfected with GFP (Fig 28 B). These data suggest that both NS2A and NS2B viroporins induces the change in mitochondrial integrity and polarizes the mitochondria membrane potential. As a positive control FCCP (carbonyl cyanide 4-(trifluoromethoxy) phenylhydrazone) was utilized. FCCP is a ionophore uncoupler of oxidative phosphorylation. Treating cells with FCCP eliminates mitochondrial membrane potential and TMRE staining (that stains the live mitochondria in cell). On the other hand, mitochondrial ROS was found to be important in NLRP3 inflammasome activation by MSU, alum, and ATP [22,27]. Therefore we tested the effect of Mito-TEMPO in the activation of NLRP3 inflammasome due to DENV viroporins. Treatment

with antioxidant Mito-TEMPO, a scavenger specific for mitochondrial ROS [30,31], had inhibitory effect on the secretion of 1L-1 $\beta$  in HMEC-1 transfected with DENV NS2A and NS2B as well as in response to ATP (Fig 28 C). Above results demonstrated a strong role of DENV viroporins in the mitochondria membrane and suggests a model through which DENV viroporins alter the mitochondrial physiology that further leads to the activation of NLRP3 inflammasome.



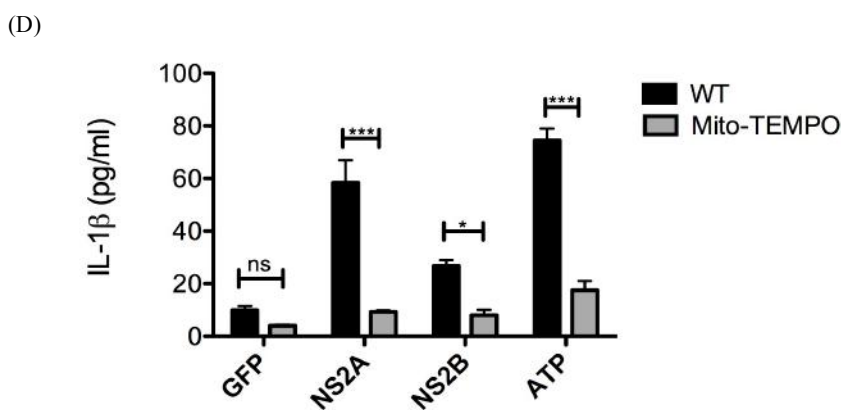
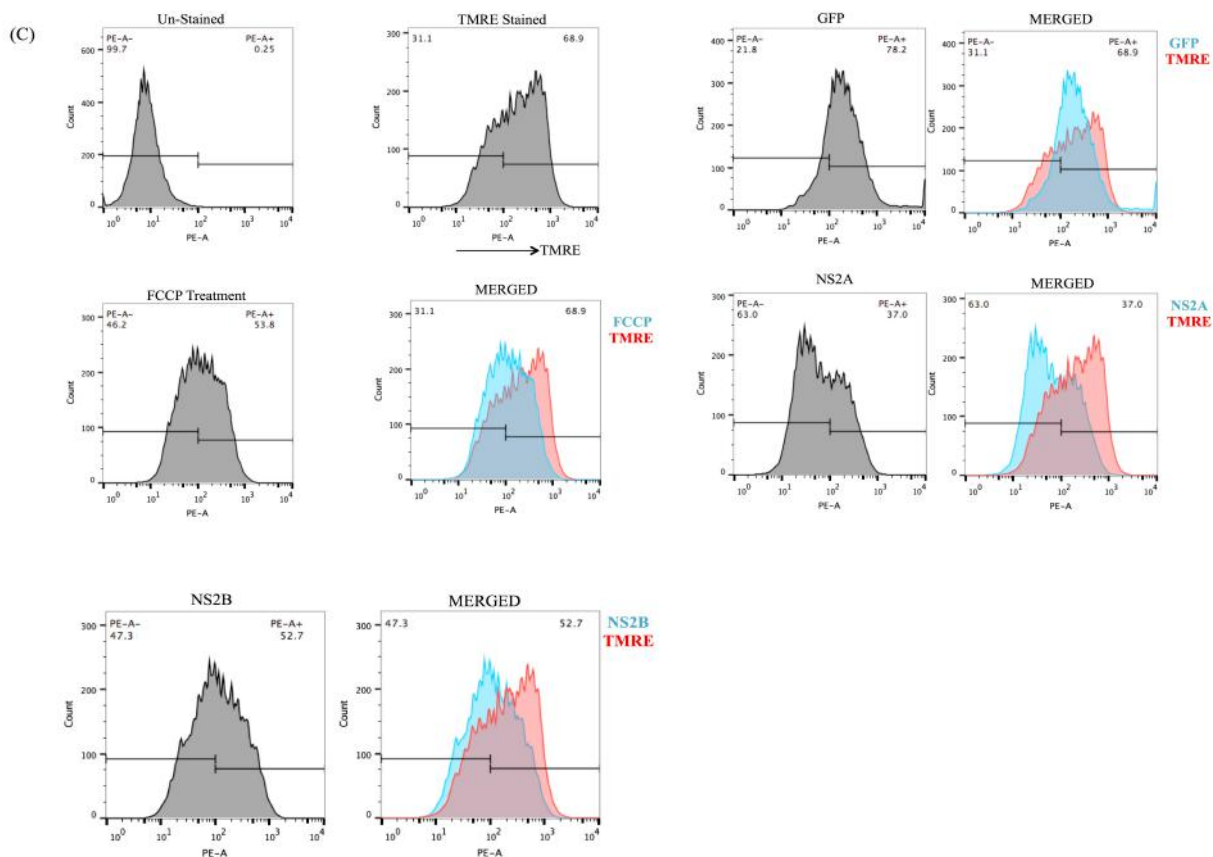


**Fig 28: DENV Viroporins induces the NLRP3 inflammasome through mitochondria.** (A) To evaluate the localization of the NS2A protein with mitochondria, HMEC-1 cells were transfected with a plasmid encoding DENV-2 NS2A-GFP for 36 h and stained with mitotracker (mitochondrial marker; red) and analyzed by confocal microscope. (B) Representation of mitochondria structure in HMEC-1 in the presence and absence of DENV-2 NS2A. (C) Mitochondrial membrane potential was detected in HMEC-1 transfected with a plasmid encoding GFP, NS2A-GFP, NS2B GFP for 36 hrs and stained with TMRE 175mM for 30 mins and analyzed in flow cytometry at 488nm (excitation peak- 595nm, emission-575nm). Cells treated with FCCP (20 mM) for 20 min were used as positive controls. (C) HMEC-1 cells were transfected with the expression plasmid encoding GFP, NS2A-GFP, NS2B-GFP for 36 hours or treated with LPS (5µg/ml) and ATP (5mM) as a positive control in the presence or absence of Mito-TEMPO (10uM) and the cell free supernatant was analyzed for IL-1 β by Elisa. Data are representative of at least three independent experiments, and indicate the mean ± S.D. (D). \*, P<0.05; \*\*, P<0.01; \*\*\*, P<0.001



## DISCUSSION

Numerous studies with different positive-strand RNA viruses, have demonstrated that many events occur during the infection cycle, such as reorganization of the intracellular membrane that can create scaffold for the replication machinery, assembly events and maturation of different virus particle (198)(199). These new structures recruit a large number of cellular factors, generating an optimum microenvironment for effective viral infections. In the flavivirus genus, DENV produces a variable cytopathic effect (depending of the target cells) in the infected cell, which is the result of the reorganization of the membranes. Another important phenomenon that has been reported to occur frequently in membranes during viral infections is the change of membrane permeability (62).

Viroporins are small, hydrophobic proteins that modulate membrane permeability towards small ions and molecules. Viroporins play crucial role during different steps in virus life cycle from entry, replication, assembly and egress. Viroporins also modulates the innate immune response by activating the inflammasome during virus infection. In our lab, we have demonstrated the membrane permeability of HMEC-1 cells during the late infection of DENV by demonstrating the inhibition of protein synthesis due to hygromycin treatment in contrast to the mock infection (200). This result suggests that viral products are able to associate with the plasma membrane promoting changes in the permeability and allowing the passage of the hygromycin B to the cytoplasm. In addition, the inhibition of protein synthesis in the late times of viral infection suggest the role of viral protein in membrane permeability as they are in higher quantity at late infection. So we can conclude that if there are changes in membrane permeability at late time of the infection with DENV, the proteins that may be involved are from the family of viral proteins called viroporin. The role of viroporin in changes the membrane permeability have been reported for other viruses including members of the flaviviridae family, such as the hepatitis C virus or Japanese encephalitis virus (35) (201).

The main goal of the present study was to determine whether the full-length DENV-2, NS2A protein possesses viroporin activity and its role in the inflammasome activation. Dengue NS2A is a 22-kDa hydrophobic protein with 5 trans-membrane domains that span the lipid bilayer of the ER membrane. It has been demonstrated that amino acids spanning these transmembrane

domains plays a crucial role in viral replication, assembly as well as in maturation (37). Significantly, study involving the flavivirus JEV revealed that small hydrophobic nonstructural proteins, including NS2A cause membrane permeability (35). To address this question, we performed an *in silico* analysis of DENV-2 NS2A to determine whether it exhibits the sequence features associated with viroporins. Therefore *In silico* analysis was performed to determine the similarity between Dengue virus NS2A proteins and NS2A of JEV in terms of sequence, and the hydrophobicity. Initially, hydropathic plots indicated the presence of six putative transmembrane helices that show significant sequence similarity with the corresponding regions in NS2A of JEV. Moreover, six transmembrane regions were observed in similar positions along with JEV NS2A protein. Furthermore, this analysis indicated that the amino and carboxyl-terminal domains of DENV-2 NS2A orient towards the lumen of the endoplasmic reticulum and the cytoplasm, respectively. Notably, these findings are consistent with the topology of flavivirus NS2A proteins generated via various bioinformatics algorithms and corroborated by biochemical approaches (202). To examine whether DENV-2 NS2A protein is able to modify the membrane permeability in different systems similarly to JEV NS2A, we compared the sequences of amino acid for these two proteins. Notably DENV and JEV NS2A exhibit 26–65% sequence identity and more than 50% sequence similarity. In addition, few amino acids within the transmembrane domains of these two proteins were identical or showed substantial similarity. This similarity suggests that the physicochemical properties of JEV and DENV-2 NS2A are comparable. In addition both proteins possess similar hydrophobic and basic residues that are important characteristic of viral proteins with membrane destabilising ability. These residues may be critical for viroporin activity, since in different studies have been reported that these amino acids participate in the oligomerization, interaction with the membranes, or selectivity of the molecule they carry, as observed for the viroporins M2, Vpu or NSP4 viroporins of Influenza virus, HIV-1 virus and rotavirus respectively(81) (203)(204). Therefore, bioinformatics analysis of the DENV-2 NS2A amino acid sequence revealed a high degree of similarity with a previously reported viroporin from a member of the Flaviviridae family(35). Recent evidence has determined that the NS2A protein have a topology with a large number of transmembranal regions, and thus the ability to associate with membranes of bacterial, eukaryotic or liposomes. However, in none of the studies have evaluated its role as permeabilizing molecules or viroporins. Given the hydrophobic nature of NS2A proteins,

expression in the bacterial system demonstrated that the protein was localized in the insoluble fraction of the bacterial extract and specifically in the inclusion bodies. Many of the already characterized viroporins are purified from these bacterial fractions (77)(205)(206)(55, 90, 91]). One of the main tools that led to the identification of viral proteins have viroporin activity, was the fact that when expressed in bacterial system, these proteins were toxic to the bacteria (Carrasco, 1987).

One of the more distinctive characteristics of viroporins is their capacity to induce alterations in membrane permeability. In this study, we provide the first evidence that NS2A exhibits pore-forming activity when it is expressed in a bacterial system, as has been demonstrated for various other viral proteins with viroporin activity (35). In prokaryotic systems, such as *E. coli*, bacterial growth can be altered directly by the expression and subsequent incorporation of viroporins within bacterial membranes, leading to a loss of membrane integrity. These data are consistent with those obtained using the NS2A viroporin from JEV, thus advocating that both the proteins may share a conserved function, as well as other viroporins characterized (35)(4). This observation is of great Importance, since it has been described that not all viroporins have the same effect on the bacterial membrane; as reported in the case of VP4 viroporin of SV40 virus, as when the protein was expressed in bacteria of PLysS strain there was no effect as observed with other viroporins(207). Subsequent studies showed that lack of a lytic activity, on the part of the VP4 protein is due to the lipid composition of bacteria membranes (77). It was observed that VP4 protein was associated with membranes with a high content of phospholipids, such as phosphatidylcholine or sphingomyelin rather associated with membranes with a high content of phosphatidyl ethanol amine, which is a conical phospholipid that induces a negative curvature in the membrane and in addition, it's the main component of bacterial membranes (77). This observation suggests that the viroporins would associate with the membranes according to the lipids that constitute it. Therefore, the results obtained suggest that DENV NS2A protein is associated with membranes preferably composed of phosphatidyl ethanolamine. The permeability result obtained in PLysS bacteria suggests strongly that the NS2A protein possibly have viroporin activity. Another important feature of viroporins is that they can oligomerize(208)(209). Hence *in silico* analysis of the NS2A sequence demonstrated the presence of five to seven transmembrane regions. Before the oligomerization assay was performed, NS2A protein was purified by preparative gels, and eluted in PBS (pH 7.0), that had

the property to form oligomer structures (dimers). We evaluated whether the recombinant NS2A proteins have the ability to oligomerize in the presence of protein crosslinker (glutaraldehyde). Glutaraldehyde cross-linking experiments revealed that NS2A could oligomerize to form a dimer, trimeric and pentameric structures under reduced conditions. Conversely, in the absence of glutaraldehyde, dimers were also observed, when the protein was stored. NS2A dimer, trimer, and pentamer formation may depend on hydrophobic interactions rather than disulphide bridges, as witnessed for other viroporins (p7-hepatitis C virus, SH-Respiratory syncytial virus) (210)(205). Once NS2A forms oligomers, it may organize into pore structures in cell membranes, which would account for the observed alterations in membrane permeability. Although, different strategies have been employed to determine the property of these pores in transporting molecules (211). Further, we demonstrated the ability of NS2A to induce membrane permeability in a model of liposomes, which comprises of lipid bilayered membrane structure similar to eukaryotic membranes and then charged with FITC (212). NS2A caused membrane disruption and release of FITC, strongly suggesting that the protein can integrate directly into membranes, leading to their structural modification. This study is supported by other viroporins (VP4 of SV40 virus, NSP4 of rotavirus,  $\mu$ 1N of reovirus), that have demonstrated to lyse liposome membrane (77)(213)(214). This study provides the first evidence that the NS2A protein is capable of oligomerisation and modifying the permeability of membranes.

Many of the viroporins described in other viruses are associated or located in the different organelles of the cell. In the case of Rotavirus, NSP4 protein is localized in mitochondria or in the endoplasmic reticulum (81)(87). Other reports suggest that the lipid composition of membranes play an important role for the viroporins to be inserted, as was demonstrated for the SV40 protein of SV40 virus, or 2B of Poliovirus (77)(215). These studies determined that viroporins are associated to the membranes with lipid composition resembles the membranes of the ER, golgi or mitochondria. To determine the cellular localization of proteins NS2A during infection with the dengue virus, we developed a polyclonal antibody, using recombinant NS2A protein as the antigen. However, we could not able to generate the high titers antibody that can recognize NS2A during dengue infection. This is due to the highly hydrophobic nature of NS2A that made it difficult to expose its relevant hydrophobic region for the antibody to bind to.

We identified that the NS2A protein has an organelle membranous localization in endoplasmic reticulum as previously reported (Xieping Xi 2013). Further, we found that NS2A colocalized in mitochondria and more specific in outer mitochondria membrane, suggesting a role of NS2A in this cellular organelle. However, we did not detect NS2A protein in the Golgi complex. The composition of the membrane organelles where the NS2A protein was located might have a percentage of between 30 to 40% of the phospholipid phosphatidylethanolamine, which as already mentioned is the main phospholipid of the bacterial membrane(216) . Additionally it is widely reported that the NS2A protein is located in the endoplasmic reticulum during the replication and assembly process of the viral genome(217). The absence of the NS2A protein in the golgi complex, probably due to the low percentage of phosphatidylethanolamine (20%) in membranes of this organelle (216).

Viroporins also participates in induction of innate immune pathway by inducing the NLRP3 inflammasome(82)(81)(80). Inflammasomes participate in pathogen recognition by sensing disturbances in cellular milieus, including intracellular ionic concentrations (121)(218). Recent studies have reported that in some viral infections, viroporin ion channel activity provides the second signal required for inflammasome activation, thereby inducing the release of active IL-1 $\beta$ . In general, viroporins induce an efflux of ions, such as H<sup>+</sup> and Ca<sup>++</sup> that move from their intracellular stores into the cytoplasm following strong electrochemical gradients, triggering the NLRP3 inflammasome(219).

During Dengue virus infection, DENV has shown to activate the NLRP3 inflammasome in platelets and macrophages and secretes IL-1 $\beta$ . However the viral factor responsible to activate inflammasome is still elusive. Although dengue virus pathogenesis is not fully elucidated, recent evidence supports the central role of proinflammatory cytokines in endothelial activation and plasma leakage during DV infection (179)(187)(188). Our study along with other study has demonstrated that microvascular endothelial cells are permissive target of DENV-2 (220)(221)(192). Considering the importance of these cells in the dengue infection, in this study we have demonstrated that DENV-2 is capable of triggering NLRP3 activation in endothelial cells (HMEC-1). We have shown the activation of the inflammasome complex by demonstrating the increased expression of NLRP3, ASC oligomerization, activation of caspase-1, and secretion of IL-1 $\beta$  in cell supernatant at late DENV infection. This data is in agreement

with the recent study demonstrating the activation of NLRP3 inflammasome in DV infected macrophages, and in platelets (194)(166). Inflammasome complex serves as platform for the activation of caspase-1 and IL-1 $\beta$  secretion. Several studies have reported NLRP3 and RIG-I inflammasome induced caspase-1 activation during RNA viruses infections (178). Our lab has demonstrated the up-regulation of RIG-1 in cells such as fibroblasts at late infection (222). Further, an array of RNA viruses has shown to induce IL-1 $\beta$  production through the NLRP3 inflammasome (144). Precisely, in flaviruses including West Nile virus, CSFV, Japanese encephalitis virus, Zika virus have shown to assemble NLRP3 inflammasome and promote IL-1 $\beta$  production during infection(144) ((223)(224)(225)(226). Our results clearly demonstrate that DENV-2 was able to activate NLRP3 inflammasome on its own, without the prerequisite for priming the cells with another PAMP as it has previously been proven necessary for other viruses, such as encephalomyocarditis virus and VSV(173)(225). An important issue is to address the molecular mechanism through which viral RNA triggers NLRP3 inflammasome activation. In this sense wide range of stimuli have been reported to activate NLRP3 inflammasome including bacterial components, environment irritants, endogenous danger signals from damaged cells, viruses (227). Among all, RNA virus viroporins have shown to activate the NLRP3 inflammasome by modulating the ionic flux (219). This is the first study where we demonstrated the role of dengue virus nonstructural hydrophobic proteins NS2A and NS2B in the activation of NLRP3 inflammasome. We have recently reported that dengue virus NS2B protein behaves as a viroporin (50). Recently, we have also shown that dengue virus NS2A is also behaves as a viroporin in DENV-2 genome and contains membrane disruptive properties. We have shown the NS2A permeabilized different membrane models and contain property of oligomerization (197). Therefore, we made a hypothesis to evaluate where these two proposed viroporin (NS2A & NS2B) of dengue virus could be able to activate the NLRP3 inflammasome. Plasmid expressing the NS2A or NS2B tagged with GFP were transfected and analyzed by Western blot, Immunofluorescence and Elisa. We demonstrated that DENV-2 NS2A and NS2B were able to activate the NLRP3 inflammasome complex following the secretion of IL-1 $\beta$  in cell supernatant. ASC punctate structures are the marker of inflammasome activation and we have shown the presence of ASC punctate structures in the presence of NS2A and NS2B further supports the hypothesis that DENV viroporins activate inflammasome. In continuation, NS2A has shown to colocalize with NLRP3. Interaction of

NS2A and NLRP3 recruits the NLRP3 to perinuclear space and this interaction could be important of activating NLRP3 inflammasome. However further study regarding the localization (ER, mitochondria) of NS2A and NLRP3 will further unravel the molecular mechanism of activation. However, we could not observe the interaction between NS2B and NLRP3. This suggests that NS2B might activate the NLRP3 inflammasome indirectly. Further, studies has reported that some RNA viruses i.e Chikungunya and Zika virus activate the AIM2 specific Inflammasome and secretes IL-1 $\beta$  (228)(229). Although AIM2 sense DNA virus for its activation, however the molecular mechanism through which AIM2 sense RNA virus is still unknown. Therefore, we have checked whether IL-1 $\beta$  secretion by NS2A and NS2B is specific to NLRP3 and caspase-1. By using the inhibitors of NLRP3 and caspase-1, we have demonstrated that secretion of IL-1 $\beta$  due to viroporins were specific to NLRP3 and caspase 1. NS2A and NS2B were found to colocalize in ER, therefore we hypothesis whether viroporins activates the inflammasome by inducing the Ca<sup>++</sup> efflux from ER to cytosol. We have used the calcium chelator and observed that the activation of caspase-1 and further secretion of IL-1 $\beta$  was decreased in the presence of NS2A followed by NS2B suggest that these viroporin modulates the Ca<sup>++</sup> concentration during dengue infection. Inducing the Ca<sup>++</sup> by viroporins is also important during viral infection as few Ca<sup>++</sup> conducting viroporins manipulate host signaling pathways, including store-operated Ca<sup>++</sup> entry, autophagy, and inflammasome activation (230).

Dengue virus interacts with cellular organelles, including mitochondria, to successfully replicate in cells. DENV infection causes an imbalance in mitochondrial dynamics and induces elongation of mitochondria that promotes viral replication and alleviates RIG-I-dependent activation of interferon responses (231)(232). Several studies have demonstrated that mitochondria play a crucial role in activating the NLRP3 inflammasome. As example, DENV impairs mitochondrial fusion by cleaving the mitochondrial fusion proteins i.e mitofusins (MFN1 and MFN2). Among them MFN2 participated in maintaining mitochondrial membrane potential (MMP) to attenuate DENV-induced cell death. Cleaving MFN2 by DENV protease suppressed mitochondrial fusion and deteriorated DENV-induced cytopathic effects through facilitating MMP disruption (233). In addition, mitofusins have demonstrated to interact with NLRP3 and play a role as potential docking sites for NLRP3 on the mitochondria for the

recruitment of NLRP3 and subsequently inflammasome activation (234). Mitochondrial ROS has also demonstrated to induce the NLRP3 inflammasome(235). It has demonstrated that during DENV infection, DENV stimulates the stress in mitochondria and induces ROS that further triggers NLRP3 inflammasome(194). Mitochondria-associated adapter molecule, MAVS has shown to be required for optimal NLRP3 inflammasome activity. MAVS mediates recruitment of NLRP3 to mitochondria, promoting production of IL-1 $\beta$  and the pathophysiologic activity of the NLRP3 inflammasome(236). By using mitotraker, we have shown that NS2A colocalize in mitochondria and further by using TOM22 as an outer mitochondria marker, we have shown that NS2A colocalize in outer membrane of mitochondria. In addition our study has also shown the presence of NS2B in mitochondria membranes through immunofluorescence (Moises et.al, 2017, unpublished data). Further we have observed the disrupted morphology of mitochondria in the presence of NS2A, suggesting that NS2A may directly disrupt mitochondria morphology due to its membrane disrupting abilities or indirectly through the Ca<sup>++</sup> influx in mitochondria or by generating ROS. This result is supported by the observation where viroporins as 2B (poliovirus) and NS4A (HCV)-expressing cells, mitochondria did not exhibit their typical long shape, appearing instead as punctate entities. In addition the expression of 6K (sindbis virus), E (MHV-A59) and 3A (polio virus) altered the normal morphology of mitochondrial network (85). Further we have observed that NS2A and NS2B changes the mitochondria membrane potential supports the hypothesis that NS2A and NS2B has a role in mitochondria. Disruption of the mitochondrial transmembrane potential has also reported by viroporins 2B (Polio virus) 3A (Polio virus) and NS4A (HCV) supporting the role of viroporins in the disruption of mitochondrial membrane potential (85). Thus we decided to use the ROS inhibitor and we demonstrated the decreased effect of NS2A and NS2B in the secretion of IL-1 $\beta$ . These results suggest that NS2A localizes in the mitochondria and disrupt the membrane permeability and induces ROS that further triggers NLRP3 inflammasome. However, further biochemical experiments are required to demonstrate the presence of NS2A and NS2B in mitochondria as we observed the presence of NS2A and NS2B protein in mitochondria only through immunofluorescence. This study is supported by the observation that DENV disrupts the mitochondria membrane potential and also DENV activates the NLRP3 inflammasome due to ROS (233)(237). This phenomenon have been reported in Influenza and EMVC virus infection where they induce a loss of mitochondrial membrane potential which was essential for NLRP3-



Mitofusin (1 & 2) interaction and subsequently inflammasome activation (234). Presence of NS2A and NS2B in ER and mitochondria and their similar roles in activation of inflammasome is supported by a study in flavivirus, demonstrated the intramolecular or intermolecular interactions between the pTMSs of DENV NS2A and NS2B are important in regulation in virus replication, assembly/secretion, and virus-induced CPE. These results expand the understanding of flavivirus replication (238). In addition, interaction of NS2B and NS2A play important role in JEV virus assembly (238). This suggests that NS2A and NS2B might function in synergistic manner, however detailed studies are required for the confirmation.

In conclusion, this study provides, for the first time, many evidences regarding to the ability of the NS2A protein to function as a viroporin. Our results indicate that NS2A can form oligomers and alter the permeability of eukaryotic and prokaryotic membrane models. Furthermore, the above results support the hypothesis that NS2A exhibits membrane-destabilising ability, a function that could be critical during the DENV replication cycle. Further, our results clearly demonstrate that DENV-2 can induce IL-1 $\beta$  secretion from HMEC-1 via activation of NLRP3 inflammasome. Our results demonstrate that DENV-2 viroporins NS2A and NS2B are able to activate NLRP3 and caspase-1 specific Inflammasome possibly by the formation of a pore or channel on the endoplasmic membrane or mitochondria. However both proteins act synergically or independently in a concerted manner is an issue that remains to be elucidated. Therefore, in DENV infected host cells, imbalance in ionic concentration could impose cellular stress that is sensed intracellularly, could be a general viral recognition pathway to triggers activation of NLRP3 inflammasomes. Further study is required regarding the role of ionic imbalance and their impact in inflammasome activation due to viroporin. In addition, research that provide the clear evidence of function of viroporins in mitochondria and their regulation will further unravel the exact mechanism by which NLRP3 detects viruses and thereby regulate pathogenesis. It will help in the designing of effective drug for the prevention of infectious disease.

## **CONCLUSION**

During Dengue virus infection, changes in membrane permeability occur, which play an important role in the cytopathic processes induced by the infection. These mechanisms are employed in various events during the virus infection cycle. The NS2A protein participates in this phenomenon of change in membrane permeability, because of the biochemical characteristics, cell location, association to membranes and the permeability tests evaluated; defines the NS2A protein as a new member of the viroporin family. NS2A and NS2B viroporin also participates in innate immune system by inducing the NLRP3 Inflammasome activation by inducing  $\text{Ca}^{++}$  efflux from ER and/or by inducing ROS from mitochondria. This phenomenon highlights the importance of viroporins mediated DENV virus induced inflammasome activation.

## **PERSPECTIVES**

1. To determine the association between Dengue virus NS2A with mitochondria membrane and the possible association between NS2A with proteins involved in the mitochondria membrane permeability VDAC and ANT.
2. To characterize the phenomenon through which NS2A induces the NLRP3 inflammasome through ROS.
3. To determine the NS2A residues, directly involved in the mitochondria or ER membrane permeability.
4. To determine and characterize the formation of ion channel in ER and mitochondria due to NS2A.
5. To determine whether NS2A and NS2B induce the inflammasome activation separately or in synergistic manner.
6. To determine the viroporins induced inflammasome by “knocking down” the inflammasome components by CRISPR Technology.

## LIST OF PUBLICATIONS

### PUBLISHED

1. **Shrivastava G**, García-Cordero J, **Cedillo-Barrón L**. NS2A comprises a putative viroporin of Dengue virus 2. **Virulence**. **2017**, doi: 10.1080/21505594.2017.1356540. PubMed PMID: 28723277
2. **Shrivastava G**, García-Cordero J, **Cedillo-Barrón L**. Commentary on the article entitled IRGB10 Liberates Bacterial Ligands for Sensing by the AIM2 and Caspase-11-NLRP3 Inflammasomes. **Public Health and Emergency** **2017**, doi:10.21037/jphe.2017.02.07
3. **Shrivastava G**, **Cedillo-Barrón L**. The Inflammasome and its importance in viral Infection, **Immunol Res**, **2016**, Oct 3, doi 10.1007/s12026-016-8873-z
4. León-Juárez M, **Shrivastava G**, García-Cordero J, **Cedillo-Barrón L**. Recombinant Dengue virus protein NS2B alters membrane permeability in different membrane models. **Virol J**. 2016 Jan 4;13(1):1. doi: 10.1186/s12985-015-0456-4.

### SUBMITTED

5. Ishita Banerjee, **Shrivastava G**, Rathinam Vijay. Regulation of Interferon during inflammasome activation. **Science Immunology** (July 2017)
6. **Cedillo-Barrón L**, García-Cordero J, **Shrivastava G**. Innate immune response against flavivirus proteins. Book Chapter. **Springer** (August 2017)

### UNDER SUBMISSION

7. **Shrivastava G**, García-Cordero J, León-Juárez M, **Cedillo-Barrón L**. Dengue Virus viroporins induce NLRP3 inflammasome in HMEC-1. **Plos Pathogen**

## REFERENCES

1. Halstead SB. Epidemiology of dengue and dengue hemorrhagic fever. *Dengue and dengue hemorrhagic fever*. 1997.
2. WHO 2017. WHO | Dengue and severe dengue. WHO [Internet]. World Health Organization; 2017 [cited 2017 Aug 17]; Available from: <http://www.who.int/mediacentre/factsheets/fs117/en/>
3. Gubler DJ, Ooi EE, Vasudevan S, Farrar J. *Dengue and dengue hemorrhagic fever: Second edition*. *Dengue and Dengue Hemorrhagic Fever: Second Edition*. 2014.
4. Ryan 16 M P, Sammis CG, Halstead SB. Pathogenesis of Dengue: Challenges to Molecular Biology. *Geol Soc Am Bull* *J Geol Soc Aust* 18 B R Lawn T R Wilshaw, *Fract of Brittk Solids* I J Smalley, *Geol Mag Nat*. 1962;
5. Gubler DJ. Dengue and dengue hemorrhagic fever: its history and resurgence as a global public health problem. *Dengue and dengue hemorrhagic fever*. 1997.
6. Leitmeyer KC, de Chacon, Leitmeyer KC, Vaughn DW, Watts DM, Vaughn DW, et al. Dengue virus structural differences that correlate with pathogenesis. *J Virol*. 1999;
7. Qi et al. Biological characteristics of dengue virus and potential targets for drug design. *Acta Biochim Biophys Sin (Shanghai)*. 2008;
8. Clyde K, Kyle JL, Harris E. Recent advances in deciphering viral and host determinants of dengue virus replication and pathogenesis. *J Virol*. 2006;
9. Surasombatpattana P, Hamel R, Patramool S, Luplertlop N, Thomas F, Despres P, et al. Dengue virus replication in infected human keratinocytes leads to activation of antiviral innate immune responses. *Infect Genet Evol*. 2011;
10. Navarro-Sanchez E, Despres P, Cedillo-Barron L. Innate immune responses to dengue virus. *Arch Med Res*. 2005;
11. Whitehead SS, Blaney JE, Durbin AP, Murphy BR. Prospects for a dengue virus vaccine. *Nat Rev Microbiol*. 2007;
12. Mukhopadhyay S, Kuhn RJ, Rossmann MG. A structural perspective of the flavivirus life cycle. *Nat Rev Microbiol*. 2005;
13. Stiasny K, Kössl C, Lepault J, Rey FA, Heinz FX. Characterization of a structural intermediate of flavivirus membrane fusion. *PLoS Pathog*. 2007;
14. Allison SL, Schalich J, Stiasny K, Mandl CW, Heinz FX. Mutational evidence for an internal fusion peptide in flavivirus envelope protein E. *J Virol*. 2001;
15. Shalem O, Sanjana NE, Hartenian E, Shi X, Scott DA, Mikkelsen TS, et al. Genome-scale CRISPR-Cas9 knockout screening in human cells. *Science*. 2014;
16. Crill WD, Roehrig JT. Monoclonal antibodies that bind to domain III of dengue virus E

- glycoprotein are the most efficient blockers of virus adsorption to Vero cells. *J Virol*. 2001;
17. Dowd KA, Pierson TC. Antibody-mediated neutralization of flaviviruses: A reductionist view. *Virology*. 2011.
  18. Alvarez DE, De Lella Ezcurra AL, Fucito S, Gamarnik A V. Role of RNA structures present at the 3'UTR of dengue virus on translation, RNA synthesis, and viral replication. *Virology*. 2005;
  19. Flamand M, Megret F, Mathieu M, Lepault J, Rey F a, Deubel V. Dengue virus type 1 nonstructural glycoprotein NS1 is secreted from mammalian cells as a soluble hexamer in a glycosylation-dependent fashion. *J Virol*. 1999;
  20. Chambers TJ, Rice CM. Molecular biology of the flaviviruses. *Microbiol Sci*. 1987;
  21. Rico-Hesse R. Dengue virus virulence and transmission determinants. *Current Topics in Microbiology and Immunology*. 2009.
  22. Srikiatkachorn A, Krautrachue A, Ratanaprakarn W, Wongtapradit L, Nithipanya N, Kalayanaroj S, et al. Natural History of Plasma Leakage in Dengue Hemorrhagic Fever: A Serial Ultrasonographic Study. *Pediatr Infect Dis J*. 2007;
  23. Fields BN, Knipe DM, Howley PM. *Fields Virology*, 5th Edition. *Fields Virology*. 2007.
  24. Chambers TJ, Hahn CS, Galler R, Rice CM. Flavivirus genome organization, expression, and replication. *Annu Rev Microbiol*. 1990;
  25. Yu I, Zhang W, Holdaway HA, Li L, Kostyuchenko VA, Chipman PR, et al. Structure of the Immature Dengue Virus at Low pH Primes Proteolytic Maturation. *Science* (80- ). 2008;
  26. Pokidysheva E, Zhang Y, Battisti AJ, Bator-Kelly CM, Chipman PR, Xiao C, et al. Cryo-EM reconstruction of dengue virus in complex with the carbohydrate recognition domain of DC-SIGN. *Cell*. 2006;
  27. Perera R, Kuhn RJ. Structural proteomics of dengue virus. *Current Opinion in Microbiology*. 2008.
  28. Sampath A, Padmanabhan R. Molecular targets for flavivirus drug discovery. *Antiviral Research*. 2009.
  29. Mercado-Curiel RF, Esquinca-Avilés HA, Tovar R, Díaz-Badillo A, Camacho-Nuez M, Muñoz M de L. The four serotypes of dengue recognize the same putative receptors in *Aedes aegypti* midgut and *Ae. albopictus* cells. *BMC Microbiol*. 2006;
  30. Jindadamrongwech S, Smith DR. Virus overlay protein binding assay (VOPBA) reveals serotype specific heterogeneity of dengue virus binding proteins on HepG2 human liver cells. *Intervirology*. 2004;
  31. Aleshin AE, Shiryaev S a, Strongin AY, Liddington RC. Structural evidence for regulation and specificity of flaviviral proteases and evolution of the Flaviviridae fold. *Protein Sci*.

- 2007;
32. FALGOUT B, PETHEL M, ZHANG YM, LAI CJ. Both Nonstructural Proteins Ns2B and Ns3 Are Required for the Proteolytic Processing of Dengue Virus Nonstructural Proteins. *J Virol.* 1991;
  33. Melino S, Fucito S, Campagna A, Wrubl F, Gamarnik A, Cicero DO, et al. The active essential CFNS3d protein complex. *FEBS J.* 2006;
  34. Garcia-Cordero J, Ramirez HR, Vazquez-Ochoa M, Gutierrez-Castaneda B, Santos-Argumedo L, Villegas-Sepulveda N, et al. Production and characterization of a monoclonal antibody specific for NS3 protease and the ATPase region of Dengue-2 virus. *Hybrid.* 2005;
  35. Chang Y-S, Liao C-L, Tsao C-H, Chen M-C, Liu C-I, Chen L-K, et al. Membrane Permeabilization by Small Hydrophobic Nonstructural Proteins of Japanese Encephalitis Virus. *J Virol.* 1999;
  36. Chambers TJ, McCourt DW, Rice CM. Yellow fever virus proteins NS2A, NS2B, and NS4B: identification and partial N-terminal amino acid sequence analysis. *Virology.* 1989;
  37. Xie X, Gayen S, Kang C, Yuan Z, Shi P-Y. Membrane topology and function of dengue virus NS2A protein. *J Virol.* 2013;
  38. Mackenzie JM, Khromykh AA, Jones MK, Westaway EG. Subcellular Localization and Some Biochemical Properties of the Flavivirus Kunjin Nonstructural Proteins NS2A and NS4A. *Virology.* 1998;
  39. Kümmerer BM, Rice CM. Mutations in the yellow fever virus nonstructural protein NS2A selectively block production of infectious particles. *J Virol.* 2002;
  40. Leung JY, Pijlman GP, Kondratieva N, Hyde J, Mackenzie JM, Khromykh AA. Role of Nonstructural Protein NS2A in Flavivirus Assembly. *J Virol.* 2008;
  41. Falgout B, Markoff L. Evidence that Flavivirus NS1-NS2A Cleavage Is Mediated by a Membrane-Bound Host Protease in the Endoplasmic Reticulum. *J Virol.* 1995;
  42. Xie X, Zou J, Puttikhunt C, Yuan Z, Shi P-Y. Two Distinct Sets of NS2A Molecules Are Responsible for Dengue Virus RNA Synthesis and Virion Assembly. *J Virol.* 2015;
  43. Liu WJ, Chen HB, Khromykh AA. Molecular and Functional Analyses of Kunjin Virus Infectious cDNA Clones Demonstrate the Essential Roles for NS2A in Virus Assembly and for a Nonconservative Residue in NS3 in RNA Replication. *J Virol.* 2003;77(14):7804–13.
  44. Liu WJ, Wang XJ, Clark DC, Lobigs M, Hall RA, Khromykh AA. A single amino acid substitution in the West Nile virus nonstructural protein NS2A disables its ability to inhibit alpha/beta interferon induction and attenuates virus virulence in mice. *J Virol.* 2006;
  45. Liu WJ, Chen HB, Wang XJ, Huang H, Khromykh A a. Analysis of adaptive mutations in Kunjin virus replicon RNA reveals a novel role for the flavivirus nonstructural protein

- NS2A in inhibition of beta interferon promoter-driven transcription. *J Virol.* 2004;
46. Robertson SJ, Mitzel DN, Taylor RT, Best SM, Bloom ME. Tick-borne flaviviruses: Dissecting host immune responses and virus countermeasures. *Immunologic Research.* 2009.
  47. Muñoz-Jordan JL, Sánchez-Burgos GG, Laurent-Rolle M, García-Sastre A. Inhibition of interferon signaling by dengue virus. *Proc Natl Acad Sci U S A.* 2003;
  48. Melian EB, Edmonds JH, Nagasaki TK, Hinzman E, Floden N, Khromykh AA. West Nile virus NS2A protein facilitates virus-induced apoptosis independently of interferon response. *J Gen Virol.* 2013;
  49. Nemésio H, Villalaín J. Membrane interacting regions of dengue virus NS2A protein. *J Phys Chem B.* 2014;
  50. León-Juárez M, Martínez-Castillo M, Shrivastava G, García-Cordero J, Villegas-Sepulveda N, Mondragón-Castelán M, et al. Recombinant Dengue virus protein NS2B alters membrane permeability in different membrane models. *Viol J.* 2016;13(1).
  51. Aguirre S, Luthra P, Sanchez-Aparicio MT, Maestre AM, Patel J, Lamothe F, et al. Dengue virus NS2B protein targets cGAS for degradation and prevents mitochondrial DNA sensing during infection. *Nat Microbiol.* 2017;
  52. Miller S, Kastner S, Krijnse-Locker J, Bühler S, Bartenschlager R. The non-structural protein 4A of dengue virus is an integral membrane protein inducing membrane alterations in a 2K-regulated manner. *J Biol Chem.* 2007;
  53. McLean JE, Wudzinska A, Datan E, Quaglino D, Zakeri Z. Flavivirus NS4A-induced autophagy protects cells against death and enhances virus replication. *J Biol Chem.* 2011;
  54. Chen X, Xia J, Zhao Q, Wang Y, Liu J, Feng L, et al. Eukaryotic initiation factor 4A1 interacts with NS4A of Dengue virus and plays an antiviral role. *Biochem Biophys Res Commun.* 2015;
  55. He Z, Zhu X, Wen W, Yuan J, Hu Y, Chen J, et al. Dengue Virus Subverts Host Innate Immunity by Targeting Adaptor Protein MAVS. *J Virol.* 2016;
  56. Nemésio H, Palomares-Jerez F, Villalaín J. NS4A and NS4B proteins from dengue virus: Membranotropic regions. *Biochim Biophys Acta - Biomembr.* 2012;
  57. Zou J, Lee LT, Wang QY, Xie X, Lu S, Yau YH, et al. Mapping the Interactions between the NS4B and NS3 proteins of dengue virus. *J Virol.* 2015;
  58. Carrasco L, Otero MJ, Castrillo J. Modification of membrane permeability by animal viruses. *Pharmacology and Therapeutics.* 1989.
  59. Mackenzie JM, Jones MK, Westaway EG. Markers for trans-Golgi membranes and the intermediate compartment localize to induced membranes with distinct replication functions in flavivirus-infected cells. *J Virol.* 1999;

60. Vázquez-Calvo Á, Saiz JC, McCullough KC, Sobrino F, Martín-Acebes MA. Acid-dependent viral entry. *Virus Research*. 2012.
61. De Castro IF, Volonté L, Risco C. Virus factories: Biogenesis and structural design. *Cellular Microbiology*. 2013.
62. Gonzalez ME, Carrasco L. Viroporins. *FEBS Lett*. 2003;
63. Grice AL, Kerr ID, Sansom MS. Ion channels formed by HIV-1 Vpu: a modelling and simulation study. *FEBS Lett*. 1997;
64. Hyser JM, Utama B, Crawford SE, Broughman JR, Estes MK. Activation of the endoplasmic reticulum calcium sensor STIM1 and store-operated calcium entry by rotavirus requires NSP4 viroporin activity. *J Virol*. 2013;
65. Wozniak AL, Griffin S, Rowlands D, Harris M, Yi M, Lemon SM, et al. Intracellular proton conductance of the hepatitis C virus p7 protein and its contribution to infectious virus production. *PLoS Pathog*. 2010;
66. Wang K, Xie S, Sun B. Viral proteins function as ion channels. *Biochim Biophys Acta*. 2010;
67. Luis Nieva J, Madan V, Carrasco L. The prevalence of pathogenic viruses and the shortage of effective treatment options for the diseases that they. 2012;
68. Lu W, Zheng B-J, Xu K, Schwarz W, Du L, Wong CKL, et al. Severe acute respiratory syndrome-associated coronavirus 3a protein forms an ion channel and modulates virus release. *Proc Natl Acad Sci U S A*. 2006;
69. Han Z, Harty RN. The NS3 protein of bluetongue virus exhibits viroporin-like properties. *J Biol Chem*. 2004;
70. Gonzalez ME, Carrasco L. Viroporins. *FEBS Letters*. 2003. p. 28–34.
71. Hyser JM, Estes MK. Pathophysiological Consequences of Calcium-Conducting Viroporins. 2015;
72. Lama J, Carrasco L. Expression of poliovirus nonstructural proteins in *Escherichia coli* cells: Modification of membrane permeability induced by 2B and 3A. *J Biol Chem*. 1992;
73. Barco A, Carrasco L. A human virus protein, poliovirus protein 2BC, induces membrane proliferation and blocks the exocytic pathway in the yeast *Saccharomyces cerevisiae*. *EMBO J*. 1995;
74. Pinto LH, Holsinger LJ, Lamb RA. Influenza virus M2 protein has ion channel activity. *Cell*. 1992;
75. Liu DX, Yuan Q, Liao Y. Coronavirus envelope protein: a small membrane protein with multiple functions. *Cell Mol Life Sci*. 2007;
76. Madan V, García MDJ, Sanz MA, Carrasco L. Viroporin activity of murine hepatitis virus E protein. *FEBS Lett*. 2005;



77. Raghava S, Giorda KM, Romano FB, Heuck AP, Hebert DN. SV40 late protein VP4 forms toroidal pores to disrupt membranes for viral release. *Biochemistry*. 2013;
78. Agirre A, Barco A, Carrasco L, Nieva JL. Viroporin-mediated membrane permeabilization: Pore formation by nonstructural poliovirus 2B protein. *J Biol Chem*. 2002;
79. Zhou Y, Frey TK, Yang JJ. Viral calciomics: Interplays between Ca<sup>2+</sup> and virus. *Cell Calcium*. 2009.
80. Van Kuppeveld FJM, De Jong AS, Melchers WJG, Willems PHGM. Enterovirus protein 2B po(u)res out the calcium: A viral strategy to survive? *Trends in Microbiology*. 2005.
81. Hyser JM, Collinson-Pautz MR, Utama B, Estes MK. Rotavirus disrupts calcium homeostasis by NSP4 viroporin activity. *MBio*. 2010;
82. Griffin SDC, Beales LP, Clarke DS, Worsfold O, Evans SD, Jaeger J, et al. The p7 protein of hepatitis C virus forms an ion channel that is blocked by the antiviral drug, Amantadine. *FEBS Letters*. 2003.
83. Hsu NY, Ilnytska O, Belov G, Santiana M, Chen YH, Takvorian PM, et al. Viral reorganization of the secretory pathway generates distinct organelles for RNA replication. *Cell*. 2010;
84. Galluzzi L, Brenner C, Morselli E, Touat Z, Kroemer G. Viral control of mitochondrial apoptosis. *Plos Pathog*. 2008;
85. Madan V, Castelló A, Carrasco L. Viroporins from RNA viruses induce caspase-dependent apoptosis. *Cell Microbiol*. 2008;
86. D'Agostino DM, Ranzato L, Arrigoni G, Cavallari I, Belleudi F, Torrisi MR, et al. Mitochondrial alterations induced by the p13II protein of human T-cell leukemia virus type 1. Critical role of arginine residues. *J Biol Chem*. 2002;
87. Bhowmick R, Halder UC, Chattopadhyay S, Chanda S, Nandi S, Bagchi P, et al. Rotaviral enterotoxin nonstructural protein 4 targets mitochondria for activation of apoptosis during infection. *J Biol Chem*. 2012;
88. Biasiotto R, Aguiari P, Rizzuto R, Pinton P, D'Agostino DM, Ciminale V. The p13 protein of human T cell leukemia virus type 1 (HTLV-1) modulates mitochondrial membrane potential and calcium uptake. *Biochim Biophys Acta*. 2010;
89. Pinto LH, Lamb RA. The M2 proton channels of influenza A and B viruses. *Journal of Biological Chemistry*. 2006.
90. Carrasco L. Entry of animal viruses and macromolecules into cells. *FEBS Letters*. 1994.
91. Steinmann E, Penin F, Kallis S, Patel AH, Bartenschlager R, Pietschmann T. Hepatitis C virus p7 protein is crucial for assembly and release of infectious virions. *PLoS Pathog*. 2007;

92. Watanabe T, Watanabe S, Ito H, Kida H, Kawaoka Y. Influenza A virus can undergo multiple cycles of replication without M2 ion channel activity. *J Virol.* 2001;
93. Griffin S, StGelais C, Owsianka AM, Patel AH, Rowlands D, Harris M. Genotype-dependent sensitivity of hepatitis C virus to inhibitors of the p7 ion channel. *Hepatology.* 2008;
94. Fernandez-Puentes C, Carrasco L. Viral infection permeabilizes mammalian cells to protein toxins. *Cell.* 1980;
95. Sanz MA, Madan V, Carrasco L, Nieva JL. Interfacial domains in sindbis virus 6K protein: Detection and functional characterization. *J Biol Chem.* 2003;
96. Hsu K, Han J, Shinlapawittayatorn K, Deschenes I, Marbán E. Membrane potential depolarization as a triggering mechanism for Vpu-mediated HIV-1 release. *Biophys J.* 2010;
97. Leiding T, Wang J, Martinsson J, DeGrado WF, Arsköld SP. Proton and cation transport activity of the M2 proton channel from influenza A virus. *Proc Natl Acad Sci U S A.* 2010;
98. Schnell JR, Chou JJ. Structure and mechanism of the M2 proton channel of influenza A virus. *Nature.* 2008;
99. Sharma M, Yi M, Dong H, Qin H, Peterson E, Busath DD, et al. Insight into the mechanism of the influenza A proton channel from a structure in a lipid bilayer. *Science.* 2010;
100. Rossman JS, Jing X, Leser GP, Lamb RA. Influenza Virus M2 Protein Mediates ESCRT-Independent Membrane Scission. *Cell.* 2010;
101. Nieva JL, Madan V, Carrasco L. Viroporins: structure and biological functions. *Nat Rev Microbiol* [Internet]. 2012;10(8):563–74. Available from: <http://www.ncbi.nlm.nih.gov/pubmed/22751485>
102. Medzhitov R, Janeway Jr. CA. Innate immunity: impact on the adaptive immune response. *Curr Opin Immunol* [Internet]. 1997;9(1):4–9. Available from: [http://www.ncbi.nlm.nih.gov/entrez/query.fcgi?cmd=Retrieve&db=PubMed&dopt=Citation&list\\_uids=9039775%5Cnhttp://www.sciencedirect.com/science?\\_ob=MIimg&\\_imagekey=B6VS1-4547CRX-B7-1&\\_cdi=6249&\\_user=4420&\\_pii=S0952791597801525&\\_orig=search&\\_coverDate=02%2F28%2F1](http://www.ncbi.nlm.nih.gov/entrez/query.fcgi?cmd=Retrieve&db=PubMed&dopt=Citation&list_uids=9039775%5Cnhttp://www.sciencedirect.com/science?_ob=MIimg&_imagekey=B6VS1-4547CRX-B7-1&_cdi=6249&_user=4420&_pii=S0952791597801525&_orig=search&_coverDate=02%2F28%2F1)
103. Medzhitov R, Janeway Jr. CA. Decoding the patterns of self and nonself by the innate immune system. *Science* (80- ) [Internet]. 2002;296(5566):298–300. Available from: [http://www.ncbi.nlm.nih.gov/entrez/query.fcgi?cmd=Retrieve&db=PubMed&dopt=Citation&list\\_uids=11951031%5Cnhttp://www.sciencemag.org/cgi/reprint/296/5566/298.pdf](http://www.ncbi.nlm.nih.gov/entrez/query.fcgi?cmd=Retrieve&db=PubMed&dopt=Citation&list_uids=11951031%5Cnhttp://www.sciencemag.org/cgi/reprint/296/5566/298.pdf)
104. Wilkins C, Gale M. Recognition of viruses by cytoplasmic sensors. *Curr Opin Immunol* [Internet]. Elsevier Ltd; 2010;22(1):41–7. Available from: <http://www.pubmedcentral.nih.gov/articlerender.fcgi?artid=3172156&tool=pmcentrez&rendertype=abstract>

105. Pothlichet J, Meunier I, Davis BK, Ting JP-Y, Skamene E, von Messling V, et al. Type I IFN triggers RIG-I/TLR3/NLRP3-dependent inflammasome activation in influenza A virus infected cells. *PLoS Pathog* [Internet]. 2013;9(4):e1003256. Available from: <http://www.pubmedcentral.nih.gov/articlerender.fcgi?artid=3623797&tool=pmcentrez&rendertype=abstract>
106. Lawrence TM, Hudacek AW, de Zoete MR, Flavell R a, Schnell MJ. Rabies virus is recognized by the NLRP3 inflammasome and activates interleukin-1 $\beta$  release in murine dendritic cells. *J Virol* [Internet]. 2013;87(10):5848–57. Available from: <http://www.pubmedcentral.nih.gov/articlerender.fcgi?artid=3648142&tool=pmcentrez&rendertype=abstract>
107. Subramanian N, Natarajan K, Clatworthy MR, Wang Z, Germain RN. The adaptor MAVS promotes NLRP3 mitochondrial localization and inflammasome activation. *Cell* [Internet]. Elsevier Inc.; 2013;153(2):348–61. Available from: <http://dx.doi.org/10.1016/j.cell.2013.02.054>
108. Park S, Juliana C, Hong S, Datta P, Hwang I, Fernandes-Alnemri T, et al. The mitochondrial antiviral protein MAVS associates with NLRP3 and regulates its inflammasome activity. *J Immunol* [Internet]. 2013;191(8):4358–66. Available from: <http://www.ncbi.nlm.nih.gov/pubmed/24048902>
109. Cai X, Chen J, Xu H, Liu S, Jiang Q-XX, Halfmann R, et al. Prion-like polymerization underlies signal transduction in antiviral immune defense and inflammasome activation. *Cell* [Internet]. Cell Press; 2014;156(6):1207–22. Available from: <http://www.ncbi.nlm.nih.gov/pubmed/24630723>
110. Franchi L, Eigenbrod T, Muñoz-Planillo R, Ozkurede U, Kim Y-G, Chakrabarti A, et al. Cytosolic double-stranded RNA activates the NLRP3 inflammasome via MAVS-induced membrane permeabilization and K<sup>+</sup> efflux. *J Immunol* [Internet]. 2014;193(8):4214–22. Available from: <http://www.ncbi.nlm.nih.gov/pubmed/25225670>
111. Huang H, Saravia J, You D, Shaw AJ, Cormier S a. Impaired gamma delta T cell-derived IL-17A and inflammasome activation during early respiratory syncytial virus infection in infants. *Immunol Cell Biol* [Internet]. Nature Publishing Group; 2014;(April):1–10. Available from: <http://www.ncbi.nlm.nih.gov/pubmed/25267484>
112. Lupfer C, Malik A, Kanneganti T-D. Inflammasome control of viral infection. *Curr Opin Virol* [Internet]. 2015;12(0):38–46. Available from: [http://www.sciencedirect.com/science/article/pii/S1879625715000310%5Cnhttp://ac.els-cdn.com/S1879625715000310/1-s2.0-S1879625715000310-main.pdf?\\_tid=2e02d30c-0469-11e5-b7ae-00000aacb35f&acdnat=1432728729\\_b1f0183acfe699745f95ce8703c61821](http://www.sciencedirect.com/science/article/pii/S1879625715000310%5Cnhttp://ac.els-cdn.com/S1879625715000310/1-s2.0-S1879625715000310-main.pdf?_tid=2e02d30c-0469-11e5-b7ae-00000aacb35f&acdnat=1432728729_b1f0183acfe699745f95ce8703c61821)
113. Lopez-Castejon G, Brough D. Understanding the mechanism of IL-1 $\beta$  secretion. *Cytokine Growth Factor Rev* [Internet]. 2011;22(4):189–95. Available from: [http://www.ncbi.nlm.nih.gov/entrez/query.fcgi?cmd=Retrieve&db=PubMed&dopt=Citation&list\\_uids=22019906](http://www.ncbi.nlm.nih.gov/entrez/query.fcgi?cmd=Retrieve&db=PubMed&dopt=Citation&list_uids=22019906)
114. Rietdijk ST, Burwell T, Bertin J, Coyle AJ. Sensing intracellular pathogens-NOD-like receptors. *Curr Opin Pharmacol* [Internet]. 2008;8(3):261–6. Available from:

<http://www.sciencedirect.com/science/article/pii/S1471489208000441>

115. Lamkanfi M, Kanneganti TD. Nlrp3: An immune sensor of cellular stress and infection. *Int J Biochem Cell Biol* [Internet]. Elsevier Ltd; 2010;42(6):792–5. Available from: <http://dx.doi.org/10.1016/j.biocel.2010.01.008>
116. Hornung V, Ablasser A, Charrel-Dennis M, Bauernfeind F, Horvath G, Caffrey DR, et al. AIM2 recognizes cytosolic dsDNA and forms a caspase-1-activating inflammasome with ASC. *Nature* [Internet]. 2009;458(7237):514–8. Available from: [http://www.ncbi.nlm.nih.gov/entrez/query.fcgi?cmd=Retrieve&db=PubMed&dopt=Citation&list\\_uids=19158675](http://www.ncbi.nlm.nih.gov/entrez/query.fcgi?cmd=Retrieve&db=PubMed&dopt=Citation&list_uids=19158675)  
<http://www.nature.com/nature/journal/v458/n7237/pdf/nature07725.pdf>
117. Martinon F, Burns K, Tschopp J. The inflammasome: a molecular platform triggering activation of inflammatory caspases and processing of proIL-beta. *Mol Cell* [Internet]. 2002;10(2):417–26. Available from: [http://ac.els-cdn.com/S1097276502005993/1-s2.0-S1097276502005993-main.pdf?\\_tid=454d667a-cfa0-11e3-84a3-00000aab0f26&acdnat=1398777481\\_c95e9f55449c17f7b023341c12e48d0b](http://ac.els-cdn.com/S1097276502005993/1-s2.0-S1097276502005993-main.pdf?_tid=454d667a-cfa0-11e3-84a3-00000aab0f26&acdnat=1398777481_c95e9f55449c17f7b023341c12e48d0b)
118. Lamkanfi M, Dixit VM. Mechanisms and functions of inflammasomes. *Cell* [Internet]. Elsevier Inc.; 2014;157(5):1013–22. Available from: <http://dx.doi.org/10.1016/j.cell.2014.04.007>
119. Cridland J a, Curley EZ, Wykes MN, Schroder K, Sweet MJ, Roberts TL, et al. The mammalian PYHIN gene family: Phylogeny, evolution and expression. *BMC Evol Biol* [Internet]. BMC Evolutionary Biology; 2012;12(1):140. Available from: BMC Evolutionary Biology
120. Gram AM, Frenkel J, Rensing ME. Inflammasomes and viruses: cellular defence versus viral offence. *J Gen Virol* [Internet]. 2012;93(Pt 10):2063–75. Available from: [http://vir.sgmjournals.org/content/93/Pt\\_10/2063.full.pdf](http://vir.sgmjournals.org/content/93/Pt_10/2063.full.pdf)
121. Shrivastava G, León-Juárez M, García-Cordero J, Meza-Sánchez DE, Cedillo-Barrón L. Inflammasomes and its importance in viral infections. *Immunol Res*. 2016;64(5–6).
122. Meylan E, Tschopp J, Karin M. Intracellular pattern recognition receptors in the host response. *Nature* [Internet]. 2006;442(7098):39–44. Available from: <http://www.ncbi.nlm.nih.gov/pubmed/16823444>
123. Fritz JH, Ferrero RL, Philpott DJ, Girardin SE. Nod-like proteins in immunity, inflammation and disease. *Nat Immunol* [Internet]. 2006;7(12):1250–7. Available from: <http://www.nature.com/doifinder/10.1038/ni1412>
124. Werts C, Girardin SE, Philpott DJ. TIR, CARD and PYRIN: three domains for an antimicrobial triad. *Cell Death Differ*. 2006;13(5):798–815.
125. Inohara N, Nunez G. NODs: intracellular proteins involved in inflammation and apoptosis. *Nat Rev Immunol* [Internet]. 2003;3(5):371–82. Available from: [http://www.ncbi.nlm.nih.gov/entrez/query.fcgi?cmd=Retrieve&db=PubMed&dopt=Citation&list\\_uids=12766759](http://www.ncbi.nlm.nih.gov/entrez/query.fcgi?cmd=Retrieve&db=PubMed&dopt=Citation&list_uids=12766759)  
<http://www.nature.com/nri/journal/v3/n5/abs/nri1086.html>  
<http://www.nature.com/nri/journal/v3/n5/pdf/nri1086.pdf>

126. Mariathasan S, Newton K, Monack DM, Vucic D, French DM, Lee WP, et al. Differential activation of the inflammasome by caspase-1 adaptors ASC and Ipaf. *Nature* [Internet]. 2004;430(6996):213–8. Available from: [http://www.ncbi.nlm.nih.gov/entrez/query.fcgi?cmd=Retrieve&db=PubMed&dopt=Citation&list\\_uids=15190255%5Cnhttp://www.nature.com/nature/journal/v430/n6996/pdf/nature02664.pdf](http://www.ncbi.nlm.nih.gov/entrez/query.fcgi?cmd=Retrieve&db=PubMed&dopt=Citation&list_uids=15190255%5Cnhttp://www.nature.com/nature/journal/v430/n6996/pdf/nature02664.pdf)
127. Faustin B, Reed JC. Sunburned skin activates inflammasomes. *Trends Cell Biol.* 2008;18(1):4–8.
128. Tattoli I, Travassos LH, Carneiro L a, Magalhaes JG, Girardin SE. The Nodosome: Nod1 and Nod2 control bacterial infections and inflammation. *Semin Immunopathol* [Internet]. 2007;29(3):289–301. Available from: <http://www.ncbi.nlm.nih.gov/pubmed/17690884>
129. Lu C, Wang A, Wang L, Dorsch M, Ocain TD, Xu Y. Nucleotide binding to CARD12 and its role in CARD12-mediated caspase-1 activation. *Biochem Biophys Res Commun* [Internet]. 2005;331(4):1114–9. Available from: <http://www.ncbi.nlm.nih.gov/pubmed/15882992>
130. Lupfer C, Kanneganti T-D. The expanding role of NLRs in antiviral immunity. *Immunol Rev* [Internet]. 2013;255(1):13–24. Available from: <http://www.ncbi.nlm.nih.gov/pubmed/23947344>
131. Gross O, Thomas CJ, Guarda G, Tschopp J. The inflammasome: An integrated view. *Immunol Rev.* 2011;243(1):136–51.
132. Martinon F, Tschopp J. Inflammatory caspases and inflammasomes: master switches of inflammation. *Cell Death Differ* [Internet]. 2007;14(1):10–22. Available from: <http://www.nature.com/cdd/journal/v14/n1/pdf/4402038a.pdf>
133. Bauernfeind FG, Horvath G, Stutz A, Alnemri ES, MacDonald K, Speert D, et al. Cutting edge: NF-kappaB activating pattern recognition and cytokine receptors license NLRP3 inflammasome activation by regulating NLRP3 expression. *J Immunol* [Internet]. 2009;183(2):787–91. Available from: <http://www.jimmunol.org/content/183/2/787.full.pdf>
134. Martinon F, Mayor A, Tschopp J. The Inflammasomes: Guardians of the Body. *Annu Rev Immunol* [Internet]. 2009;27(1):229–65. Available from: <http://www.annualreviews.org/doi/abs/10.1146/annurev.immunol.021908.132715>
135. Hornung V, Bauernfeind F, Halle A, Samstad EO, Kono H, Rock KL, et al. Silica crystals and aluminum salts activate the NALP3 inflammasome through phagosomal destabilization. *Nat Immunol* [Internet]. 2008;9(8):847–56. Available from: <http://www.nature.com/ni/journal/v9/n8/pdf/ni.1631.pdf>
136. Cruz CM, Rinna A, Forman HJ, Ventura AL, Persechini PM, Ojcius DM. ATP activates a reactive oxygen species-dependent oxidative stress response and secretion of proinflammatory cytokines in macrophages. *J Biol Chem* [Internet]. 2007;282(5):2871–9. Available from: <http://www.ncbi.nlm.nih.gov/pubmed/17132626>
137. Kanneganti TD, Lamkanfi M, Kim YG, Chen G, Park JH, Franchi L, et al. Pannexin-1-mediated recognition of bacterial molecules activates the cryopyrin inflammasome

- independent of Toll-like receptor signaling. *Immunity* [Internet]. 2007;26(4):433–43. Available from: [http://www.ncbi.nlm.nih.gov/entrez/query.fcgi?cmd=Retrieve&db=PubMed&dopt=Citation&list\\_uids=17433728%5Chttp://www.sciencedirect.com/science?\\_ob=MIimg&\\_imagekey=B6WSP-4NGCYF0-1-2&\\_cdi=7052&\\_user=10&\\_pii=S1074761307002117&\\_coverDate=04%252F27%252F2007&\\_sk=%2523TOC%25](http://www.ncbi.nlm.nih.gov/entrez/query.fcgi?cmd=Retrieve&db=PubMed&dopt=Citation&list_uids=17433728%5Chttp://www.sciencedirect.com/science?_ob=MIimg&_imagekey=B6WSP-4NGCYF0-1-2&_cdi=7052&_user=10&_pii=S1074761307002117&_coverDate=04%252F27%252F2007&_sk=%2523TOC%25)
138. Murakami T, Ockinger J, Yu J, Byles V, McColl A, Hofer AM, et al. Critical role for calcium mobilization in activation of the NLRP3 inflammasome. *Proc Natl Acad Sci U S A* [Internet]. 2012;109(28):11282–7. Available from: <http://www.pnas.org/content/109/28/11282.full.pdf>
  139. Lee G-S, Subramanian N, Kim AI, Aksentijevich I, Goldbach-Mansky R, Sacks DB, et al. The calcium-sensing receptor regulates the NLRP3 inflammasome through Ca<sup>2+</sup> and cAMP. *Nature* [Internet]. Nature Publishing Group; 2012;492(7427):123–7. Available from: <http://www.ncbi.nlm.nih.gov/pubmed/23143333>
  140. Feldmeyer L, Keller M, Niklaus G, Hohl D, Werner S, Beer HD. The inflammasome mediates UVB-induced activation and secretion of interleukin-1beta by keratinocytes. *Curr Biol* [Internet]. 2007;17(13):1140–5. Available from: [http://ac.els-cdn.com/S0960982207015084/1-s2.0-S0960982207015084-main.pdf?\\_tid=525bc6be-15c1-11e5-bf65-00000aab0f26&acdnat=1434635755\\_fd4b4c042b55488be5fc6bf7b346ff7a](http://ac.els-cdn.com/S0960982207015084/1-s2.0-S0960982207015084-main.pdf?_tid=525bc6be-15c1-11e5-bf65-00000aab0f26&acdnat=1434635755_fd4b4c042b55488be5fc6bf7b346ff7a)
  141. Triantafilou K, Hughes TR, Triantafilou M, Morgan BP. The complement membrane attack complex triggers intracellular Ca<sup>2+</sup> fluxes leading to NLRP3 inflammasome activation. *J Cell Sci* [Internet]. 2013;126(Pt 13):2903–13. Available from: <http://www.ncbi.nlm.nih.gov/pubmed/23613465%5Chttp://jcs.biologists.org/content/126/13/2903.full.pdf>
  142. Munoz-Planillo R, Kuffa P, Martinez-Colon G, Smith BL, Rajendiran TM, Nunez G. K(+) efflux is the common trigger of NLRP3 inflammasome activation by bacterial toxins and particulate matter. *Immunity* [Internet]. 2013;38(6):1142–53. Available from: [http://ac.els-cdn.com/S1074761313002434/1-s2.0-S1074761313002434-main.pdf?\\_tid=0f8d9aa6-15c1-11e5-b154-00000aab0f01&acdnat=1434635643\\_f7265a75a220cac61f254b65f6c0a50f](http://ac.els-cdn.com/S1074761313002434/1-s2.0-S1074761313002434-main.pdf?_tid=0f8d9aa6-15c1-11e5-b154-00000aab0f01&acdnat=1434635643_f7265a75a220cac61f254b65f6c0a50f)
  143. Guo HC, Jin Y, Zhi XY, Yan D, Sun SQ. NLRP3 Inflammasome Activation by Viroporins of Animal Viruses. *Viruses*. 2015;7(7):3380–91.
  144. Chen IY, Ichinohe T. Response of host inflammasomes to viral infection. *Trends Microbiol* [Internet]. 2015;23(1):55–63. Available from: [http://www.sciencedirect.com/science/article/pii/S0966842X1400198X%5Chttp://ac.els-cdn.com/S0966842X1400198X/1-s2.0-S0966842X1400198X-main.pdf?\\_tid=cf561720-9d6a-11e4-9da1-00000aacb35e&acdnat=1421404459\\_596ffd8fd5493907102a9ddd971a4844](http://www.sciencedirect.com/science/article/pii/S0966842X1400198X%5Chttp://ac.els-cdn.com/S0966842X1400198X/1-s2.0-S0966842X1400198X-main.pdf?_tid=cf561720-9d6a-11e4-9da1-00000aacb35e&acdnat=1421404459_596ffd8fd5493907102a9ddd971a4844)
  145. Lupfer C, Kanneganti TD. The expanding role of NLRs in antiviral immunity. *Immunological Reviews*. 2013.

146. Kanneganti TD, Body-Malapel M, Amer A, Park JH, Whitfield J, Franchi L, et al. Critical role for Cryopyrin/Nalp3 in activation of caspase-1 in response to viral infection and double-stranded RNA. *J Biol Chem* [Internet]. 2006;281(48):36560–8. Available from: [http://www.ncbi.nlm.nih.gov/entrez/query.fcgi?cmd=Retrieve&db=PubMed&dopt=Citation&list\\_uids=17008311%5Cnhttp://www.jbc.org/content/281/48/36560.full.pdf](http://www.ncbi.nlm.nih.gov/entrez/query.fcgi?cmd=Retrieve&db=PubMed&dopt=Citation&list_uids=17008311%5Cnhttp://www.jbc.org/content/281/48/36560.full.pdf)
147. Rajan J V, Rodriguez D, Miao E a, Aderem A. The NLRP3 inflammasome detects encephalomyocarditis virus and vesicular stomatitis virus infection. *J Virol*. 2011;85(9):4167–72.
148. Ito M, Yanagi Y, Ichinohe T. Encephalomyocarditis virus viroporin 2B activates NLRP3 inflammasome. *PLoS Pathog* [Internet]. 2012;8(8):e1002857. Available from: <http://www.plospathogens.org/article/fetchObjectAttachment.action?uri=info%3Adoi%2F10.1371%2Fjournal.ppat.1002857&representation=PDF>
149. Komune N, Ichinohe T, Ito M, Yanagi Y. Measles Virus V Protein Inhibits NLRP3 Inflammasome-Mediated Interleukin-1 Secretion. *J Virol*. 2011;85(24):13019–26.
150. Triantafilou K, Kar S, Van Kuppeveld FJM, Triantafilou M. Rhinovirus-induced calcium flux triggers NLRP3 and NLRC5 activation in bronchial cells. *Am J Respir Cell Mol Biol*. 2013;49:923–34.
151. Shrivastava S, Mukherjee a., Ray R, Ray RB. Hepatitis C Virus Induces Interleukin-1 (IL-1)/IL-18 in Circulatory and Resident Liver Macrophages. *J Virol* [Internet]. 2013;87(22):12284–90. Available from: <http://jvi.asm.org/cgi/doi/10.1128/JVI.01962-13>
152. Negash AA, Ramos HJ, Crochet N, Lau DTY, Doehle B, Papic N, et al. IL-1 $\beta$  Production through the NLRP3 Inflammasome by Hepatic Macrophages Links Hepatitis C Virus Infection with Liver Inflammation and Disease. *PLoS Pathog* [Internet]. Public Library of Science; 2013;9(4):e1003330. Available from: <http://dx.doi.org/10.1371%2Fjournal.ppat.1003330%5Cnhttp://www.ncbi.nlm.nih.gov/pmc/articles/PMC3635973/pdf/ppat.1003330.pdf>
153. Chen W, Xu Y, Li H, Tao W, Xiang Y, Huang B, et al. HCV Genomic RNA Activates the NLRP3 Inflammasome in Human Myeloid Cells. *PLoS One* [Internet]. Public Library of Science; 2014;9(1):e84953. Available from: <http://dx.doi.org/10.1371%2Fjournal.pone.0084953%5Cnhttp://www.ncbi.nlm.nih.gov/pmc/articles/PMC3882267/pdf/pone.0084953.pdf>
154. Owen DM, Gale M. Fighting the flu with inflammasome signaling. *Immunity* [Internet]. Elsevier Inc.; 2009;30(4):476–8. Available from: <http://www.ncbi.nlm.nih.gov/pubmed/19371712>
155. Pang IK, Iwasaki A. Inflammasomes as mediators of immunity against influenza virus. *Trends Immunol* [Internet]. 2011;32(1):34–41. Available from: [http://ac.els-cdn.com/S1471490610001651/1-s2.0-S1471490610001651-main.pdf?\\_tid=880973ac-f9e-11e3-a765-00000aacb361&acdnat=1398776734\\_8192527a100528cca2b6020b2444308b](http://ac.els-cdn.com/S1471490610001651/1-s2.0-S1471490610001651-main.pdf?_tid=880973ac-f9e-11e3-a765-00000aacb361&acdnat=1398776734_8192527a100528cca2b6020b2444308b)
156. Allen IC, Scull MA, Moore CB, Holl EK, McElvania-TeKippe E, Taxman DJ, et al. The NLRP3 inflammasome mediates in vivo innate immunity to influenza A virus through

- recognition of viral RNA. *Immunity* [Internet]. 2009;30(4):556–65. Available from: [http://www.ncbi.nlm.nih.gov/entrez/query.fcgi?cmd=Retrieve&db=PubMed&dopt=Citation&list\\_uids=19362020%5Cnhttp://www.sciencedirect.com/science?\\_ob=MImg&\\_imagekey=B6WSP-4W1K8T0-1-2&\\_cdi=7052&\\_user=4420&\\_pii=S1074761309001393&\\_orig=search&\\_coverDate=04%2F17%2F2](http://www.ncbi.nlm.nih.gov/entrez/query.fcgi?cmd=Retrieve&db=PubMed&dopt=Citation&list_uids=19362020%5Cnhttp://www.sciencedirect.com/science?_ob=MImg&_imagekey=B6WSP-4W1K8T0-1-2&_cdi=7052&_user=4420&_pii=S1074761309001393&_orig=search&_coverDate=04%2F17%2F2)
157. Thomas PG, Dash P, Aldridge Jr. JR, Ellebedy AH, Reynolds C, Funk AJ, et al. The intracellular sensor NLRP3 mediates key innate and healing responses to influenza A virus via the regulation of caspase-1. *Immunity* [Internet]. 2009;30(4):566–75. Available from: [http://ac.els-cdn.com/S107476130900140X/1-s2.0-S107476130900140X-main.pdf?\\_tid=5c8c4e10-cf9f-11e3-8cc2-00000aacb35d&acdnat=1398777091\\_b4918beee2b05755a5fbbd823125dbb3](http://ac.els-cdn.com/S107476130900140X/1-s2.0-S107476130900140X-main.pdf?_tid=5c8c4e10-cf9f-11e3-8cc2-00000aacb35d&acdnat=1398777091_b4918beee2b05755a5fbbd823125dbb3)
  158. Ichinohe T, Pang IK, Iwasaki A. Influenza virus activates inflammasomes via its intracellular M2 ion channel. *Nat Immunol* [Internet]. 2010;11(5):404–10. Available from: <http://www.nature.com/ni/journal/v11/n5/pdf/ni.1861.pdf>
  159. Segovia J, Sabbah A, Mgbemena V, Tsai SY, Chang TH, Berton MT, et al. TLR2/MyD88/NF-kappaB pathway, reactive oxygen species, potassium efflux activates NLRP3/ASC inflammasome during respiratory syncytial virus infection. *PLoS One* [Internet]. 2012;7(1):e29695. Available from: <http://www.plosone.org/article/fetchObjectAttachment.action?uri=info%3Adoi%2F10.1371%2Fjournal.pone.0029695&representation=PDF>
  160. Triantafilou K, Kar S, Vakakis E, Kotecha S, Triantafilou M. Human respiratory syncytial virus viroporin SH: a viral recognition pathway used by the host to signal inflammasome activation. *Thorax* [Internet]. 2013;68(1):66–75. Available from: <http://thorax.bmj.com/content/68/1/66.full.pdf>
  161. Pontillo A, Silva LT, Oshiro TM, Finazzo C, Crovella S, Duarte AJS. HIV-1 induces NALP3-inflammasome expression and interleukin-1 $\beta$  secretion in dendritic cells from healthy individuals but not from HIV-positive patients. *AIDS* [Internet]. 2012;26(1):11–8. Available from: <http://www.ncbi.nlm.nih.gov/pubmed/21971358>
  162. Ramos HJ, Lanteri MC, Blahnik G, Negash A, Suthar MS, Brassil MM, et al. IL-1 $\beta$  signaling promotes CNS-intrinsic immune control of West Nile virus infection. *PLoS Pathog* [Internet]. 2012;8(11):e1003039. Available from: <http://www.pubmedcentral.nih.gov/articlerender.fcgi?artid=3510243&tool=pmcentrez&rendertype=abstract>
  163. Kumar M, Roe K, Orillo B, Muruve DA, Nerurkar VR, Gale M, et al. Inflammasome adaptor protein Apoptosis-associated speck-like protein containing CARD (ASC) is critical for the immune response and survival in west Nile virus encephalitis. *J Virol* [Internet]. 2013;87(7):3655–67. Available from: <http://www.pubmedcentral.nih.gov/articlerender.fcgi?artid=3624239&tool=pmcentrez&rendertype=abstract>
  164. Kaushik DK, Gupta M, Kumawat KL, Basu A. NLRP3 inflammasome: key mediator of neuroinflammation in murine Japanese encephalitis. *PLoS One* [Internet]. 2012;7(2):e32270. Available from:



<http://www.pubmedcentral.nih.gov/articlerender.fcgi?artid=3290554&tool=pmcentrez&rendertype=abstract>

165. Hottz ED, Lopes JF, Freitas C, Valls-de-Souza R, Oliveira MF, Bozza MT, et al. Platelets mediate increased endothelium permeability in dengue through NLRP3-inflammasome activation. *Blood* [Internet]. 2013;122(20):3405–14. Available from: <http://www.pubmedcentral.nih.gov/articlerender.fcgi?artid=3829114&tool=pmcentrez&rendertype=abstract>
166. Wu M-F, Chen S-T, Yang A-H, Lin W-W, Lin Y-L, Chen NJ, et al. CLEC5A is critical for dengue virus-induced inflammasome activation in human macrophages. *Blood*. 2013;121(1):95–106.
167. Ermler ME, Traylor Z, Patel K, Schattgen SA, Vanaja SK, Fitzgerald KA, et al. Rift Valley fever virus infection induces activation of the NLRP3 inflammasome. *Virology* [Internet]. Academic Press Inc.; 2014;449:174–80. Available from: <http://www.scopus.com/inward/record.url?eid=2-s2.0-84896983616&partnerID=tZOtx3y1>
168. Wikan N, Khongwichit S, Phuklia W, Ubol S, Thonsakulprasert T, Thannagith M, et al. Comprehensive proteomic analysis of white blood cells from chikungunya fever patients of different severities. *J Transl Med* [Internet]. Journal of Translational Medicine; 2014;12(1):96. Available from: <http://www.ncbi.nlm.nih.gov/pubmed/24721947>
169. Zhi X-Y, Guo H-C, Jin Y, Yan D, Sun S-Q. NLRP3 Inflammasome Activation by Viroporins of Animal Viruses. *Viruses* (1999-4915). 2015;
170. Allen IC, Scull MA, Moore CB, Holl EK, McElvania-TeKippe E, Taxman DJ, et al. The NLRP3 Inflammasome Mediates In Vivo Innate Immunity to Influenza A Virus through Recognition of Viral RNA. *Immunity*. 2009;
171. Segovia J, Sabbah A, Mgbemena V, Tsai SY, Chang TH, Berton MT, et al. TLR2/MyD88/NF- $\kappa$ B pathway, reactive oxygen species, potassium efflux activates NLRP3/ASC inflammasome during respiratory syncytial virus infection. *PLoS One*. 2012;
172. Triantafilou K, Kar S, Vakakis E, Kotecha S, Triantafilou M. Human respiratory syncytial virus viroporin SH: a viral recognition pathway used by the host to signal inflammasome activation. *Thorax*. 2013;
173. Ito M, Yanagi Y, Ichinohe T. Encephalomyocarditis Virus Viroporin 2B Activates NLRP3 Inflammasome. *PLoS Pathog*. 2012;
174. Triantafilou K, Kar S, Van Kuppeveld FJM, Triantafilou M. Rhinovirus-induced calcium flux triggers NLRP3 and NLRC5 activation in bronchial cells. *Am J Respir Cell Mol Biol*. 2013;
175. Shrivastava S, Mukherjee A, Ray R, Ray RB. Hepatitis C virus induces interleukin-1 $\beta$  (IL-1 $\beta$ )/IL-18 in circulatory and resident liver macrophages. *J Virol*. 2013;
176. Negash AA, Ramos HJ, Crochet N, Lau DTY, Doehle B, Papic N, et al. IL-1 $\beta$  Production through the NLRP3 Inflammasome by Hepatic Macrophages Links Hepatitis C Virus Infection with Liver Inflammation and Disease. *PLoS Pathog*. 2013;

177. Chen W, Xu Y, Li H, Tao W, Xiang Y, Huang B, et al. HCV genomic RNA activates the NLRP3 inflammasome in human myeloid cells. *PLoS One*. 2014;
178. Chen IY, Ichinohe T. Response of host inflammasomes to viral infection. *Trends in Microbiology*. 2015.
179. Bozza F a, Cruz OG, Zagne SMO, Azeredo EL, Nogueira RMR, Assis EF, et al. Multiplex cytokine profile from dengue patients: MIP-1beta and IFN-gamma as predictive factors for severity. *BMC Infect Dis* [Internet]. 2008;8(1):86. Available from: <http://www.biomedcentral.com/1471-2334/8/86%5Cnhttp://www.pubmedcentral.nih.gov/articlerender.fcgi?artid=2474613&tool=pmcentrez&rendertype=abstract>
180. Davis BK, Wen H, Ting JP-Y. The inflammasome NLRs in immunity, inflammation, and associated diseases. *Annu Rev Immunol* [Internet]. 2011;29:707–35. Available from: <http://www.pubmedcentral.nih.gov/articlerender.fcgi?artid=4067317&tool=pmcentrez&rendertype=abstract>
181. Netea MG, Kullberg BJ, Van der Meer JW. Circulating cytokines as mediators of fever. *Clin Infect Dis*. 2000;
182. Dinarello CA. Infection, fever, and exogenous and endogenous pyrogens: some concepts have changed. *J Endotoxin Res*. 2004;
183. Callaway JB, Smith SA, McKinnon KP, De Silva AM, Crowe JE, Ting JPY. Spleen tyrosine kinase (Syk) mediates IL-1 $\beta$  induction by primary human monocytes during antibody-enhanced dengue virus infection. *J Biol Chem*. 2015;
184. Bozza FA, Cruz OG, Zagne SM, Azeredo EL, Nogueira RM, Assis EF, et al. Multiplex cytokine profile from dengue patients: MIP-1beta and IFN-gamma as predictive factors for severity. *BMC Infect Dis*. 2008;
185. Wu M-F, Chen S-T, Hsieh S-L. Distinct regulation of dengue virus-induced inflammasome activation in human macrophage subsets. *J Biomed Sci*. 2013;
186. Hottz ED, Medeiros-de-Moraes IM, Vieira-de-Abreu A, de Assis EF, Vals-de-Souza R, Castro-Faria-Neto HC, et al. Platelet activation and apoptosis modulate monocyte inflammatory responses in dengue. *J Immunol*. 2014;
187. Suharti C, Van Gorp ECM, Setiati TE, Dolmans WM V, Djokomoeljanto RJ, Hack CE, et al. The role of cytokines in activation of coagulation and fibrinolysis in dengue shock syndrome. *Thromb Haemost*. 2002;87(1):42–6.
188. Pang T, Cardosa MJ, Guzman MG. Of cascades and perfect storms: the immunopathogenesis of dengue haemorrhagic fever-dengue shock syndrome (DHF/DSS). *Immunol Cell Biol*. 2007;85:43–5.
189. Nasirudeen AMA, Liu DX. Gene expression profiling by microarray analysis reveals an important role for caspase-1 in dengue virus-induced p53-mediated apoptosis. *J Med Virol*. 2009;

190. Wu MF, Chen ST, Yang AH, Lin WW, Lin YL, Chen NJ, et al. CLEC5A is critical for dengue virus-induced inflammasome activation in human macrophages. *Blood*. 2013;
191. Welsch S, Miller S, Romero-Brey I, Merz A, Bleck CKE, Walther P, et al. Composition and Three-Dimensional Architecture of the Dengue Virus Replication and Assembly Sites. *Cell Host Microbe*. 2009;
192. Vasquez Ochoa M, Garcia Cordero J, Gutierrez Castaneda B, Santos Argumedo L, Villegas Sepulveda N, Cedillo Barron L. A clinical isolate of dengue virus and its proteins induce apoptosis in HMEC-1 cells: a possible implication in pathogenesis. *Arch Virol*. 2009;
193. Ma Q, Chen S, Hu Q, Feng H, Zhang JH, Tang J. NLRP3 inflammasome contributes to inflammation after intracerebral hemorrhage. *Ann Neurol*. 2014;
194. Hottz ED, Lopes JF, Freitas C, Valls-de-Souza R, Oliveira MF, Bozza MT, et al. Platelets mediate increased endothelium permeability in dengue through NLRP3-in fl ammasome activation. *Blood*. 2013;
195. Ran F, Hsu P, Wright J, Agarwala V. Genome engineering using the CRISPR-Cas9 system. *Nat Protoc*. 2013;
196. Sanjana NE, Shalem O, Zhang F. Improved vectors and genome-wide libraries for CRISPR screening. *Nat Methods*. 2014;
197. Shrivastava G, García-Cordero J, León-Juárez M, Oza G, Tapia-Ramírez J, Villegas-Sepulveda N, et al. NS2A comprises a putative viroporin of Dengue virus 2.
198. Netherton CL, Wileman T. Virus factories, double membrane vesicles and viroplasm generated in animal cells. *Curr Opin Virol*. 2011;
199. den Boon JA, Ahlquist P. Organelle-like membrane Ccompartmentalization of positive-strand RNA virus replication factories. *Annu Rev Microbiol Vol 64, 2010*. 2010;
200. Madan V, Sanz MA, Carrasco L. Requirement of the vesicular system for membrane permeabilization by Sindbis virus. *Virology*. 2005;
201. Aweya JJ, Mak TM, Lim SG, Tan YJ. The p7 protein of the hepatitis C virus induces cell death differently from the influenza A virus viroporin M2. *Virus Res*. 2013;
202. Xie X, Gayen S, Kang C, Yuan Z, Shi P-Y. Membrane topology and function of dengue virus NS2A protein. *J Virol [Internet]*. 2013;87(8):4609–22. Available from: <http://www.pubmedcentral.nih.gov/articlerender.fcgi?artid=3624351&tool=pmcentrez&rendertype=abstract>
203. Herrero L, Monroy N, González ME. HIV-1 Vpu protein mediates the transport of potassium in *Saccharomyces cerevisiae*. *Biochemistry*. 2013;
204. Pielak RM, Chou JJ. Influenza M2 proton channels. *Biochimica et Biophysica Acta - Biomembranes*. 2011.

205. Clarke D, Griffin S, Beales L, Gelais CS, Burgess S, Harris M, et al. Evidence for the formation of a heptameric ion channel complex by the hepatitis C virus p7 protein in vitro. *J Biol Chem*. 2006;
206. S.D. C, K.C. D, E. A, T.L. F, M. V, P. G, et al. Direct visualization of the small hydrophobic protein of human respiratory syncytial virus reveals the structural basis for membrane permeability. *FEBS Letters*. 2010.
207. Daniels R, Sadowicz D, Hebert DN. A very late viral protein triggers the lytic release of SV40. *PLoS Pathog*. 2007;
208. Ao D, Guo HC, Sun SQ, Sun DH, Fung TS, Wei YQ, et al. Viroporin activity of the foot-and-mouth disease virus non-structural 2B protein. *PLoS One*. 2015;
209. Giorda KM, Raghava S, Zhang MW, Hebert DN. The viroporin activity of the minor structural proteins VP2 and VP3 is required for SV40 propagation. *J Biol Chem*. 2013;
210. Gan SW, Tan E, Lin X, Yu D, Wang J, Tan GMY, et al. The small hydrophobic protein of the human respiratory syncytial virus forms pentameric ion channels. *J Biol Chem*. 2012;
211. Fischer WB, Hsu HJ. Viral channel forming proteins - Modeling the target. *Biochimica et Biophysica Acta - Biomembranes*. 2011.
212. Spector AA, Yorek MA. Membrane lipid composition and cellular function. *J Lipid Res*. 1985;
213. Pham T, Perry JL, Dosey TL, Delcour AH, Hyser JM. The Rotavirus NSP4 Viroporin Domain is a Calcium-conducting Ion Channel. *Sci Rep*. 2017;
214. Agosto MA, Ivanovic T, Nibert ML. Mammalian reovirus, a nonfusogenic nonenveloped virus, forms size-selective pores in a model membrane. *Proc Natl Acad Sci U S A*. 2006;
215. Madan V, Sánchez-Martínez S, Carrasco L, Nieva JL. A peptide based on the pore-forming domain of pro-apoptotic poliovirus 2B viroporin targets mitochondria. *Biochim Biophys Acta - Biomembr*. 2010;
216. van Meer G, Voelker DR, Feigenson GW. Membrane lipids: where they are and how they behave. *Nat Rev Mol Cell Biol*. 2008;
217. Mackenzie JM, Westaway EG. Assembly and maturation of the flavivirus Kunjin virus appear to occur in the rough endoplasmic reticulum and along the secretory pathway, respectively. *J Virol*. 2001;
218. Broz P, Dixit VM. Inflammasomes: mechanism of assembly, regulation and signalling. *Nat Rev Immunol* [Internet]. 2016;16(7):407–20. Available from: <http://www.nature.com/doi/10.1038/nri.2016.58><http://www.nature.com/doi/10.1038/nri.2016.58><http://www.ncbi.nlm.nih.gov/pubmed/27291964>
219. Guo H-C, Jin Y, Zhi X-Y, Yan D, Sun S-Q. NLRP3 Inflammasome Activation by Viroporins of Animal Viruses. *Viruses* [Internet]. 2015;7(7):3380–91. Available from: <http://www.ncbi.nlm.nih.gov/pubmed/26114475><http://www.ncbi.nlm.nih.gov/pubmed/26114475><http://www.pubmedcentral.nih.gov/>

articlerender.fcgi?artid=PMC4517106

220. Talavera D, Castillo AM, Dominguez MC, Escobar Gutierrez A, Meza I. IL8 release, tight junction and cytoskeleton dynamic reorganization conducive to permeability increase are induced by dengue virus infection of microvascular endothelial monolayers. *J Gen Virol.* 2004;
221. Dalrymple N, Mackow ER. Productive dengue virus infection of human endothelial cells is directed by heparan sulfate-containing proteoglycan receptors. *J Virol.* 2011;
222. Bustos-Arriaga J, Garcia-Machorro J, Leizaola-Munoz M, Garcia-Cordero J, Santos-Argumedo L, Flores-Romo L, et al. Activation of the innate immune response against dengue in normal non-transformed human fibroblasts. *PLoS Negl Trop Dis.* 2011;
223. Kaushik DK, Gupta M, Kumawat KL, Basu A. Nlrp3 inflammasome: Key mediator of neuroinflammation in murine japanese encephalitis. *PLoS One.* 2012;7(2).
224. Negash AA, Ramos HJ, Crochet N, Lau DTY, Doehle B, Pappas N, et al. IL-1 $\beta$  Production through the NLRP3 Inflammasome by Hepatic Macrophages Links Hepatitis C Virus Infection with Liver Inflammation and Disease. *PLoS Pathog.* 2013;9(4).
225. Ramos HJ, Lanteri MC, Blahnik G, Negash A, Suthar MS, Brassil MM, et al. IL-1 $\beta$  signaling promotes CNS-intrinsic immune control of West Nile virus infection. *PLoS Pathog* [Internet]. 2012;8(11):e1003039. Available from: <http://www.ncbi.nlm.nih.gov/pubmed/23209411> <http://www.ncbi.nlm.nih.gov/pmc/articles/PMC3510243/pdf/ppat.1003039.pdf>
226. Tricarico PM, Caracciolo I, Crovella S, D'Agaro P. Zika virus induces inflammasome activation in the glial cell line U87-MG. *Biochem Biophys Res Commun.* 2017;
227. Bauernfeind F, Ablasser A, Bartok E, Kim S, Schmid-Burgk J, Cavlar T, et al. Inflammasomes: Current understanding and open questions. *Cellular and Molecular Life Sciences.* 2011. p. 765–83.
228. Ekchariyawat P, Hamel R, Bernard E, Wichit S, Surasombatpattana P, Talignani L, et al. Inflammasome signaling pathways exert antiviral effect against Chikungunya virus in human dermal fibroblasts. *Infect Genet Evol* [Internet]. Elsevier B.V.; 2015;32:401–8. Available from: <http://linkinghub.elsevier.com/retrieve/pii/S1567134815001100>
229. Hamel R, Dejarnac O, Wichit S, Ekchariyawat P, Neyret A, Natthanej L, et al. BIOLOGY OF ZIKA VIRUS INFECTION IN HUMAN SKIN CELLS. *J Virol* [Internet]. 2015;JVI.00354-15-. Available from: <http://jvi.asm.org/content/early/2015/06/11/JVI.00354-15.abstract>
230. Hyser JM, Estes MK. Pathophysiological Consequences of Calcium-Conducting Viroporins. *Annu Rev Virol.* 2015;
231. Barbier V, Lang D, Valois S, Rothman AL, Medin CL. Dengue virus induces mitochondrial elongation through impairment of Drp1-triggered mitochondrial fission. *Virology.* 2017;

232. Chatel-Chaix L, Cortese M, Romero-Brey I, Bender S, Neufeldt CJ, Fischl W, et al. Dengue Virus Perturbs Mitochondrial Morphodynamics to Dampen Innate Immune Responses. *Cell Host Microbe*. 2016;
233. Yu CY, Liang JJ, Li JK, Lee YL, Chang BL, Su CI, et al. Dengue Virus Impairs Mitochondrial Fusion by Cleaving Mitofusins. *PLoS Pathog*. 2015;
234. Ichinohe T, Yamazaki T, Koshiba T, Yanagi Y. Mitochondrial protein mitofusin 2 is required for NLRP3 inflammasome activation after RNA virus infection. *Proc Natl Acad Sci U S A*. 2013;
235. Cruz CM, Rinna A, Forman HJ, Ventura ALM, Persechini PM, Ojcius DM. ATP activates a reactive oxygen species-dependent oxidative stress response and secretion of proinflammatory cytokines in macrophages. *J Biol Chem*. 2007;
236. Subramanian N, Natarajan K, Clatworthy MR, Wang Z, Germain RN. The adaptor MAVS promotes NLRP3 mitochondrial localization and inflammasome activation. *Cell*. 2013;
237. Campbell A, Daher N, Solaimani P, Mendoza K, Sioutas C. Human brain derived cells respond in a type-specific manner after exposure to urban particulate matter (PM). *Toxicol Vitro*. 2014;
238. Li X-D, Deng C-L, Ye H-Q, Zhang H-L, Zhang Q-Y, Chen D-D, et al. Transmembrane Domains of NS2B Contribute to Both Viral RNA Replication and Particle Formation in Japanese Encephalitis Virus. *J Virol*. 2016;